USGS
science for a changing world

Prepared in cooperation with the Hood Canal Dissolved Oxygen Program

HCDOP

Estimates of Nutrient Loading by Ground-Water Discharge into the Lynch Cove Area of Hood Canal, Washington

Seepage meter No.	Average seepage rate, in centimeters per day: Incoming tide
Twanoh Sta	
T1	4.4
T2	1.2
T3	3.6
T4	.1
T5	–
Average net discharge rate.....	
Merrim	
M20	-37.8
M25	-31.6
Average net discharge rate.....	
Sunset B	
SB1	[1]9.1
SB2	-1.4
SB3	-.1
SB4	-1.2
SB5	-.3
SB6	1.9

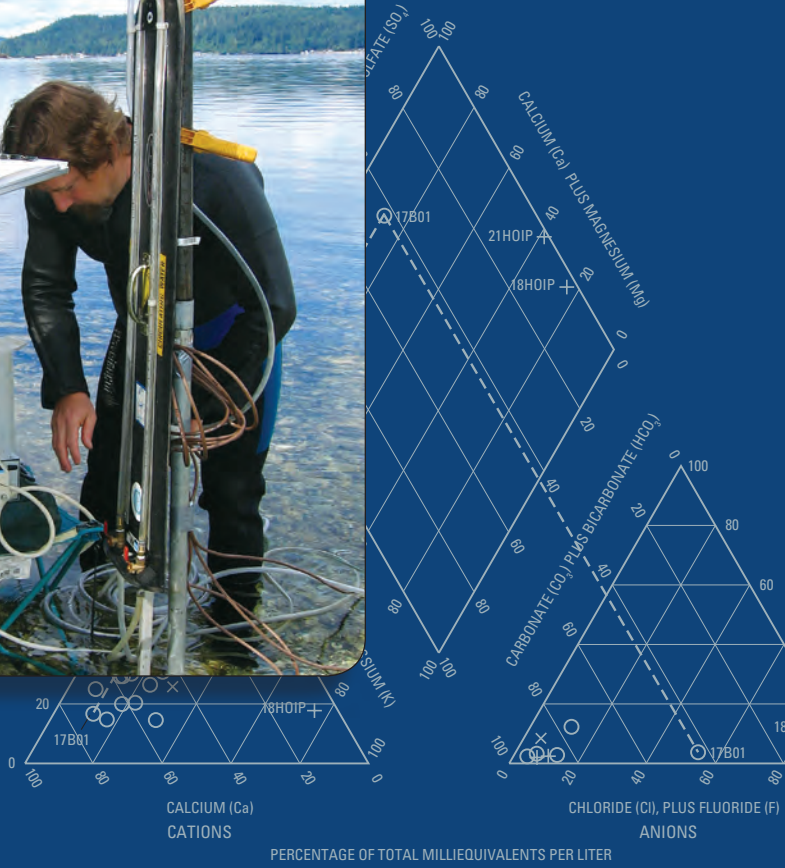

Scientific Investigations Report 2008–5078

U.S. Department of the Interior
U.S. Geological Survey

Cover: Seth Book, Mason County Health Department, and F. William Simonds, U.S. Geological Survey, measuring vertical hydraulic gradient at Twanoh State Park on the south shore of Hood Canal, Washington. (Photograph taken by Donald Rosenberry, U.S. Geological Survey, June 9, 2005.)

Estimates of Nutrient Loading by Ground-Water Discharge into the Lynch Cove Area of Hood Canal, Washington

By F. William Simonds, Peter W. Swarzenski, Donald O. Rosenberry, Christopher D. Reich, and Anthony J. Paulson

Prepared in cooperation with the Hood Canal Dissolved Oxygen Program

Scientific Investigations Report 2008–5078

U.S. Department of the Interior
U.S. Geological Survey

U.S. Department of the Interior
DIRK KEMPTHORNE, Secretary

U.S. Geological Survey
Mark D. Myers, Director

U.S. Geological Survey, Reston, Virginia: 2008

For product and ordering information:
World Wide Web: http://www.usgs.gov/pubprod
Telephone: 1-888-ASK-USGS

For more information on the USGS--the Federal source for science about the Earth, its natural and living resources, natural hazards, and the environment:
World Wide Web: http://www.usgs.gov
Telephone: 1-888-ASK-USGS

Suggested citation:
Simonds, F.W., Swarzenski, P.W., Rosenberry, D.O., Reich, C.D., and Paulson, A.J., 2008, Estimates of nutrient loading by ground-water discharge into the Lynch Cove area of Hood Canal, Washington: U.S. Geological Survey Scientific Investigations Report 2008–5078, 54 p.

Contents

Figures

Figures—Continued

Tables

Conversion Factors, Datums, and Acronyms

Conversion Factors

Multiply	By	To obtain
	Length	
centimeter (cm)	0.3937	inch (in.)
centimeter per day (cm/d)	0.3937	inch per day (in/d)
meter (m)	3.281	foot (ft)
kilometer (km)	0.6214	mile (mi)
	Area	
square meter (m^2)	10.76	square foot (ft^2)
square centimeter (cm^2)	0.001076	square foot (ft^2)
	Volume	
liter (L)	0.2642	gallon (gal)
	Flow rate	
meter per day (m/d)	3.281	foot per day (ft/d)
cubic meter per second (m^3/s)	35.31	cubic foot per second (ft^3/s)
	Mass	
kilogram (kg)	2.205	pound avoirdupois (lb)
metric ton per day (MT/d)	1.102	ton per day (ton/d)
metric ton per year (MT/yr)	1.102	ton per year (ton/yr)
	Density	
milligram per cubic meter (mg/m^3)	$6.243 \times 10\text{-}8$	pound per cubic foot (lb/ft^3)

Temperature in degrees Celsius (°C) may be converted to degrees Fahrenheit (°F) as follows:

$$°F = (1.8 \times °C) + 32.$$

Specific conductance is given in microsiemens per centimeter at 25 degrees Celsius (μS/cm at 25°C) for freshwater.

Specific conductance is given in millisiemens per centimeter at 25 degrees Celsius (mS/cm at 25°C) for seawater.

Concentrations of chemical constituents in water are given either in milligrams per liter (mg/L) or micrograms per liter (μg/L).

Datums

Vertical coordinate information is referenced to the North American Vertical Datum of 1988 (NAVD 88).

Horizontal coordinate information is referenced to the State Plane North, zone 5601, North American Datum of 1983 (NAD 83).

Altitude, as used in this report, refers to distance above the vertical datum.

Acronyms

Acronym	Meaning
AGI	Advanced Geosciences, Inc.
CTD	conductivity, temperature, and depth
DC	direct current
DEM	digital elevation model
DIN	dissolved inorganic nitrogen
DO	dissolved oxygen
dpm	decays per minute
ESM	electromagnetic seepage meter
GPS	global positioning system
HCDOP	Hood Canal Dissolved Oxygen Program
ID	inside diameter
LIDAR	Light Detection and Ranging
ppt	parts per thousand
SGD	submarine ground-water discharge
TDN	total dissolved nitrogen
USGS	U.S. Geological Survey

This page intentionally left blank

Estimates of Nutrient Loading by Ground-Water Discharge into the Lynch Cove Area of Hood Canal, Washington

By F. William Simonds, Peter W. Swarzenski, Donald O. Rosenberry, Christopher D. Reich, and Anthony J. Paulson

Abstract

Low dissolved oxygen concentrations in the waters of Hood Canal threaten marine life in late summer and early autumn. Oxygen depletion in the deep layers and landward reaches of the canal is caused by decomposition of excess phytoplankton biomass, which feeds on nutrients (primarily nitrogen compounds) that enter the canal from various sources, along with stratification of the water column that prevents mixing and replenishment of oxygen. Although seawater entering the canal is the largest source of nitrogen, ground-water discharge to the canal also contributes significant quantities, particularly during summer months when phytoplankton growth is most sensitive to nutrient availability. Quantifying ground-water derived nutrient loads entering an ecologically sensitive system such as Hood Canal is a critical component of constraining the total nutrient budget and ultimately implementing effective management strategies to reduce impacts of eutrophication. The amount of nutrients entering Hood Canal from ground water was estimated using traditional and indirect measurements of ground-water discharge, and analysis of nutrient concentrations. Ground-water discharge to Hood Canal is variable in space and time because of local geology, variable hydraulic gradients in the ground-water system adjacent to the shoreline, and a large tidal range of 3 to 5 meters. Intensive studies of ground-water seepage and hydraulic-head gradients in the shallow, nearshore areas were used to quantify the freshwater component of submarine ground-water discharge (SGD), whereas indirect methods using radon and radium geochemical tracers helped quantify total SGD and recirculated seawater. In areas with confirmed ground-water discharge, shore-perpendicular electrical resistivity profiles, continuous electromagnetic seepage-meter measurements, and continuous radon measurements were used to visualize temporal variations in ground-water discharge over several tidal cycles. The results of these field investigations show that ground-water discharge into the Lynch Cove area of Hood Canal is highly dynamic and strongly affected by the large tidal range. In areas with a steep shoreline and steep hydraulic gradient, ground-water discharge is spatially concentrated in or near the intertidal zone, with increased discharge during low tide. Topographically flat areas with weak hydraulic gradients had more spatial variability, including larger areas of seawater recirculation and more widely dispersed discharge. Measured total-dissolved-nitrogen concentrations in ground water ranged from below detection limits to 2.29 milligrams per liter and the total load entering Lynch Cove was estimated to be approximately 98 ± 10.3 metric tons per year (MT/yr). This estimate is based on net freshwater seepage rates from Lee-type seepage meter measurements and can be compared to estimates derived from geochemical tracer mass balance estimates (radon and radium) of 231 to 749 MT/yr, and previous water-mass-balance estimates (14 to 47 MT/yr). Uncertainty in these loading estimates is introduced by complex biogeochemical cycles of relevant nutrient species, the representativeness of measurement sites, and by energetic dynamics at the coastal aquifer-seawater interface caused by tidal forcing.

Introduction

In 2003, the U.S. Geological Survey (USGS) was asked to assist in the study of the causes of low dissolved oxygen concentrations in Hood Canal, Wash. (fig. 1) in collaboration with the Hood Canal Dissolved Oxygen Program (HCDOP). The HCDOP is a partnership of more than 30 organizations that monitor and study Hood Canal, and evaluate potential corrective actions to address the low dissolved oxygen problem. Working with the HCDOP partners, the USGS began to assess the loading of nitrogen-based compounds to Hood Canal. A study focusing on nitrogen loading from surface-water sources landward of the Great Bend was conducted in 2004 because severe instances of low dissolved oxygen occur in this region. The USGS also investigated the processes that affect nitrogen concentrations in the Lynch Cove area by analyzing the water column from July to October 2004 for various constituents including nitrogen isotopes. The study described in this report is a continuation of efforts to better understand and quantify nitrogen loading to Hood Canal by focusing on the role of ground water as a nutrient source.

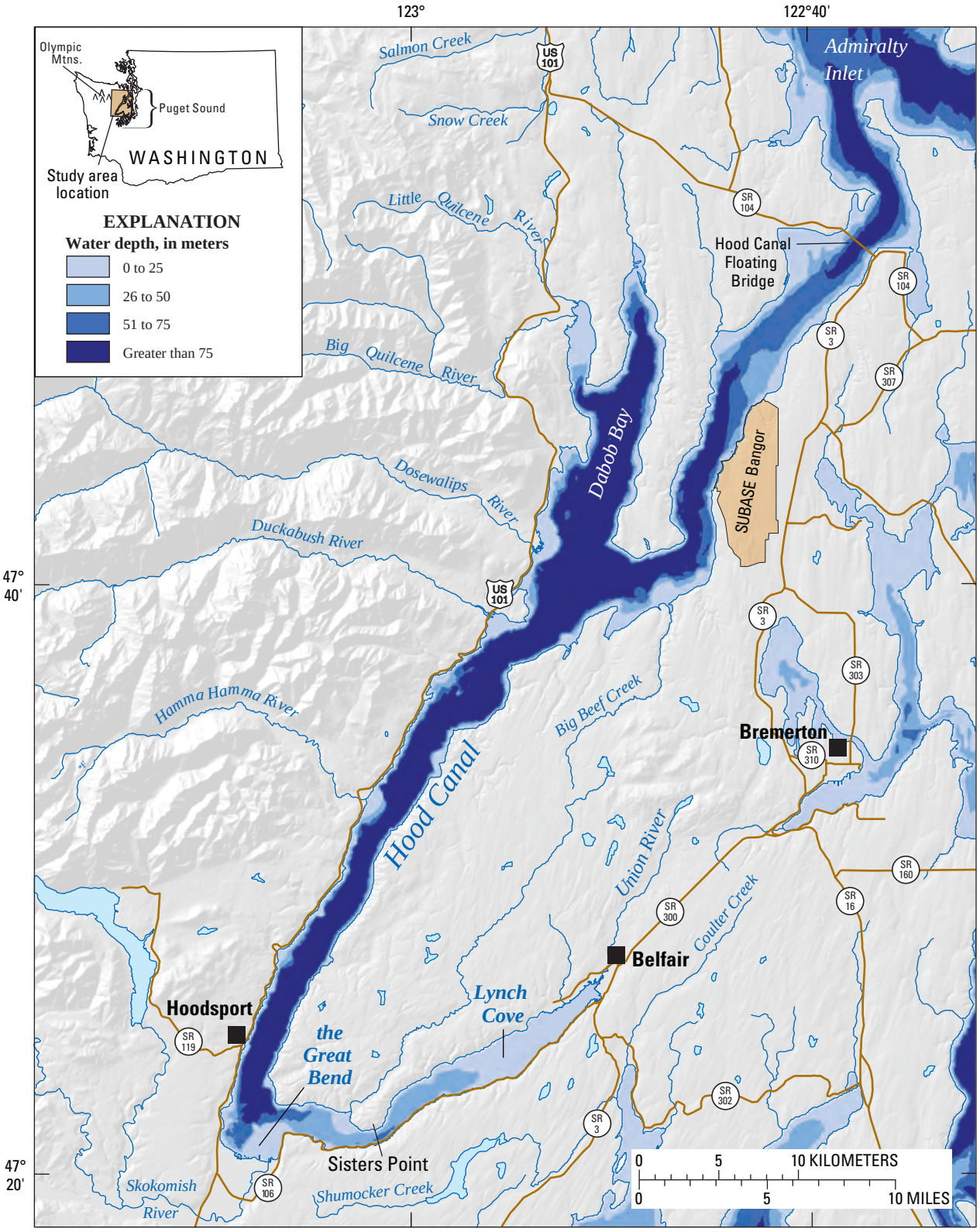

Figure 1. Location of Hood Canal on the west side of the Puget Sound lowland adjacent to the Olympic Mountains in western Washington.

Dissolved oxygen depletion in the marine waters of Hood Canal is a natural phenomenon. Hypoxic conditions are primarily caused by the combined effects of three factors: (1) the bathymetry of the fjord-shaped water body, in which a series of shallow sills near the entrance to Hood Canal limits the amount of exchange with the open ocean; (2) mixing within Hood Canal that is inhibited by a strong temperature and salinity gradient that separates an upper layer of warm, fresher water from a lower layer of cold, denser saline water; and (3) high primary productivity of planktonic algae (phytoplankton) that, after blooming, die and sink to the bottom where they decay, consuming oxygen in the process. Under certain conditions, typically in the late summer and early autumn, prevailing southerly winds push oxygenated surface water aside and cause upwelling of deeper, poorly oxygenated water that stresses marine life to the point of mortality. Although these events have probably been occurring in Hood Canal since its formation at the end of the last ice age (Crecelius and others, 2007), recent fish kill events have catalyzed monitoring and research efforts to better understand the problem and the role of humans. Observations of dissolved oxygen concentrations since the 1950s suggest that hypoxic conditions have become more frequent and are spreading northward (Jan Newton, University of Washington, oral commun., 2007). Urbanization of drainages adjacent to Hood Canal and residential development along the shoreline is suspected of increasing the nutrient load entering the Hood Canal estuary. The effects of increased nutrient availability and the dynamic interaction with estuarine processes within Hood Canal are topics of intensive study. Although the causes of hypoxia in the Hood Canal estuary are fairly well known, the processes that affect the spatial and temporal distribution and severity of hypoxia events are less clear. This study contributes to the overall understanding of nutrient loading to Hood Canal by examining the role of ground-water discharge as a nutrient source in the most landward reach, referred to here as the Lynch Cove area.

To estimate the nutrient load entering the Lynch Cove area from ground water, ground-water discharge entering the estuary must be quantified. Hydrologists have been pursuing methods for measuring the exchange of water and solutes between ground-water and surface-water bodies since the mid-1940s. Instruments designed specifically to measure ground-water discharge have undergone significant technological improvements in recent years, but are still based on original concepts developed by Fokkens and Weijenberg (1968), Lee (1977), and Lee and Cherry (1978). The need to quantify the exchange between ground water and surface water has become increasingly important as resource managers seek to use refined nutrient budgets that include submarine ground-water discharge (SGD) loading estimates.

Much recent research has focused on hyporheic exchange (the exchange of water that occurs through the streambed between shallow aquifers and rivers and streams) and the biogeochemical processes that occur in these settings (Stanford and Ward, 1988; Harvey and Bencala, 1993; Bencala, 2000; Jones and Mulholland, 2000; Woessner, 2000). A key component of the study of terrestrial river systems is quantifying the extent of exchange, and the spatial and temporal variability of exchange (Worman and others, 2002; Malcolm and others, 2003; Mutz and Rohde, 2003; Storey and others, 2003; Salehin and others, 2004; Gooseff and others, 2005). Some studies have used natural and anthropogenic tracers (Bencala and others, 1990; Harvey and Bencala, 1993; Triska and others, 1993; Scott and others, 2003; Gooseff and others, 2005), chemical-mixing models (Atekwana and Krishnamurthy, 2004; Liu and others, 2004), measurement of vertical temperature gradients (Silliman and Booth, 1993; Constantz and others, 1994; Conant, 2004; Stonestrom and Constantz, 2004; Hatch and others, 2006), or measurement of local-scale hydraulic gradients and streambed hydraulic conductivity (Valett and others, 1994; Landon and others, 2001; Baxter and others, 2003; Storey and others, 2003; Malcolm and others, 2004; Anderson and others, 2005) to calculate flow across the sediment-water interface.

Parallel research efforts have focused on coastal systems and aquifer dynamics, which may include SGD and submarine recharge processes and saltwater intrusion issues. One driving force behind many coastal aquifer studies is the need to understand the role of SGD in supplying nutrient-enriched ground water to coastal ecosystems. Most studies conducted on the east coast of North America focus on the effects of SGD on material and water budgets (Moore, 1996; 1999; 2000; Charette and others, 2001; Burnett and others, 2003a; Charette, 2007; Swarzenski, 2007), nutrient enrichments that contribute to phytoplankton blooms (LaRoche and others, 1997; Gobler and Sanudo-Wilhelmy, 2001; Hwang and others, 2005; Hu and others, 2006), as well as eutrophication and general ecosystem deterioration (Johannes, 1980; Capone and Bautista, 1985; Giblin and Gaines, 1990). Recent technological advances in geochemical tracer techniques (Burnett and others, 2002; Burnett and others, 2003b; Moore, 2003) and multi-electrode direct-current (DC) geophysical methods (Manheim and others, 2004; Swarzenski and others, 2006a) have greatly enhanced the ability to constrain SGD rates and the factors that influence spatial and temporal variability. An improved understanding of the processes that control ground-water discharge helps in evaluating potential ecological impacts.

Purpose and Scope

The purposes of this report are to (1) describe the processes that control the spatial distribution and timing of ground-water discharge into the Lynch Cove area of Hood Canal, where the dissolved oxygen problem is most severe, and (2) present estimates of ground-water discharge entering the estuary and the associated nutrient load delivered through the ground-water pathway. Understanding the dynamics of ground-water discharge and nutrient loading is part of a larger effort by the HCDOP to quantify all sources of nutrients and better understand how they are cycled through the marine ecosystem (see http://www.hoodcanal.washington.edu; Nobel and others, 2006). The Lynch Cove area (fig. 1) was selected for this study because of its sensitivity to hypoxic conditions—its distance from the entrance to Hood Canal reduces transport and flushing, the proximity to urbanized areas (Belfair) and intense development of the shoreline increases potential nutrient loading, and the hydrogeology is characterized by steep hydraulic gradients that drive ground-water flow toward the estuary.

During June 2005 and 2006, the freshwater component of SGD was quantified using intensive studies of ground-water seepage and hydraulic-head gradients in the shallow nearshore areas of Lynch Cove. Indirect methods using radon and radium geochemical tracers helped quantify total SGD and the extent of seawater recirculation. In areas with confirmed ground-water discharge, shore-perpendicular electrical resistivity profiles, continuous electromagnetic seepage-meter measurements, and continuous radon measurements were used to visualize temporal variations in ground-water discharge over several tidal cycles. Water samples from domestic wells, springs, and minipiezometers were collected for nutrient analysis and provide information necessary to estimate the nutrient load entering the estuary through the ground-water pathway. When compared to other sources, the nutrient load entering Hood Canal from ground-water discharge is especially important during the dry summer months when surface-water discharge is at a minimum (Michael and others, 2005).

Description of Study Area

Hood Canal is a 110-km-long, 2- to 4-km-wide fjord estuary on the west side of the Puget Sound lowland, adjacent to the Olympic Mountains (fig. 1). The entrance to Hood Canal at Admiralty Inlet is restricted by shallow sills that rise to within 65 m of the surface. The main channel of Hood Canal trends northeast to southwest and reaches a maximum depth of 175 m before turning abruptly eastward at the Great Bend. Inland of the Great Bend, Hood Canal becomes much shallower (55 m or less) and narrows to about 1 km wide at Sisters Point. Lynch Cove is located at the eastward-projecting terminus of Hood Canal near the town of Belfair, Washington.

Although Tertiary bedrock is locally exposed on the west side of Hood Canal, most of the fjord is underlain by unconsolidated glacial and glacio-lacustrine sediments as much as 350 m thick or more. These sediments were deposited by advancing and retreating glaciers and lakes formed during multiple cycles of continental glaciation and by streams flowing off mountains to the west. The last glacial advance, known as the Vashon Stade of the Frasier Glaciation, covered the Hood Canal area with about 300 m of ice at the south end and as much as 1,200 m of ice at the north end between 17,000 and 12,000 years ago (Easterbrook, 1979). The modern landscape, including possibly Hood Canal itself, is dominated by geomorphic features that were formed during the Frasier Glaciation (the subtle north-south lineations visible in figure 1 were caused by glacier movement). The glacial outwash deposits of the Hood Canal area consist of compacted sand, silt, and gravel with interbedded silt and clay layers, and occasional peat. These deposits form the principal aquifers that discharge ground water to the nearshore of Lynch Cove and supply the wells and springs that residents living along the shoreline of Lynch Cove rely on for their potable water supply. To avoid seawater intrusion problems, most wells are located at the landward end of residential lots, but small lot sizes are common and many wells are located very close to the shoreline. Ground water also discharges to numerous small creeks and streams adjacent to the Lynch Cove shoreline. The part of streamflow derived from springs and diffuse seepage emanating from permeable horizons adjacent to the streambed is called “baseflow,” which can be the majority of streamflow during the late summer. Ground-water seepage also can be seen in road cuts where lenses of fine-grained silt form local confining layers that direct ground-water flow laterally. Such areas typically support distinctive wetland vegetation (sidebar A).

Sidebar A. Downward movement of ground water through thick glacial sediments is directed laterally by thin lenses of silt creating a seepage face along this road cut. Wetland plants take advantage of the consistent source of water. Photograph taken by Seth Book, Mason County Health Department, May 25, 2005.

concentration for ground water. On the basis of these estimates of ground-water discharge and nitrogen concentrations, Paulson and others (2006) estimated a ground-water load of 138±77 MT/yr for the entire Hood Canal drainage basin.

A more detailed study of nitrogen mass balance was conducted in the Lynch Cove area during September and October 2004. Paulson and others (2006) calculated dissolved inorganic nitrogen loads from atmospheric deposition, runoff, regional ground-water flow, shallow flow from shoreline septic systems, and estuarine circulation. Although estuarine circulation transports about 98.7 percent of the total annual nutrient load to Lynch Cove, a portion of this load does not reach the surface layer (euphotic zone) to supply phytoplankton with nutrients. Regional ground water was the second largest source during the late summer period when surface-water inputs are smallest. This load is important because it would be discharged into the surface layer and available for phytoplankton. Annual loading from regional ground water into the Lynch Cove area was about 20.4 MT/yr, based on monthly loads from the five subbasins that drain to Lynch Cove through direct discharge and stream baseflow.

In the study described in this report, traditional physical measurements of ground-water discharge and indirect methods using geochemical tracers were used to improve the general understanding of the processes that control ground-water discharge and to verify the annual loading based on the mass-balance approaches previously used.

Methods

Previous Mass-Balance Estimates of Nutrient Loading

Average annual rainfall of 217 cm for the Hood Canal drainage basin (U.S. Soil Conservation Service, 1965) provides the primary source for recharge to the ground-water system. Water-mass-balance estimates that include precipitation, evapotranspiration, and surface-water runoff have residual terms for ground-water recharge of 2.9 to 6.9 m^3/s to the Puget Sound basin (Vaccaro and others, 1998) and 7.3 m^3/s to the Hood Canal drainage basin (Paulson and others, 2006). Under steady-state conditions these recharge rates are assumed to equal the rate of ground-water discharge that eventually enters the marine ecosystem by direct discharge and stream baseflow. To calculate nutrient loads, Paulson and others (2006) used a median inorganic nitrogen concentration of 0.6 mg/L as a nominal background

Traditional Methods for Estimating Ground-Water Discharge

Relatively few methods are available for direct measurement of ground-water discharge. These methods rely on physical measurement of seepage over a given area during a specific period of time. Because these measurements are only representative of small spatial and temporal scales, it can be challenging to evaluate variability at larger scales, as required to meet the goals of this study. In addition, measured SGD includes components of fresh ground water and recirculated seawater, which carry distinct nutrient loads and are difficult to differentiate once they have mixed. Multiple approaches using direct and indirect methods of quantifying ground-water discharge were used to help quantify the components of SGD and to increase the reliability of the estimates at various scales.

Seepage Meters

A seepage meter provides the most direct method for quantifying exchange across the sediment-water interface by isolating a part of the sediment-water interface and physically measuring the amount of exchange that occurs over time. Seepage meters have been successfully used to quantify exchange between ground water and surface water in wetlands, ponds, lakes, estuaries, and oceans (Cable and others, 1997). With appropriate consideration to minimize several sources of error (Shaw and Prepas, 1990; Belanger and Montgomery, 1992; Shinn and others, 2002; Murdoch and Kelly, 2003) and adjustment for meter inefficiencies (Belanger and Montgomery, 1992; Murdoch and Kelly, 2003; Rosenberry and Menheer, 2006) and impacts of bioirrigation (Cable and others, 2006), measurements can be made to within about 10 percent of actual seepage rates.

Manual Seepage Meters

An initial reconnaissance to identify areas and rates of nearshore ground-water discharge was conducted using "Lee-type" seepage meters (Lee, 1977) deployed within the intertidal zone and near the low tide line at seven sites around the perimeter of Lynch Cove (fig. 2). Multiple seepage meters also were deployed about 3 m apart in lines both parallel and perpendicular to the shoreline within the intertidal zone at four intensive study sites: Twanoh State Park, Merrimont, Sunset Beach, and Landon Road. The Lee-type seepage meters were made from the top of a 55-gal steel drum with a cross-sectional area of 2,550 cm^2, cut off approximately 38 cm from the top edge. Handles were attached and a 2.5-cm hole was drilled near the top edge and fitted with 1.6-cm-inside-diameter (ID) tubing. Collection bags were 3.2-L plastic packing bags with attached 1.6-cm-ID tube and valve assemblies. The collection bags were housed in a plastic box

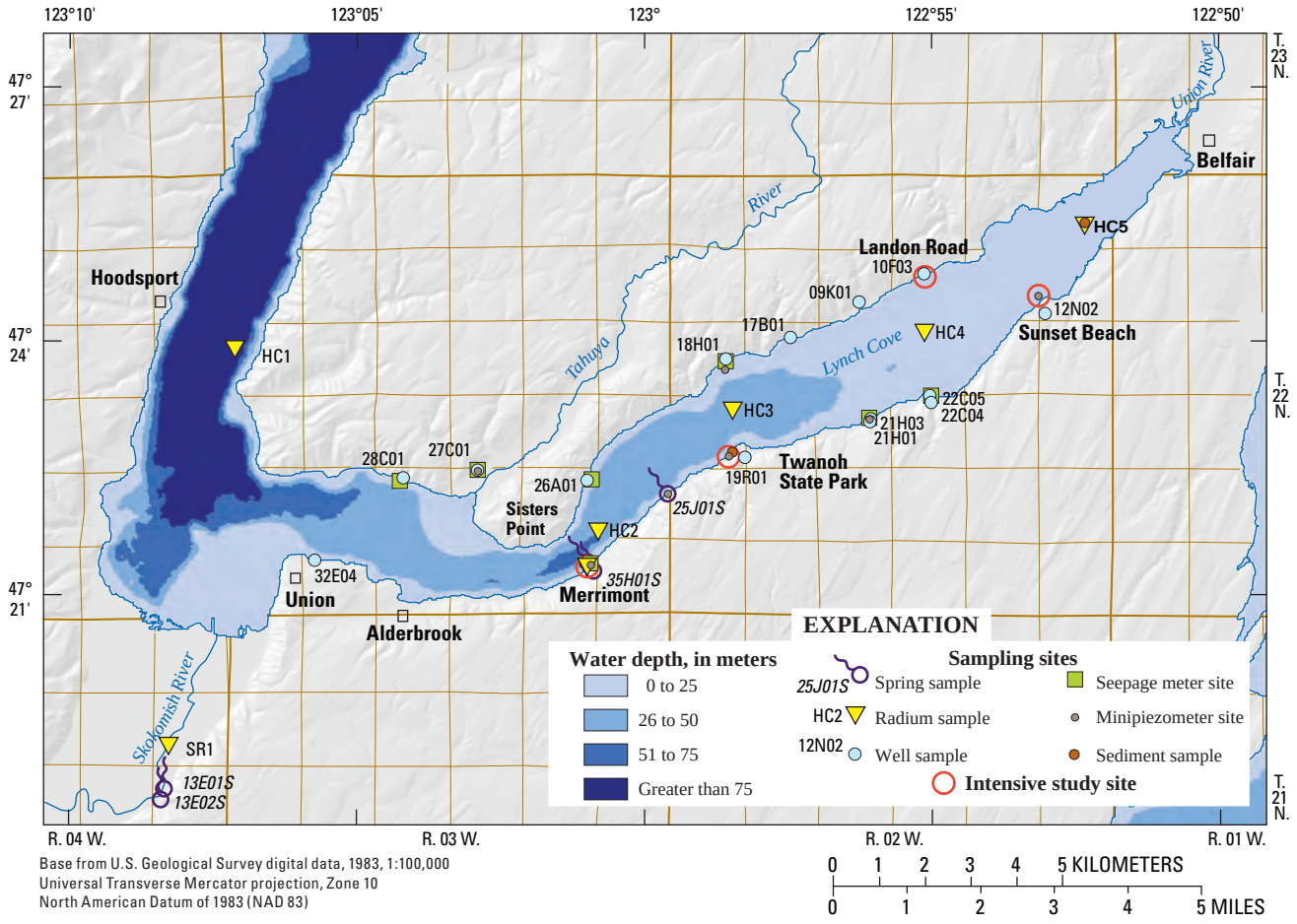

Figure 2. Location of domestic wells, minipiezometers, springs, and intensive study sites and other point measurements in the Lynch Cove area of Hood Canal, Washington.

that was secured to the top of the seepage meter with a bungee cord to reduce the effects of waves and currents. Seepage meters were installed by pressing the open end of the drum at least 15 cm into the sediments. Collection bags containing a known mass of fresh water (about 1 kg) were then connected to the seepage meter. The valve was then opened and the time noted. After an arbitrary period of time (before the collection bag could overfill), the valve was closed and the time noted. The collection bags were then reweighed, and the change in mass per unit time was calculated and converted to a flux by dividing by the sediment surface area isolated by the seepage meter. At the intensive study sites, multiple measurements were made from each seepage meter during both incoming and outgoing tides.

Electromagnetic Seepage Meters

In addition to the Lee-type seepage meters, seepage domes equipped with built-in electromagnetic flow meters were used at each of the four intensive study sites. One electromagnetic seepage meter (ESM) generally was deployed near the center of an array of Lee-type seepage meters and minipiezometers. The design and function of the ESM are described by Rosenberry and Morin (2004) and Swarzenski and others (2004). The advantage of the ESM is that it provides continuous measurement of seepage that can be recorded at 1-minute intervals. This method provides much higher temporal resolution of variations in total SGD over the area of the seepage dome than the manual Lee-type meters. Conductivity, Temperature and Depth (CTD) loggers also were used on the inside and outside of the domes to track changes in salinity and temperature over the measurement period, typically several tidal cycles.

Minipiezometers

Minipiezometers are miniature monitoring wells that can be used to provide information about the hydraulic head and direction of ground-water flow. Although minipiezometers do not provide direct measurements of ground-water discharge, they can be used to estimate hydraulic gradients and hydraulic conductivity. Using Darcy's Law, these estimates can be used to calculate the ground-water flux. The lack of thin confining units in the shallow unconfined aquifer along the shoreline of Hood Canal makes minipiezometers useful for reconnaissance of large areas and qualitatively identifying areas of concentrated ground-water discharge.

Minipiezometers used in this study were made from 1.72-cm-diameter galvanized pipe with a flattened tip and multiple (16 to 24) 0.3-cm holes drilled in the lower 15 cm of the pipe. The pipe was pounded into the ground with a slide hammer to a depth of about 152 cm. Once installed and cleared of sediment using a peristaltic pump, the minipiezometers usually provided an open connection to the water–table aquifer through which ground-water samples could be obtained, head measurements made, and slug tests conducted. A manometer was used to measure the difference in hydraulic head between ground water and the adjacent sea surface (sidebar B). The design and use of the manometer in conjunction with a minipiezometer are based on the work of Winter and others (1988). The manometer provides a means for direct measurement of vertical hydraulic gradient and an immediate indication of potential upward or downward exchange between surface water and ground water. Density corrections due to variable salinity were assumed to be negligible and were not included in the calculations.

Sidebar B. Difference in vertical hydraulic head between surface water and ground water can be directly measured using a manometer in conjunction with a minipiezometer. Relative ground–water head, on the right side of the manometer, is higher than the relative surface-water head, on the left side of the board, indicating an upward vertical hydraulic gradient. Photograph taken by F. William Simonds, U.S. Geological Survey, June 26, 2005.

In the initial reconnaissance phase of this study, minipiezometers were installed in the intertidal zone (and where possible, adjacent to a seepage meter) at the seven reconnaissance sites and four intensive study sites around the perimeter of Lynch Cove (fig. 2). Specialized 2.5-cm-diameter minipiezometers were installed next to seepage meters in an array at each of the intensive study sites. These minipiezometers were instrumented with a Solinst™ level logger set to record water level (hydraulic head) every minute. Because of the large tidal range, minipiezometers were installed with the rigid pipe projecting slightly above the sediment-water interface and extended using flexible tubing to a large float that kept the tops of the minipiezometer tubes a constant distance above the water surface. The continuous data collected from each minipiezometer could be compared to surface water-level data to determine continuous changes in vertical hydraulic gradient. However, instrument problems, poor venting, and clogged minipiezometer screens precluded collection of a complete vertical gradient dataset from all minipiezometers.

Indirect Methods for Estimating Ground-Water Discharge Using Geochemical Tracers

Recent advances in analytical techniques have enhanced the usefulness of geochemical tracers in quantifying SGD in coastal settings (Burnett and Dulaiova, 2003; Dulaiova and others, 2005; Moore, 2006). Geochemical tracers such as radon and radium can be used as proxies to derive SGD rates. Previous work has shown that although radon appears to be an effective tracer of total (fresh plus saline) ground-water discharge (Burnett and Dulaiova, 2003; Burnett and Dulaiova, 2006; Crusius and others, 2005; Dulaiova and others, 2005), radium isotopes typically track mostly the saline contribution (Moore, 2000; Charette and others, 2001; Moore, 2003; Hwang and others, 2005; Moore, 2006; Charette, 2007; Swarzenski, 2007). A combined radon/radium study yields information on the various components of ground-water discharge (Swarzenski and others, 2006a; 2007a).

Radon (Rn)

Radon-222 ($t^{1/2}$ = 3.8 d) activity, when measured in surface waters, may provide useful insight into rates and magnitudes of aquifer/ocean exchange and SGD. To determine the contribution of SGD to Lynch Cove, spatial and temporal variation of radon in the surface-water column was measured in survey and time-series experiments. Measurements were made using mobile and stationary deployments of two commercial radon-in-air detectors connected in series to one gas/water exchanger (Martens and others, 1980; Burnett and Dulaiova, 2003; Dulaiova and others, 2005; Burnett and others, 2007). These new measurement techniques have greatly simplified the collection and subsequent detection of radon, such that radon activities can now be measured in-place in near real time.

Radon variation over time, due to tides and other factors, was measured in surface water at a stationary point at Merrimont. Water was delivered to the gas/water exchanger by placing a submersible pump 15 cm above the seabed just below the low-tide line. Continuous measurements of bottom-water radon were made over a 5-day interval in June 2006 using two Durridge, Inc., RAD 7™ radon monitors placed in series (Swarzenski and others, 2007b). Concurrent temperature, conductivity, and water depth data were collected using a calibrated YSI® multiparameter probe.

As a potential reconnaissance tracer for SGD "hot spots," near-continuous radon measurements also were made in survey mode from a boat following the perimeter of Lynch Cove at 2-4 knots. In this configuration, a submersible pump drew surface water into the gas/water exchanger from a depth of about 50 cm. Salinity and temperature were measured from the same stream of water using an In-Situ® Troll® probe. Background concentrations of radon in air were continuously recorded over the entire period of the field study using a single radon monitor positioned on the south shore of Lynch Cove near the community of Alderbrook (fig. 2). Background concentrations in ground water were determined from discrete grab samples collected using a drive-point minipiezometer from an equilibrated horizon 185 cm below the sea floor at the high-tide line at the Merrimont site. Samples were analyzed using a RAD H20™ accessory connected to a RAD 7™ monitor.

Radium (Ra)

To examine the saline contribution of SGD into Lynch Cove, the distribution of four naturally occurring Ra isotopes (^{223,224,226,228}Ra) also was determined in surface waters and ground water of Lynch Cove. Surface-water samples were pumped from 0.5-m-water-column depth, where 75–100 L of water was slowly filtered through preweighed manganese-impregnated fiber columns with a peristaltic pump. Ground-water samples were obtained from a minipiezometer at the Merrimont site using the same protocol. The fiber columns were analyzed first for the short-lived ^{223,224}Ra isotopes at Woods Hole Oceanographic Institute using delayed coincidence counters, and then a high-resolution gamma well detector was used for the long-lived ^{226,228}Ra isotopes. Expected error for the short-lived isotopes and long-lived isotopes is about 10 and 7 percent, respectively. A simple mass balance of radium input and loss terms (Swarzenski and others, 2007b) was used to derive SGD rates for the entire Lynch Cove estuary based on excess ^{226}Ra. Radium isotope

samples were collected in Hood Canal, Lynch Cove, and the Skokomish River, and a mean apparent residence time of 32 days (range for Lynch Cove, 25-40 days) was calculated using $^{223}Ra/^{228}Ra$ isotope ratios as described by Moore (1996; 1999; 2000; 2003) and used in studies by Charette and others (2001) and Swarzenski and others (2006a; 2007a) (fig. 2). For the radium-based residence time approach, the upper layer of surface water impacted by SGD was assumed to become isolated from bottom sediments so that radioactive decay processes alone could be used as water-mass proxies. Such an assumption was valid in this situation because of a persistent thermocline in Lynch Cove and Hood Canal, which deepened from 2 m on June 2, 2006, to about 7 m on June 9, 2006, that effectively separated bottom water from surface water (Paulson and others, 2006). Because radium is only mobilized in water with salinities greater than 2 ppt, this radium approach represents a best estimate of the saline component of SGD for the time period studied (Charette, 2007). Additional sampling locations and winter sample collection would better constrain end-member variability and seasonality, and thus better refine these estimates.

Indirect Methods for Visualizing the Freshwater-Saltwater Interface

Recent advances in geophysical instrumentation and analytical techniques have led to the use of new tools for identifying, measuring, and visualizing SGD (Swarzenski and others, 2006a). Two electrical resistivity methods were applied for the first time in the Pacific Northwest as part of this study. Electrical resistivity can be applied in a stationary (land-based) time-series mode or in a streaming (marine-based) survey mode. Both methods are useful for identifying ground-water discharge areas and visualizing subsurface salinity gradients and how they change under various hydrologic forces.

Stationary (Land-Based) Electrical-Resistivity Time Series

Stationary multi-electrode electrical-resistivity time-series measurements were made at two of the intensive study sites—Merrimont and Sunset Beach. An Advanced Geosciences, Inc., (AGI) SuperSting™ eight-channel receiver was connected to a 56-electrode, 112-m cable (2-m electrode spacing) through an external switching box (sidebar C).

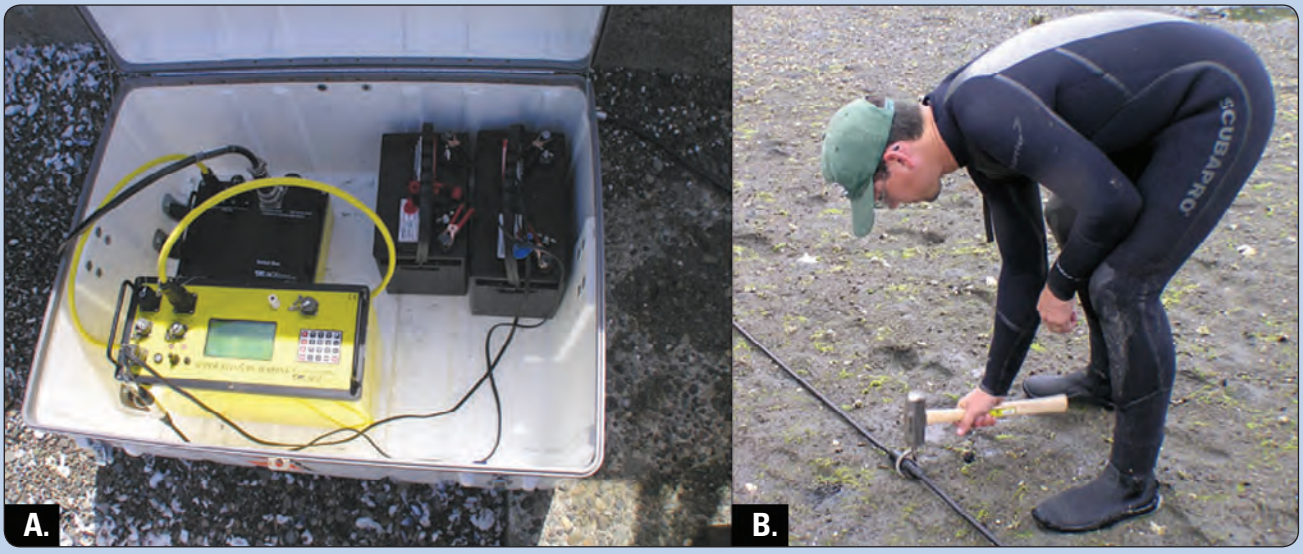

Sidebar C. Land-based electrical-resistivity time-series data are acquired using an AGI SuperSting™ marine resistivity meter (*A*) interfaced with a 110-meter cable with 56 electrodes spaced every 2 meters. The cable is anchored to the seabed with stainless-steel spikes in a line perpendicular to the shoreline (*B*). Photographs taken by F. William Simonds, U.S. Geological Survey, June 9, 2006.

To maximize resolution and the signal-to-noise ratio, while minimizing data acquisition time, current potentials were measured in a distributed dipole-dipole array pairwise between the first electrode and each successive electrode down the line, followed by the second electrode and each successive electrode, and so on until potentials between all combinations of electrodes were measured. Resistivity values were processed with AGI's 2D EarthImager™ software using a homogeneous starting model and water-depth data collected at the midpoint of the cable using a Solinist™ Diver submersible pressure transducer. Details of the method and image processing are described by Swarzenski and others (2007b). Each electrode along the cable was connected to the seabed with 30-cm-long stainless-steel spikes in a line perpendicular to the shoreline. The cable extended from about 15 m landward of the high-tide line to well below the low tide line at Merrimont, and from a cement seawall out to just above the extreme low-tide line at Sunset Beach. At both sites, the cable was left in place over one or more tidal cycles. The rate of data acquisition and processing capability of the SuperSting™ receiver was about one image per hour. Thus, multiple snapshot images were obtained as the surface-water stage changed with the tides.

Streaming (Marine-Based) Electrical-Resistivity Surveys

Streaming multi-electrode electrical resistivity surveys were conducted by trailing a 130-m cable behind a boat in a series of transects parallel to the shoreline around the perimeter of Lynch Cove (sidebar D). In this configuration, electrodes are spaced 10 m apart with two source electrodes nearest the boat followed by nine receiver electrodes. The cable is kept near the surface of the water by foam floats as it is towed behind a boat traveling at 2 to 4 knots. Electrical-resistivity data are collected in streaming mode as the boat travels parallel to the shoreline in about 3 to 10 m of water. During the survey, a Global Positioning System (GPS) receiver was used to record the position of the boat while a depth sounder measured water depth and an In-Situ® Troll® probe recorded temperature and specific conductivity at a depth of 0.5 m. In total, about 30 km of the Lynch Cove shoreline were surveyed yielding 16 profiles that provide electrical resistivity data to depths of as much as 20 m below the sea floor (appendix A).

Sidebar D. A streaming resistivity survey was conducted using a boat towing a 130-meter cable near the surface of the water. The cable, which is wrapped with pieces of styrofoam to stay afloat, has two source electrodes nearest the boat and nine receiver electrodes spaced 10 meters apart. Data are collected as the cable is towed parallel to the shoreline in about 3 to 10 meters of water. Photograph taken by F. William Simonds, U.S. Geological Survey, June 8, 2006.

Ground-Water Sampling

To determine nutrient concentrations and other aqueous constituents in fresh ground water, samples were collected around the perimeter of Lynch Cove from domestic wells, springs and seeps, and from selected minipiezometers installed in the intertidal zone (fig. 2). Using standard USGS sampling procedures (U.S. Geological Survey, variously dated), samples were collected from 14 domestic wells, 5 springs or seeps, and 5 minipiezometers; 2 duplicate samples and 2 deionized water blanks also were collected for quality-assurance purposes. Samples collected in August 2005 were filtered and shipped on ice to the USGS National Water Quality Laboratory in Denver, Colo., for analysis. Samples were analyzed for major element chemistry and nutrients, plus total phosphorus and nitrogen using the methods described by Fishman (1993).

In June 2006, additional samples were collected from minipiezometers at Merrimont and Sunset Beach sites to further evaluate temporal and spatial variability. These samples were analyzed for trace metals and nutrients at Woods Hole Oceanographic Institute using standard colorimetric techniques (Charette and others, 2001; Swarzenski and others, 2006b).

Domestic Wells and Springs

The domestic wells evaluated in this study ranged in depth from 7 to 54 m, with an average depth of 26 m. Available well logs describe glacial lithologies consisting of compacted sand and gravel with occasional layers or lenses of fine silt or blue clay. Although most residents of the Lynch Cove area use ground water from wells for their potable water supply, some residents use gravity systems that collect spring water originating from hillslopes adjacent to the Lynch Cove shoreline. Two spring-fed water systems were sampled at the source, along with two other natural springs near the mouth of the Skokomish River (fig. 2). A fifth sample was collected in 2006 from a seep emanating from the beach face at Merrimont during an outgoing tide.

Minipiezometers

Minipiezometers installed in the intertidal zone around the perimeter of Lynch Cove provided measurements of vertical hydraulic head gradients and collection points for water samples close to the point of discharge. Due to the large tidal range, minipiezometers were generally installed and sampled during low-tide stages. Most minipiezometers, when sampled at high-tide stages, yielded primarily saline water. Samples with high specific conductances indicative of significant saline water intrusion were not submitted for analysis. To further evaluate temporal and spatial variability, a series of minipiezometers was installed along a transect perpendicular to the shoreline at Sunset Beach (sidebar E) in June 2006. Minipiezometers were installed at distances of 20, 40, 60, and 80 m from the shoreline (a concrete seawall), and samples were collected at 1.5-m (shallow) and 3-m (deep) depths below the seabed (no samples were collected at 60 m from the shoreline and only the 1.5-m depth was sampled at 80 m from the shoreline). All samples were collected during low tide.

Another series of samples was collected from a single minipiezometer installed at a depth of 1.85 m below the seabed, just below the high tide line at the Merrimont site. Here, samples of surface water and ground water were collected for comparison purposes at 1-hour intervals over a 10-hour period encompassing an incoming tide on June 6, 2006.

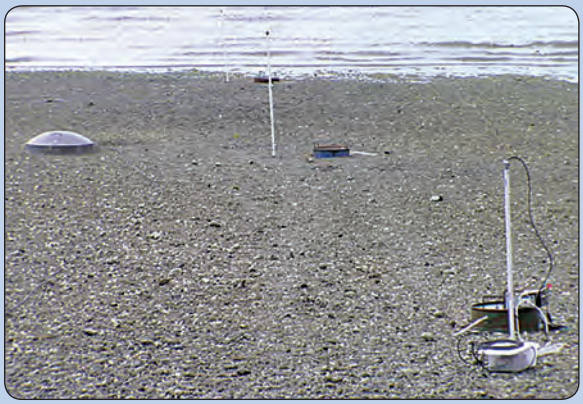

Sidebar E. Linear array of minipiezometers (white pipes), Lee-type seepage meters (partly buried colored barrels), and electromagnetic seepage meter (ESM) (aluminum dome) at Sunset Beach are exposed at low tide. When the beach is submerged at high tide, the ESM is capable of measuring and recording seepage rates at 1-minute intervals. Photograph taken by F. William Simonds, U.S. Geological Survey, June 9, 2006.

Chemical Composition of Ground Water

In general, the quality of drinking water reported by residents of the Lynch Cove area was good, and chemical data (table 1) show a tight clustering of analyses (fig. 3). Nutrient analyses from wells indicated that total nitrogen occurs in the form of nitrate; ammonia and nitrite concentrations were less than detection limits of 0.04 and 0.008 mg/L, respectively. The average total nitrogen concentration from all samples was 0.33 mg/L, which is similar to concentrations of 1.0 mg/L reported for dissolved inorganic nitrogen in ground water in the Puget Sound Basin (Inkpen and others, 2000) and 0.06 mg/L near the Naval Submarine Base Bangor (Greene, 1997). Chemical analysis of the spring water yielded essentially identical results to those of the wells sampled in this study, and constituent concentrations cluster in the same area (fig. 3). The average total nitrogen concentration from springs was 0.5 mg/L.

Table 1. Field measurements and concentrations of dissolved constituents in ground water collected in the Lynch Cove area of Hood Canal, Washington, August 2005.

[Constituent averages do not include estimated values and values less than reporting limit. Samples analyzed at the National Water Quality Laboratory, Denver, CO. Locations of sample points shown in figure 2. **Local name:** B, blank sample; P, minipiezometer sample; R, replicate sample; S, spring sample. Quality assurance samples shown in **bold**. **Abbreviations:** N, nitrogen, P, phosphorus; m, meter; mV, millivolt; mg/L, milligram per liter; µS/cm, microsiemen per centimeter; µg/L, microgram per liter; ºC, degree Celsius; E, estimated value below reporting limit; <, less than reporting limit; –, parameter not analyzed; nd, no data]

Station No.	Local name	Sample date	Time	Well depth (m)	Altitude of land surface (m)	Oxidation reduction potential (mV)	Dissolved oxygen (mg/L)	pH (standard units)	Specific conductance (µS/cm)
471833123083101	13E01S	08-25-05	1600	–	18.0	108	10.9	6.9	110
471836123082301	13E02S	08-30-05	1400	–	52.3	215	11.0	6.8	108
471836123082301	**13E02SR**	**08-30-05**	**1401**	**–**	**52.3**	**–**	**–**	**–**	**–**
471836123082301	**13E02SB**	**08-31-05**	**1415**	**–**	**52.3**	**–**	**–**	**–**	**–**
472418122563201	09K01	08-10-05	1040	21.6	11.0	444	5.5	7.2	111
472447122551301	10F03	08-16-05	1210	21.3	6.4	189	4.5	6.7	105
472420122530501	12N02	08-16-05	1315	54.3	6.4	190	7.5	7.5	111
472402122573201	17B01	08-09-05	1415	35.4	5.2	68	6.7	6.8	194
472402122573201	**17B01B**	**08-31-05**	**1405**	**35.4**	**5.2**	**–**	**–**	**–**	**–**
472350122582701	18H01	08-03-05	1115	24.4	5.6	100	1.2	7.7	119
472350122582702	18H01P	08-03-05	1156	–	.3	86	3.5	7.2	3,260
472239122581801	19R01	08-17-05	1210	22.9	10.9	152	10.7	7.8	103
472239122581801	**19R01R**	**08-17-05**	**1211**	**22.9**	**10.9**	**–**	**–**	**–**	**–**
472239122581802	19R01P	08-24-05	1145	–	.9	152	5.1	6.0	93
472309122555001	21H01	08-16-05	1420	7.3	5.3	–	–	–	–
472309122555002	21H01P	08-17-05	1115	–	0.8	101	8.9	5.9	7,590
472304122560801	21H03	08-16-05	1450	nd	3.9	187	9.7	7.5	95
472316122550501	22C04	08-09-05	1100	23.7	14.0	90	8.7	6.4	141
472321122550701	22C05	08-09-05	1325	nd	2.4	–	nd	–	103
472203122591501	25J01S	08-24-05	1300	–	28.5	186	11.2	6.8	87
472203122591502	25J01P	08-24-05	1400	–	1.7	174	9.9	6.9	98
472252123003501	26A01	08-10-05	1200	19.8	7.2	135	4.4	6.2	113
472228123030001	27C01	08-04-05	1315	15.8	13.9	49	7.6	7.0	116
472228123030002	27C01P	08-04-05	1315		1.3	166	6.7	5.9	115
472223123041601	28C01	08-05-05	1215	19.8	10.1	–	–	–	–
472124123054901	32E04	08-25-05	1050	34.4	2.0	184	8.9	7.5	108
472117123010201	35H01S	08-11-05	1120	–	16.1	204	10.4	6.1	142
Average well depth				25.6					

Chemical analyses of minipiezometer samples produced slightly lower average total nitrogen (0.2 mg/L) when compared to domestic well samples (0.3 mg/L). Two of the minipiezometer samples (18H01P and 21H01P) showed higher values for most major constituents, especially sodium, chloride, and sulfate, indicating that these samples were at least partially contaminated by seawater infiltration during a previous high tidal stage. These samples plot as distinct outliers in figure 3.

Chemical analyses for nutrients and trace metals (table 2) at the Sunset Beach minipiezometer array showed a range of total-dissolved-nitrogen concentrations from 0.42 to 2.29 mg/L, with decreasing concentrations in the seaward direction (fig. 4). The average total nitrogen concentration at this site was 1.1 mg/L, which is slightly higher than was measured in domestic wells and other minipiezometers around Lynch Cove.

Table 1. Field measurements and concentrations of dissolved constituents in ground water collected in the Lynch Cove area of Hood Canal, Washington, August 2005.—Continued

[Constituent averages do not include estimated values and values less than reporting limit. Samples analyzed at the National Water Quality Laboratory, Denver, CO. Locations of sample points shown in figure 2. **Local name:** B, blank sample; P, minipiezometer sample; R, replicate sample; S, spring sample. Quality assurance samples shown in **bold**. **Abbreviations:** N, nitrogen, P, phosphorus; m, meter; mV, millivolt; mg/L, milligram per liter; µS/cm, microsiemen per centimeter; µg/L, microgram per liter; ºC, degree Celsius; E, estimated value below reporting limit; <, less than reporting limit; –, parameter not analyzed; nd, no data]

Station No.	Local name	Sample date	Time	Temperature (ºC)	Ammonia (mg/L as N)	Nitrate (mg/L as N)	Nitrite (mg/L as N)	Orthophosphate (mg/L as P)	Phosphorus (mg/L as P)
471833123083101	13E01S	08-25-05	1600	9.9	<0.04	0.56	<0.008	0.038	0.04
471836123082301	13E02S	08-30-05	1400	9.0	<.04	.45	<.008	.028	.034
471836123082301	**13E02SR**	**08-30-05**	**1401**	**–**	**<.04**	**.45**	**<.008**	**.029**	**.033**
471836123082301	**13E02SB**	**08-31-05**	**1415**	**–**	**<.04**	**<.06**	**<.008**	**<.006**	**E.002**
472418122563201	09K01	08-10-05	1040	9.4	<.04	E.03	<.008	.087	.099
472447122551301	10F03	08-16-05	1210	11.6	<.04	<.06	<.008	.065	.07
472420122530501	12N02	08-16-05	1315	9.5	<.04	.25	<.008	.046	.055
472402122573201	17B01	08-09-05	1415	14.5	<.04	E.03	<.008	.061	.075
472402122573201	**17B01B**	**08-31-05**	**1405**	**–**	**<.04**	**<.06**	**<.008**	**<.006**	**<.004**
472350122582701	18H01	08-03-05	1115	10.6	<.04	<.06	<.008	.145	.154
472350122582702	18H01P	08-03-05	1156	16.7	<.04	E.04	<.008	.021	.026
472239122581801	19R01	08-17-05	1210	14.2	<.04	<.06	<.008	.046	.053
472239122581801	**19R01R**	**08-17-05**	**1211**	**–**	**<.04**	**<.06**	**<.008**	**.045**	**.052**
472239122581802	19R01P	08-24-05	1145	12.2	<.04	.08	<.008	.02	.023
472309122555001	21H01	08-16-05	1420	–	<.04	.43	<.008	.017	.018
472309122555002	21H01P	08-17-05	1115	14.7	<.04	.65	<.008	<.006	E.003
472304122560801	21H03	08-16-05	1450	10.6	<.04	.07	<.008	.06	.069
472316122550501	22C04	08-09-05	1100	11.3	<.04	.93	<.008	.022	.028
472321122550701	22C05	08-09-05	1325	10.3	<.04	.34	<.008	.059	.074
472203122591501	25J01S	08-24-05	1300	9.4	<.04	<.06	<.008	.056	.065
472203122591502	25J01P	08-24-05	1400	13.2	<.04	.06	<.008	.04	.044
472252123003501	26A01	08-10-05	1200	10.8	<.04	.07	<.008	.016	.02
472228123030001	27C01	08-04-05	1315	10.6	<.04	.06	<.008	.053	.06
472228123030002	27C01P	08-04-05	1315	16.3	<.04	.08	<.008	.023	.023
472223123041601	28C01	08-05-05	1215	–	<.04	E.04	<.008	.127	.135
472124123054901	32E04	08-25-05	1050	10.1	<.04	<.06	<.008	.12	.13
472117123010201	35H01S	08-11-05	1120	9.0	<.04	<.06	<.008	.026	.032
Average nitrate						0.31			

Table 1. Field measurements and concentrations of dissolved constituents in ground water collected in the Lynch Cove area of Hood Canal, Washington, August 2005.—Continued

[Constituent averages do not include estimated values and values less than reporting limit. Samples analyzed at the National Water Quality Laboratory, Denver, CO. Locations of sample points shown in figure 2. **Local name:** B, blank sample; P, minipiezometer sample; R, replicate sample; S, spring sample. Quality assurance samples shown in **bold**. **Abbreviations:** N, nitrogen, P, phosphorus; m, meter; mV, millivolt; mg/L, milligram per liter; µS/cm, microsiemen per centimeter; µg/L, microgram per liter; ºC, degree Celsius; E, estimated value below reporting limit; <, less than reporting limit; –, parameter not analyzed; nd, no data]

Station No.	Local name	Sample date	Time	Total nitrogen (mg/L)	Calcium (mg/L)	Magnesium (mg/L)	Sodium (mg/L)	Acid neutralizing capacity (mg/L)	Chloride (mg/L)
471833123083101	13E01S	08-25-05	1600	0.61	11.3	5.02	3.13	52	1.98
471836123082301	13E02S	08-30-05	1400	.47	11.4	5.08	2.97	–	2.63
471836123082301	**13E02SR**	**08-30-05**	**1401**	**.47**	**11.4**	**5.01**	**2.96**	**–**	**2.61**
471836123082301	**13E02SB**	**08-31-05**	**1415**	**E.06**	**–**	**–**	**–**	**–**	**–**
472418122563201	09K01	08-10-05	1040	<.06	13.3	2.84	3.97	52	1.27
472447122551301	10F03	08-16-05	1210	<.06	12.3	2.52	4.24	49	1.2
472420122530501	12N02	08-16-05	1315	.28	10	4.97	4.01	54	1.43
472402122573201	17B01	08-09-05	1415	E.04	35.4	5.44	6.82	50	44.8
472402122573201	**17B01B**	**08-31-05**	**1405**	**E.03**	**.02**	**<.008**	**<.2**	**–**	**<.20**
472350122582701	18H01	08-03-05	1115	<.06	16.3	2.33	4.64	57	1.19
472350122582702	18H01P	08-03-05	1156	.06	58	98.8	786	84	1,340
472239122581801	19R01	08-17-05	1210	<.06	8.96	3.11	3.05	42	1.44
472239122581801	**19R01R**	**08-17-05**	**1211**	**E.03**	**9.00**	**3.13**	**3.04**	**42**	**1.44**
472239122581802	19R01P	08-24-05	1145	.08	–	–	–	–	–
472309122555001	21H01	08-16-05	1420	.48	6.8	2.87	3.96	37	1.53
472309122555002	21H01P	08-17-05	1115	.7	91.3	285	1,012	46	2,383
472304122560801	21H03	08-16-05	1450	.09	11.6	3.11	3.49	48	1.47
472316122550501	22C04	08-09-05	1100	1	13.8	6.78	3.98	65	1.58
472321122550701	22C05	08-09-05	1325	.4	13.5	4.36	3.8	56	1.47
472203122591501	25J01S	08-24-05	1300	E.03	10.1	3.14	2.89	42	1.61
472203122591502	25J01P	08-24-05	1400	.11	10.9	3.91	3.12	–	1.68
472252123003501	26A01	08-10-05	1200	.1	11.1	3.63	5.95	49	4.34
472228123030001	27C01	08-04-05	1315	.1	11.9	3.75	3.35	50	1.25
472228123030002	27C01P	08-04-05	1315	.12	11.8	4.41	4.18	51	3.24
472223123041601	28C01	08-05-05	1215	E.04	13.4	2.87	4.32	52	1.24
472124123054901	32E04	08-25-05	1050	<.06	12	2.67	5.31	46	4.03
472117123010201	35H01S	08-11-05	1120	<.06	8.1	3.56	2.86	42	1.4
Average total N				0.33					

The high nutrient values close to the seawall (concrete bulkhead, fig. 4) indicate possible anthropogenic sources just landward of the seawall where individual septic drain fields are located. Samples from nested minipiezometers indicated that ammonia, silica, total dissolved nitrogen (TDN), and manganese increase in concentration with depth below the seabed (table 2).

At the Merrimont site, time-series samples were collected during an incoming tide from a minipiezometer installed on the beach and from surface water near the boat dock. An additional sample was collected from a spring that emerged on the beach face near the low tide line at the beginning of the time series (beach-face seep, table 2). The chemical analyses

Table 1. Field measurements and concentrations of dissolved constituents in ground water collected in the Lynch Cove area of Hood Canal, Washington, August 2005.—Continued

[Constituent averages do not include estimated values and values less than reporting limit. Samples analyzed at the National Water Quality Laboratory, Denver, CO. Locations of sample points shown in figure 2. **Local name:** B, blank sample; P, minipiezometer sample; R, replicate sample; S, spring sample. Quality assurance samples shown in **bold**. **Abbreviations:** N, nitrogen, P, phosphorus; m, meter; mV, millivolt; mg/L, milligram per liter; µS/cm, microsiemen per centimeter; µg/L, microgram per liter; ºC, degree Celsius; E, estimated value below reporting limit; <, less than reporting limit; –, parameter not analyzed; nd, no data]

Station No.	Local name	Sample date	Time	Fluoride (mg/L)	Silica (mg/L)	Sulfate (mg/L)	Iron (µg/L)	Manganese (µg/L)
471833123083101	13E01S	08-25-05	1600	<0.1	19.4	1.14	34	0.8
471836123082301	13E02S	08-30-05	1400	E.06	20.2	1.21	<6	<.6
471836123082301	**13E02SR**	**08-30-05**	**1401**	**<.1**	**20.5**	**1.2**	**<6**	**<.6**
471836123082301	**13E02SB**	**08-31-05**	**1415**	**–**	**–**	**–**	**–**	**–**
472418122563201	09K01	08-10-05	1040	<.1	19.2	1.4	<6	<.6
472447122551301	10F03	08-16-05	1210	<.1	20.2	1.2	11	<.6
472420122530501	12N02	08-16-05	1315	<.1	26	.94	<6	<.6
472402122573201	17B01	08-09-05	1415	<.1	19.4	3.92	24	1.2
472402122573201	**17B01B**	**08-31-05**	**1405**	**<.1**	**<.20**	**<.18**	**6**	**<.6**
472350122582701	18H01	08-03-05	1115	<.1	17.5	1.4	<6	E.6
472350122582702	18H01P	08-03-05	1156	<.1	19.1	200	E13	2.2
472239122581801	19R01	08-17-05	1210	<.1	19.8	.66	<6	<.6
472239122581801	**19R01R**	**08-17-05**	**1211**	**<.1**	**19.9**	**.68**	**<6**	**<.6**
472239122581802	19R01P	08-24-05	1145	–	–	–	–	–
472309122555001	21H01	08-16-05	1420	<.1	22.8	1.2	<6	<.6
472309122555002	21H01P	08-17-05	1115	<.1	29.9	293	<30	E2.2
472304122560801	21H03	08-16-05	1450	<.1	20.7	.9	<6	<.6
472316122550501	22C04	08-09-05	1100	<.1	27	1.78	22	6.0
472321122550701	22C05	08-09-05	1325	<.1	20.7	1.72	<6	E.36
472203122591501	25J01S	08-24-05	1300	E.06	19.8	.8	<6	<.6
472203122591502	25J01P	08-24-05	1400	E.07	21.9	.84	8	.9
472252123003501	26A01	08-10-05	1200	E.1	18.9	1.6	22	3.7
472228123030001	27C01	08-04-05	1315	<.1	19.3	1.1	9	2.4
472228123030002	27C01P	08-04-05	1315	<.1	21.8	1.6	<6	1.0
472223123041601	28C01	08-05-05	1215	<.1	17.9	1.5	<6	<.6
472124123054901	32E04	08-25-05	1050	<.1	18.2	1.5	<6	<.6
472117123010201	35H01S	08-11-05	1120	<.1	19.1	0.8	<6	<.6

from the minipiezometer (table 2) show very small variation in TDN (0.36 to 0.48 mg/L), and no consistent trends in trace metal concentrations over the 10-hour sampling period. Average total nitrogen concentration in ground water over the sampling period was 0.41 mg/L, which is consistent with domestic well concentrations. Similarly, analyses of surface water also show little variation in TDN (0.12 to 0.25 mg/L), with an average concentration of 0.17 mg/L (table 2). The total dissolved nitrogen concentration in a single grab sample from the beach-face seep near the low-tide line was 0.2 mg/L (table 2). Additional analysis of the time-series data is presented in Swarzenski and others (2007b).

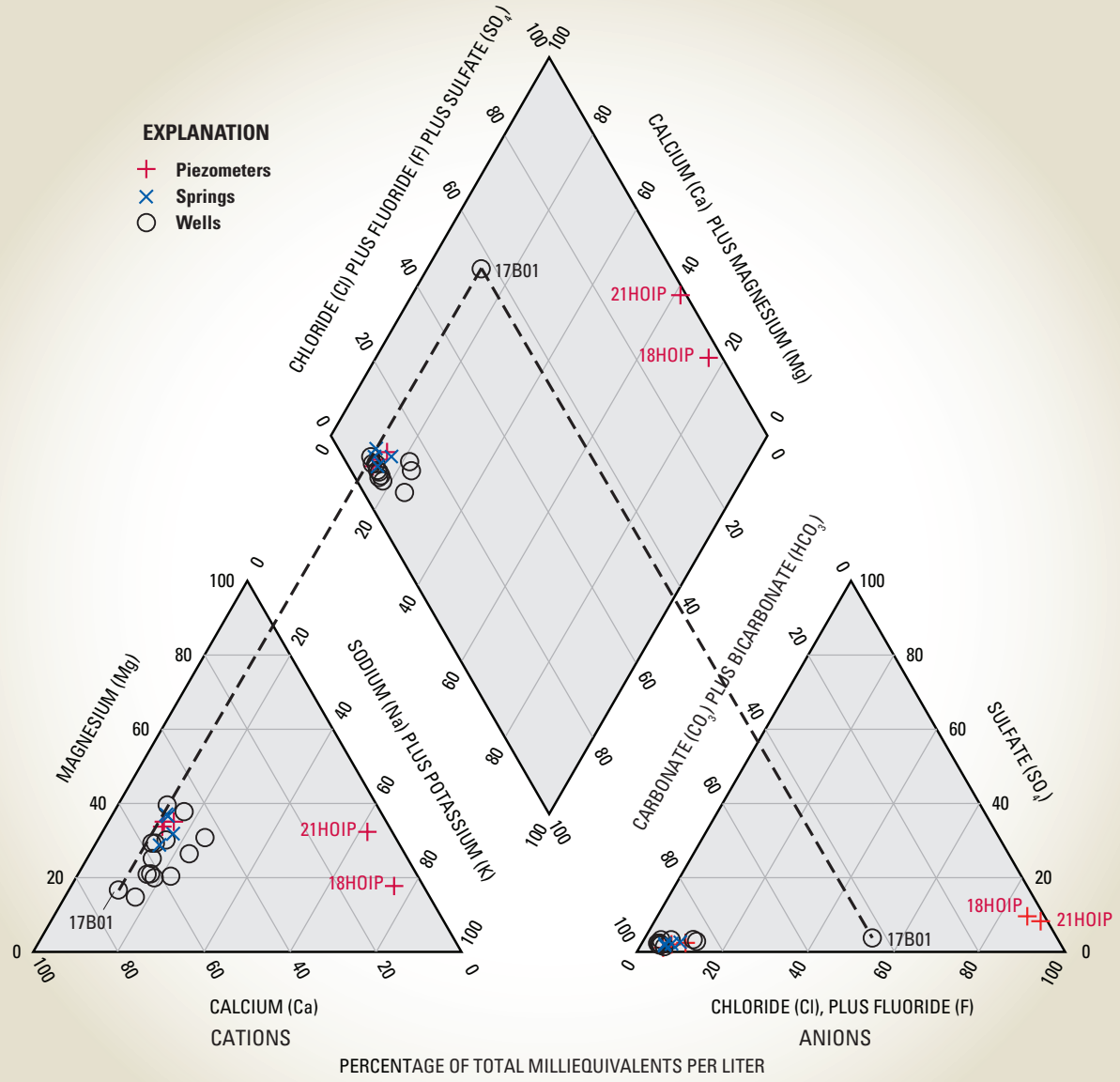

Figure 3. Chemical composition of water samples from wells, springs, and minipiezometers in the Lynch Cove area of Hood Canal, Washington.

Table 2. Field measurements and nutrient and trace metal concentrations from minipiezometers and surface water at Sunset Beach and Merrimont, Lynch Cove area of Hood Canal, Washington, June 2006.

[Samples analyzed at Woods Hole Oceanographic Institute. Locations of sample points shown in figures 7 and 11. **Abbreviations:** N, nitrogen; P, phosphorus; cm, centimeter; mg/L, milligram per liter; µS/cm, microsiemens per centimeter; –, parameter not measured; nd, not detected at specified detection limit]

Station No.	Date	Time	Temperature (ºC)	Specific conductance (µS/cm)	pH (standard units)	Dissolved oxygen (mg/L)	Ammonium (mg/L as N)	Silica (mg/L as SiO_2)	Phosphate (mg/L as P)	Nitrate plus nitrite (mg/L as N)
Sunset Beach										
2006 minipiezometer array (depth - shallow, 1.5 m; deep, 3 m)										
M20 (shallow)	06-15-06	13:20	21.0	37.5	–	–	0.001	8.35	0.08	0.413
M20 (deep)	06-15-06	14:00	19.0	15	–	–	.007	12.50	.02	1.919
M40 (shallow)	06-15-06	14:30	20.9	34.4	–	–	.003	9.49	.07	.709
M40 (deep)	06-15-06	15:30	19.8	29.7	–	–	.045	10.28	.03	1.152
M80 (shallow)	06-15-06	16:15	21.7	34.4	–	–	.018	7.45	.03	.247
					Detection limit.....		0.001	0.003	0.002	0.001

Station No.	Date	Time	Dissolved inorganic nitrogen (mg/L as N)	Dissolved organic nitrogen (mg/L as N)	Total dissolved nitrogen (mg/L as N)	Barium (mg/L)	Cobalt (mg/L)	Chromium (mg/L)	Iron (mg/L)	Manganese (mg/L)
2006 minipiezometer array (depth - shallow, 1.5 m; deep, 3 m)										
M20 (shallow)	06-15-06	13:20	0.41	0.14	0.55	9.46	0.03	0.4	1.78	1
M20 (deep)	06-15-06	14:00	1.93	.36	2.29	9.97	.78	.8	159.23	25
M40 (shallow)	06-15-06	14:30	.71	.20	.92	11.42	.13	.4	7.35	5
M40 (deep)	06-15-06	15:30	1.20	.22	1.41	16.54	1.97	.4	7.55	100
M80 (shallow)	06-15-06	16:15	.26	.16	.42	13.23	1.58	.8	30.47	24
				Detection limit.....		0.906	0.005	0.062	1.508	0.093
Average total nitrogen					1.12					

Station No.	Date	Time	Molybdenum (mg/L)	Lead (mg/L)	Rhenium (mg/L)	Uranium (mg/L)	Vanadium (mg/L)
2006 minipiezometer array (depth - shallow, 1.5 m; deep, 3 m)							
M20 (shallow)	06-15-06	13:20	7	nd	0.004	1.6	2.4
M20 (deep)	06-15-06	14:00	2	0.15	nd	.1	2.3
M40 (shallow)	06-15-06	14:30	6	nd	.005	2.1	2.3
M40 (deep)	06-15-06	15:30	5	nd	.004	1.5	1.9
M80 (shallow)	06-15-06	16:15	7	nd	.005	4.0	3.1
	Detection limit.....		0.058	0.112	0.004	0.038	0.061

Table 2. Field measurements and nutrient and trace metal concentrations from minipiezometers and surface water at Sunset Beach and Merrimont, Lynch Cove area of Hood Canal, Washington, June 2006.—Continued.

[Samples analyzed at Woods Hole Oceanographic Institute. Locations of sample points shown in figures 7 and 11. **Abbreviations:** N, nitrogen; P, phosphorus; cm, centimeter; mg/L, milligram per liter; µS/cm, microsiemens per centimeter; –, parameter not measured; nd, not detected at specified detection limit]

Station No.	Date	Time	Temperature (°C)	Salinity (parts per thousand)	pH (standard units)	Dissolved oxygen (mg/L)	Ammonium (mg/L as N)	Silica (mg/L as SiO_2)	Phosphate (mg/L as P)	Nitrate plus nitrite (mg/L as N)
Merrimont (time series)										
Minipiezometer HC0606 (depth - 185 cm)										
1 GW	06-07-06	9:45	nd	14.60	–	–	0.001	9.43	0.01	0.277
2 GW	06-07-06	10:45	nd	17.60	–	–	.001	8.77	.02	.269
3 GW	06-07-06	11:45	nd	14.70	–	–	nd	9.07	.03	.287
4 GW	06-07-06	12:45	nd	14.50	–	–	nd	9.43	.03	.296
5 GW	06-07-06	13:45	nd	15.50	–	–	nd	8.71	.04	.332
6 GW	06-07-06	14:45	nd	16.80	–	–	nd	8.95	.02	.380
7 GW	06-07-06	15:45	nd	17.30	–	–	nd	8.23	.04	.405
8 GW	06-07-06	16:45	nd	18.10	–	–	nd	8.05	.04	.423
9 GW	06-07-06	17:45	nd	17.10	–	–	nd	8.71	.05	.368
10 GW	06-07-06	18:45	nd	17.10	–	–	nd	8.23	.05	.346
					Detection limit.....		0.001	0.003	0.002	0.001
Average total phosphorus									0.03	

Station No.	Date	Time	Dissolved inorganic nitrogen (mg/L as N)	Dissolved organic nitrogen (mg/L as N)	Total dissolved nitrogen (mg/L as N)	Barium (mg/L)	Cobalt (mg/L)	Chromium (mg/L)	Iron (mg/L)	Manganese (mg/L)
Minipiezometer HC0606 (depth - 185 cm)										
1 GW	06-07-06	9:45	0.28	0.09	0.37	9.46	0.20	0.4	6.76	17
2 GW	06-07-06	10:45	.27	.10	.37	7.38	.28	.4	6.25	29
3 GW	06-07-06	11:45	.29	.07	.36	3.47	.02	.4	4.66	6
4 GW	06-07-06	12:45	.30	.07	.37	6.27	.04	.4	3.88	3
5 GW	06-07-06	13:45	.33	.05	.38	7.92	.10	.4	6.11	11
6 GW	06-07-06	14:45	.38	.05	.43	7.29	.08	.4	nd	8
7 GW	06-07-06	15:45	.40	.06	.47	7.98	.05	.4	nd	4
8 GW	06-07-06	16:45	.42	.06	.48	9.59	.17	.4	nd	20
9 GW	06-07-06	17:45	.37	.09	.46	5.67	.15	.3	nd	16
10 GW	06-07-06	18:45	.35	.08	.43	9.21	.05	.3	nd	4
				Detection limit.....		0.906	0.005	0.062	1.508	0.093
Average total N					0.41					

Station No.	Date	Time	Molybdenum (mg/L)	Lead (mg/L)	Rhenium (mg/L)	Uranium (mg/L)	Vanadium (mg/L)
Minipiezometer HC0606 (depth - 185 cm)							
1 GW	06-07-06	9:45	5	nd	0.004	3.2	1.6
2 GW	06-07-06	10:45	6	0.13	nd	3.0	1.8
3 GW	06-07-06	11:45	2	nd	nd	.9	1.4
4 GW	06-07-06	12:45	5	nd	nd	1.7	1.8
5 GW	06-07-06	13:45	5	.20	.004	2.2	1.8
6 GW	06-07-06	14:45	5	nd	.004	2.1	1.8
7 GW	06-07-06	15:45	5	nd	.004	2.3	1.9
8 GW	06-07-06	16:45	6	nd	.006	3.2	1.8
9 GW	06-07-06	17:45	5	nd	nd	1.9	1.6
10 GW	06-07-06	18:45	5	nd	.006	2.7	1.7
	Detection limit.....		0.058	0.112	0.004	0.038	0.061

Table 2. Field measurements and nutrient and trace metal concentrations from minipiezometers and surface water at Sunset Beach and Merrimont, Lynch Cove area of Hood Canal, Washington, June 2006.—Continued.

[Samples analyzed at Woods Hole Oceanographic Institute. Locations of sample points shown in figures 7 and 11. **Abbreviations:** N, nitrogen; P, phosphorus; cm, centimeter; mg/L, milligram per liter; µS/cm, microsiemens per centimeter; –, parameter not measured; nd, not detected at specified detection limit]

Station No.	Date	Time	Temperature (°C)	Salinity (parts per thousand)	pH (standard units)	Dissolved oxygen (mg/L)	Ammonium (mg/L as N)	Silica (mg/L as SiO_2)	Phosphate (mg/L as P)	Nitrate plus nitrite (mg/L as N)
Merrimont (time series)										
Surface water at boat dock										
11 SW	06-07-06	9:45	15.40	25.30	8.40	11.80	0.006	3.77	0.03	0.019
12 SW	06-07-06	10:45	16.30	24.60	8.30	11.50	.018	3.68	.05	.017
13 SW	06-07-06	11:45	15.90	25.10	8.40	12.10	.010	9.55	.12	.010
14 SW	06-07-06	12:45	15.10	25.80	8.40	12.50	.022	4.89	.06	.010
15 SW	06-07-06	13:45	13.90	26.70	8.40	12.50	.019	3.74	.02	.003
16 SW	06-07-06	14:45	14.90	25.90	8.40	12.30	.009	3.38	.03	.001
17 SW	06-07-06	15:45	14.70	26.00	8.30	12.40	.004	3.17	.03	.001
18 SW	06-07-06	16:45	13.90	26.60	8.30	12.30	.004	3.23	.03	.003
19 SW	06-07-06	17:45	13.70	26.70	8.30	11.90	.001	3.33	.03	.017
20 SW	06-07-06	18:45	14.00	26.50	8.30	12.10	.008	3.77	.03	.031
					Detection limit.....		0.001	0.003	0.002	0.001
Average total P									0.04	

Station No.	Date	Time	Dissolved inorganic nitrogen (mg/L as N)	Dissolved organic nitrogen (mg/L as N)	Total dissolved nitrogen (mg/L as N)	Barium (mg/L)	Cobalt (mg/L)	Chromium (mg/L)	Iron (mg/L)	Manganese (mg/L)
Surface water at boat dock										
11 SW	06-07-06	9:45	0.03	0.23	0.25	4.76	0.06	0.2	3.36	14
12 SW	06-07-06	10:45	.03	.11	.14	7.74	.06	.2	3.06	16
13 SW	06-07-06	11:45	.02	.12	.14	12.15	.07	.4	4.51	6
14 SW	06-07-06	12:45	.03	.18	.21	8.87	.08	.3	6.20	16
15 SW	06-07-06	13:45	.02	.14	.16	7.45	.05	.3	5.74	13
16 SW	06-07-06	14:45	.01	.16	.17	5.51	.05	.2	6.08	11
17 SW	06-07-06	15:45	.00	.15	.15	5.28	.05	.2	2.94	10
18 SW	06-07-06	16:45	.01	.11	.12	4.40	.04	.2	3.04	10
19 SW	06-07-06	17:45	.02	.15	.16	6.03	.05	.4	3.60	10
20 SW	06-07-06	18:45	.04	.11	.15	5.94	.05	.3	3.63	11
				Detection limit.....		0.906	0.005	0.062	1.508	0.093
Average total N					0.17					

Station No.	Date	Time	Molybdenum (mg/L)	Lead (mg/L)	Rhenium (mg/L)	Uranium (mg/L)	Vanadium (mg/L)
Surface water at boat dock							
11 SW	06-07-06	9:45	7	nd	0.005	2.2	1.8
12 SW	06-07-06	10:45	7	nd	.007	3.4	2.1
13 SW	06-07-06	11:45	5	nd	.007	3.2	1.7
14 SW	06-07-06	12:45	8	0.12	.007	2.9	2.4
15 SW	06-07-06	13:45	8	nd	.007	3.0	2.1
16 SW	06-07-06	14:45	8	.18	.006	2.5	1.9
17 SW	06-07-06	15:45	8	nd	.006	2.6	2.0
18 SW	06-07-06	16:45	8	nd	.006	2.5	1.9
19 SW	06-07-06	17:45	8	nd	.007	2.9	1.9
20 SW	06-07-06	18:45	8	nd	.006	2.5	1.9
	Detection limit.....		0.058	0.112	0.004	0.038	0.061

Table 2. Field measurements and nutrient and trace metal concentrations from minipiezometers and surface water at Sunset Beach and Merrimont, Lynch Cove area of Hood Canal, Washington, June 2006.—Continued.

[Samples analyzed at Woods Hole Oceanographic Institute. Locations of sample points shown in figures 7 and 11. **Abbreviations:** N, nitrogen; P, phosphorus; cm, centimeter; mg/L, milligram per liter; µS/cm, microsiemens per centimeter; –, parameter not measured; nd, not detected at specified detection limit]

Station No.	Date	Time	Tempe-rature (°C)	Salinity (parts per thousand)	pH (standard units)	Dissolved oxygen (mg/L)	Ammonium (mg/L as N)	Silica (mg/L as SiO_2)	Phosphate (mg/L as P)	Nitrate plus nitrite (mg/L as N)
Merrimont (time series)										
Seepage water – low tide line										
Beach-face seep	06-09-06	10:00	19.85	4.60	7.00	7.60	0.001	10.22	0.13	0.09
					Detection limit.....		0.001	0.003	0.002	0.001

Station No.	Date	Time	Dissolved inorganic nitrogen (mg/L as N)	Dissolved organic nitrogen (mg/L as N)	Total dissolved nitrogen (mg/L as N)	Barium (mg/L)	Cobalt (mg/L)	Chromium (mg/L)	Iron (mg/L)	Manganese (mg/L)
Seepage water – low tide line										
Beach-face seep	06-09-06	10:00	0.10	0.11	0.20	3.67	0.04	2.1	3.11	4
				Detection limit.....		0.906	0.005	0.062	1.508	0.093

Station No.	Date	Time	Molybdenum (mg/L)	Lead (mg/L)	Rhenium (mg/L)	Uranium (mg/L)	Vanadium (mg/L)
Seepage water – low tide line							
Beach-face seep	06-09-06	10:00	2	nd	nd	0.4	5.8
	Detection limit.....		0.058	0.112	0.004	0.038	0.061

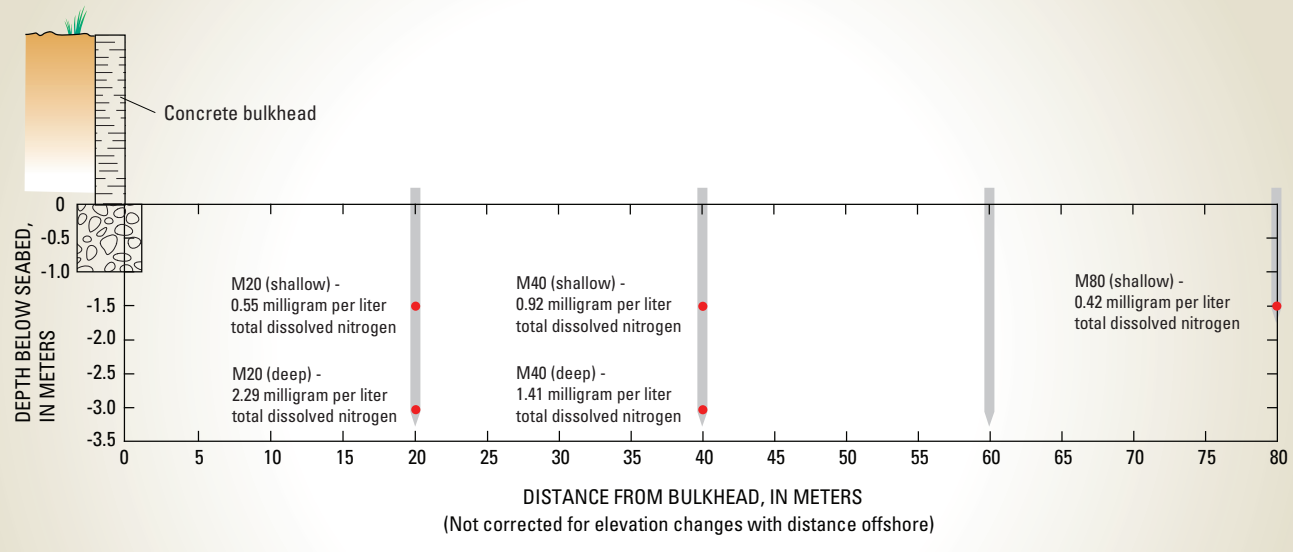

Figure 4. Total-dissolved-nitrogen concentrations at the Sunset Beach minipiezometer array, Lynch Cove area of Hood Canal, Washington, June 15, 2006. Plot represents a cross-sectional view perpendicular to the shoreline (concrete bulkhead).

Ground-Water Discharge Estimates

Estimating the amount of ground-water discharge into the Lynch Cove area of Hood Canal is complicated by spatial and temporal variability of SGD and by the fact that total SGD consists of freshwater and seawater components. To address these challenges, multiple approaches were used to quantify the components of SGD at various scales. Traditional methods for directly measuring ground-water discharge at a local scale were used for identifying SGD processes at four intensive study sites. Indirect methods using geochemical tracers were used to help place point measurements and data from the intensive study sites into a more regional context, and to understand the role of recirculated seawater. Although the independent estimates of SGD derived from each method have inherent assumptions and uncertainties, the fact that independent methods of measurement yielded overlapping ranges of SGD rates that are similar to the previous mass-balance estimate provides some confidence that the assumptions and measuring techniques were valid.

Intensive Study Sites

To evaluate small-scale spatial variability, intensive study sites were established consisting of arrays of piezometers and seepage meters. Each array was designed to provide information about variability both parallel and perpendicular to the shoreline in an area of about 30×30 m. Larger scale variability was evaluated by comparing four intensive study sites, each of which represents a distinct geomorphic setting around the perimeter of Lynch Cove (fig. 2). Twanoh State Park and the Merrimont sites, both on the south shore, represent steep, densely populated areas along the shoreline with large hydraulic gradients landward from the shore. Sunset Beach near the terminus of Lynch Cove represents a low-angle, densely populated area with a lower hydraulic gradient landward from the shore. The Landon Road site is typical of the north shore of Lynch Cove and represents a moderately steep, sparsely populated area with a moderate hydraulic gradient landward from the shore. These sites were selected for detailed study on the basis of their distinct geomorphic settings and accessibility. During an initial reconnaissance of the study area, visible seeps were mapped and combinations of minipiezometers and (or) seepage meters were installed at multiple sites around the perimeter of Lynch Cove (fig. 2). Widespread ground-water discharge was confirmed around the perimeter of Lynch Cove based on observed seeps along road cuts, measured upward vertical hydraulic gradients in minipiezometers, and measured total seepage (fresh plus saline) rates that ranged from of 0.5 to 30 cm/d in Lee-type seepage meters.

Twanoh State Park

A T-shaped array of minipiezometers and Lee-type seepage meters was installed at Twanoh State Park (fig. 5 and sidebar F) so that measurements could be made both perpendicular and parallel to the shoreline. An ESM was installed near the center of the array. The water levels recorded in the minipiezometers were close to or slightly higher than the recorded surface-water stage indicating upward vertical hydraulic gradients during low tides (fig. 6). Although continuous minipiezometer stage data during high tides were lost due to the range limitations of the pressure transducers, manometer measurements confirmed small upward gradients even during high tides at this site. Barometric pressure recorded during the same time period was used to correct the transducer data. The ESM data show the temporal variation in seepage relative to tidal stage over several tidal cycles (fig. 6). Short-term fluctuations in the continuous data may be due to wind, currents, or wave action.

Sidebar F. Intertidal area of Lynch Cove at Twanoh State Park has small springs and a large upward vertical hydraulic gradient that indicates ground-water discharge. The beach here is covered with oysterbeds, which are common throughout the intertidal zone of Hood Canal. Photograph taken by Don Rosenberry, U.S. Geological Survey, June 15, 2005.

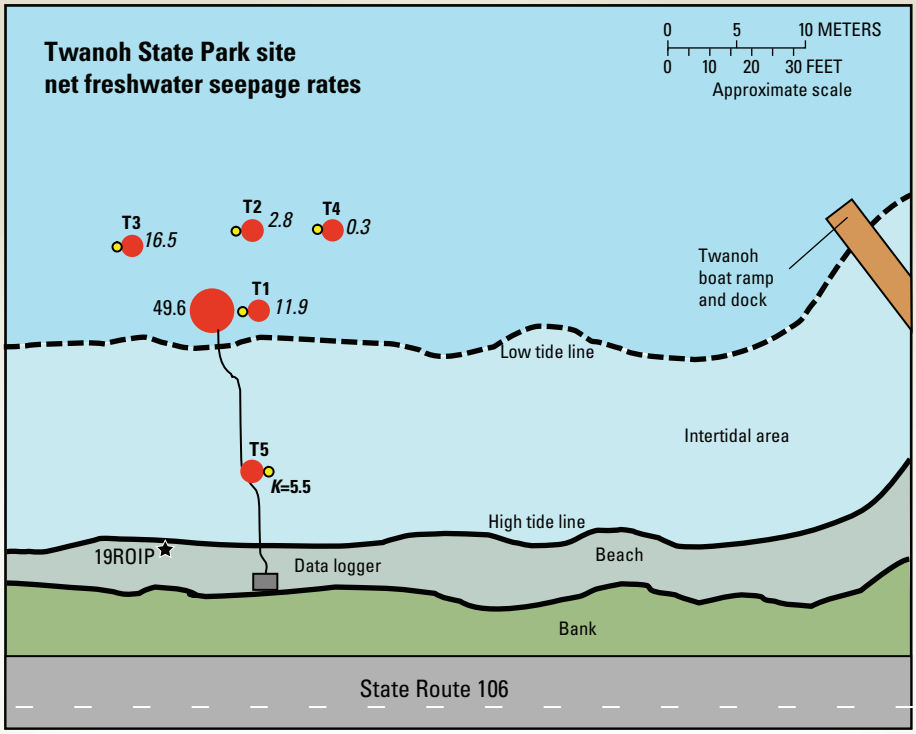

EXPLANATION

Net freshwater seepage rates—Calculated by adding average seepage rates during incoming tides (generally positive) and average seepage rates during outgoing tides (positive but smaller in magnitude). Location of intensive study site shown in figure 2

49.6 **Electromagnetic seepage meter (ESM)**—Number is average seepage rate, in centimeters per day, measured by ESM

11.9 T2 **Lee-type seepage meter and number**—Number is seepage meter number (see table 3). Italicized number is net freshwater seepage rate, in centimeters per day (see table 3), and represents the freshwater component of submarine ground-water discharge

K=5.5 **Minipiezometer**—Bold number is hydraulic conductivity (***K***), in meters per day, measured using three drawdown and three slug tests in the minipiezometer adjacent to seepage meter T5

19ROIP **Minipiezometer used for water-sample collection**—A single grab sample was collected from minipiezometer 19R01P. Data are shown in table 1

Figure 5. Minipiezometer and seepage-meter array at Twanoh State Park intensive study site, Lynch Cove area of Hood Canal, Washington.

At the Twanoh State Park site, all Lee-type seepage meters except T4, consistently measured continuous ground-water discharge (positive values). Seepage meter T4 measured occasional ground-water recharge (negative values) and very low seepage rates overall. In general, most seepage meters measured larger seepage rates during outgoing tides. For each Lee-type seepage meter, the net freshwater seepage rate was determined by adding the average rates of seepage during outgoing tides to the average rates of seepage during incoming tides. At the Twanoh State Park site, the average net freshwater discharge rate was 8 cm/d for the entire array of Lee-type seepage meters (table 3). The net seepage rates measured by individual Lee-type seepage meters (0.3 to 16.5 cm/d) were lower than the average seepage rate measured by the ESM (49.6 cm/d) (fig. 5). This spatial variability at the scale of the array could be due to heterogeneities in seabed materials.

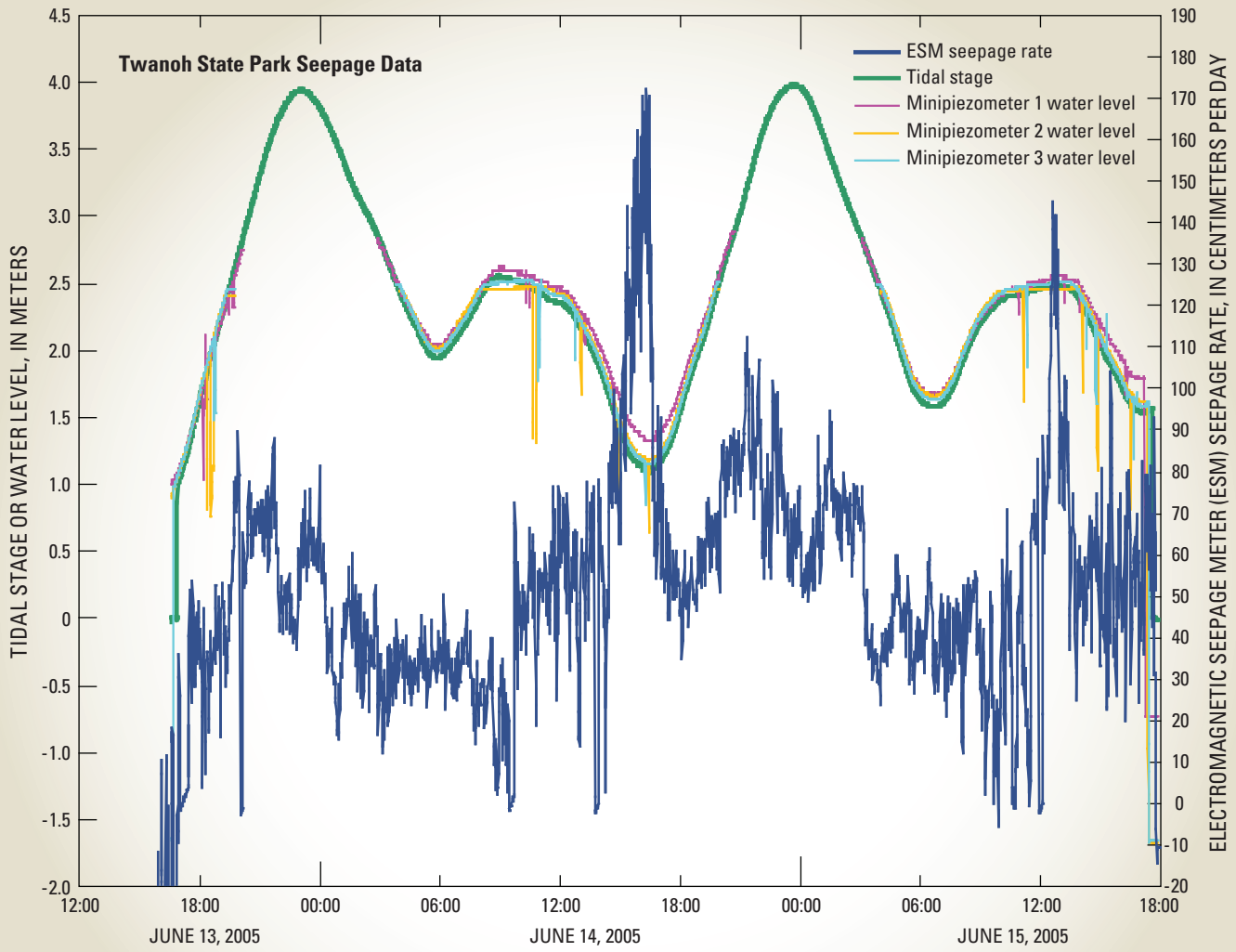

Figure 6. Continuous seepage data from the electromagnetic seepage meter (ESM) at the intensive study site at Twanoh State Park relative to surface-water stage, Lynch Cove area of Hood Canal, Washington. Measured water levels in minipiezometers closely track the surface-water stage except during high tides when ranges of transducers used to measure water levels were exceeded.

Variations in hydraulic conductivity may restrict ground-water discharge in some areas while creating preferential flowpaths in other areas. Detailed measurements of hydraulic conductivity would be needed to determine precise subsurface variations. In the minipiezometer adjacent to seepage meter T5, a series of three drawdown and three slug tests were conducted where water was either withdrawn from the pipe or poured into the pipe and the water level was monitored while it re-equilibrated. These tests yielded an average hydraulic conductivity of 5.5 m/d.

Table 3. Summary of Lee-type seepage-meter measurements at intensive study sites, Lynch Cove area of Hood Canal, Washington.

[Study site sample points shown in figures 5, 7, 11, and 14. **Incoming tide:** Average seepage rates for all measurements made during incoming tides at a given seepage meter. **Outgoing tide:** Average seepage rates for all measurements made during outgoing tides at a given seepage meter. Positive values indicate upward flow or discharge, negative values indicate downward flow or recharge. **Net freshwater discharge or saline water recharge:** Calculated as the sum of average seepage rates during incoming tides and average seepage rates during outgoing tides. **Average net discharge rate:** Average net discharge rate for all measurements made at the intensive study site. –, no data]

Seepage meter No.	Average seepage rate, in centimeters per day		
	Incoming tide	Outgoing tide	Net freshwater discharge or saline water recharge
Twanoh State Park, 2005			
T1	4.4	7.4	11.9
T2	1.2	1.6	2.8
T3	3.6	12.9	16.5
T4	.1	.2	.3
T5	–	6.1	
Average net discharge rate.....			8
Merrimont, 2006			
M20	-37.8	72.5	34.7
M25	-31.6	50.6	19.0
Average net discharge rate.....			27
Sunset Beach, 2005			
SB1	[1]9.1	[1]11.4	[1]20.6
SB2	-1.4	-1.4	-2.8
SB3	-.1	.6	.5
SB4	-1.2	-.9	-2.1
SB5	-.3	-.7	-1.0
SB6	1.9	-.1	1.8
Average net recharge rate.....			-0.72
Sunset Beach, 2006			
M20	-0.9	7.5	6.7
M40	-10.2	17.7	7.5
M60	-6.9	22.8	15.9
M80	1.7	23.2	24.9
Average net discharge rate.....			14
Landon Road, 2005			
LR1	3.8	20.4	24.2
LR2	3.3	3.7	7.0
LR3	1.9	11.7	13.6
LR4	1.6	3.0	4.5
LR5	6.6	9.2	15.8
LR6	1.5	–	–
Average net discharge rate.....			13

[1]Measurement affected by ghost shrimp and data not used.

Merrimont

The Merrimont site, located on the south shore of Lynch Cove, has a moderately steep slope landward of the shore similar to Twanoh State Park (sidebar G). A large hydraulic gradient is suggested by numerous springs that emanate from the hillside and year-round flow in the small drainage that forms Merrimont Creek. The intertidal area at Merrimont was the focus of a detailed study in 2006 in which a number of experiments were conducted to specifically examine temporal variability in ground-water discharge. An array of minipiezometers and seepage meters was deployed at the site as depicted in figure 7. ESMs were deployed at three different positions to compare time-series seepage rates as a function of position (fig. 8). ESM A was positioned just below the low-tide line near a boat dock. ESM B was initially positioned near ESM A for comparison purposes, but later moved to position ESM C near the middle of the intertidal area (fig. 7). It is unclear if the difference in average seepage rates between ESM A (-12.7 cm/d) and ESM B (80.8 cm/d) was due to spatial variability or differences in ESM operation. A comparison of seepage rates between ESM A and ESM C

Sidebar G. The intertidal zone at the Merrimont intensive study site has a moderately steep intertidal area. Seepage measurements and electrical-resistivity profiles indicate large amounts of ground-water discharge within the intertidal area, especially during outgoing tides. Photograph taken by F. William Simonds, U.S. Geological Survey, June 7, 2006.

(38.8 cm/d) show substantial differences in seepage within the intertidal area (fig. 8). ESM C was not submerged during low tides, but clearly shows downward flow or decreased upward flow during high tides. Increased SGD during intermediate low tides was more pronounced higher on the intertidal area (ESM C) than near the low tide line (ESM A). Two Lee-type seepage meters (M20 and M25) placed in the intertidal area (fig. 7) indicated ground-water recharge of saline water during incoming tides and ground-water discharge of saline plus freshwater during outgoing tides. When the average seepage rates are added, the resulting net freshwater discharge rates of 34.7 cm/d (M20) and 19.0 cm/d (M25) suggest that there is variability in seepage throughout the intertidal zone with an average net discharge rate of 27 cm/d for both Lee-type seepage meters (table 3).

At the Merrimont site, the stationary (land based) electrical-resistivity method was used to acquire a series of 12 subsurface profiles perpendicular to the shoreline during an outgoing tide (Swarzenski and others, 2007b). The images clearly show a plume of fresh water with higher resistivity water that extends seaward as the tidal stage decreases (fig. 9). During the later stages of the outgoing tide (fig. 9, profiles F, G, and H), an upper saline plume is evident and a "tongue" of inferred fresh ground water connects to the seabed just landward of the receding shoreline, similar to tide-induced recirculation models published by Robinson and others (2006). This "tongue" of freshwater discharge is consistent with observations of bubbling springs and seeps that migrate down the beach face as the tide goes out. One of these springs, the beach-face seep shown in figure 7, was sampled near the low tide line and had a salinity of 4.6 ppt (table 2) indicating that freshwater does reach land surface. The profiles show a plume of fresh ground water that extends to depths of at least 20 m below the seabed, but does not extend seaward beyond the low-tide line before mixing with saline water (fig. 9, profile J). The plume of fresh ground water is most pronounced at low tide. As the tide begins to rise again, seawater infiltrates into the sediments and mixes with fresh ground water, thereby decreasing the electrical resistivity of the mixed fluid causing the plume to appear to recede (fig. 9, profiles J, K, and L).

Continuous radon activity in water was monitored at the surface water sampling site located 15 cm above the seabed just below the low tide line at Merrimont (fig. 7). The time series of radon activity shows a strong inverse correlation with the tidal stage (fig. 10*A*), where the radon activity increases by up to a factor of eight during low tides, and decreases during high tides. To calculate total SGD (fresh plus saline), the methods of Lambert and Burnett (2003) and Burnett and Dulaiova (2003) were applied by converting radon inventories to radon fluxes after accounting for losses of radon due to atmospheric evasion and mixing. The calculated net radon flux ranged from -24,700 to 25,400 decays per minute (dpm)/m^2hr, whereas a mixing-loss corrected total flux ranged up to 29,500 dpm/m^2hr, depending on the tide (Swarzenski and others, 2007b). To correct for supported radon in the water column, a mean ^{226}Ra activity of 5 dpm/100L measured at the surface water sampling site located at the Merrimont boat dock was subtracted from the ^{222}Rn values (table 4). For the 5-day time series, water column ^{222}Rn activity ranged from 1,700 to 25,000 dpm/m^3, with a mean of 5,273 dpm/m^3 (fig. 10*A*). Ground-water discharge based on radon advection rates was estimated by dividing the calculated radon fluxes by the representative radon activities in ground water. A mean ground-water radon activity (142 dpm/L) was derived from three piezometer samples (^{222}Rn = 158±11, 129±25, and 140±35 dpm/L), which were collected as part of the time series sampling at a depth of 185 cm in piezometer HC0606 near the high-tide line and during an incoming tide (table 4). The radon activity of discrete grab samples were measured using a RAD H2O™ accessory attached to a RAD 7™ monitor. Radon activity measured hourly in ground water at minipiezometer HC0606 changed little under different tidal regimes, and was of the same order of magnitude as radon activity measured in the nearby Merrimont spring sample (274±21 dpm/L; table 4). The instantaneous radon advection rates calculated using this method (fig. 10*B*) yield an average SGD (fresh plus saline) of 85.8±84.5 cm/d. The large error range reflects the dynamic mixing imposed by the large tidal range (Burnett and others, 2007).

ESM data for the same 5-day period show that seepage rates peak at low tide, and illustrate the tidal modulation of ground-water discharge and recharge (fig. 10*C*). As the tidal range increased during the time-series experiment (an increase of almost 2 m), the measured seepage rates also increased. The ESM data collected during the last tidal cycle show clear discharge events (seepage rates greater than 80 cm/d) coincident with low tidal stages, and significant recharge of saline water into the sediments during high tidal stages (seepage rates of less than -40 cm/d).

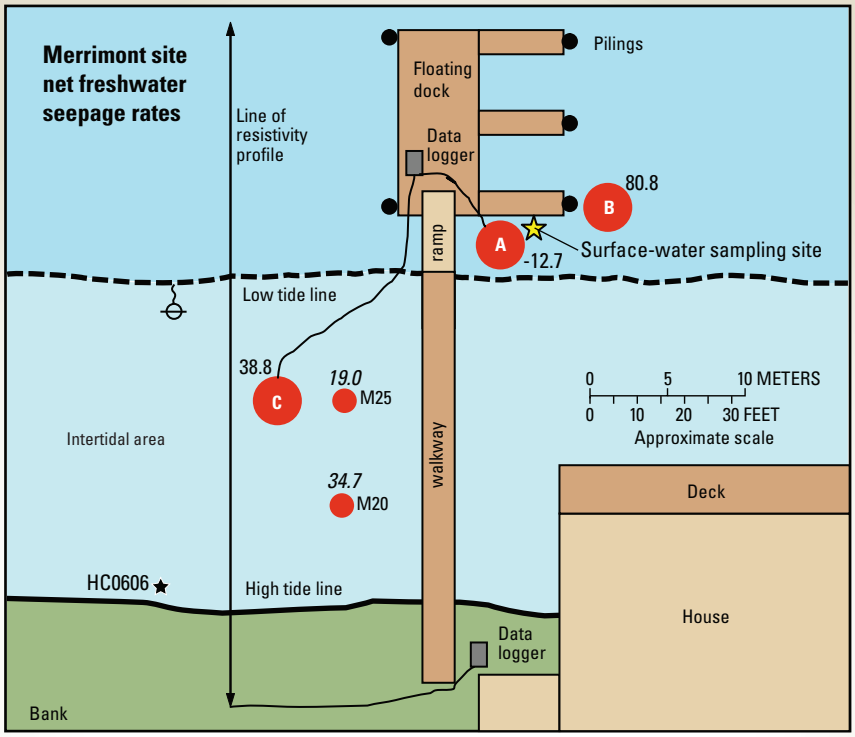

EXPLANATION

Net freshwater seepage rates—Calculated by adding average seepage rates during incoming tides (generally positive) and average seepage rates during outgoing tides (generally negative). Location of intensive study site shown in figure 2

80.8 A **Electromagnetic seepage meter (ESM)**—Number is average seepage rate, in centimeters per day, measured by ESM

19.0 M25 **Lee-type seepage meter and number**—Number is seepage meter number (see table 3). Italicized number is net freshwater seepage rate, in centimeters per day (see table 3), and represents the freshwater component of submarine ground-water discharge

HC0606 **Minipiezometer used for time-series water-quality samples**—Time-series water quality samples were collected from minipiezometer HC0606 near the high-tide line. Data are shown in table 2

Surface-water sampling site used for time-series samples and continuous radon measurements—Time-series samples were collected from surface water adjacent to the dock. Data are shown in table 2

Spring—Beach-face seep

Figure 7. Minipiezometer and seepage-meter array at the Merrimont intensive study site, Lynch Cove area of Hood Canal, Washington.

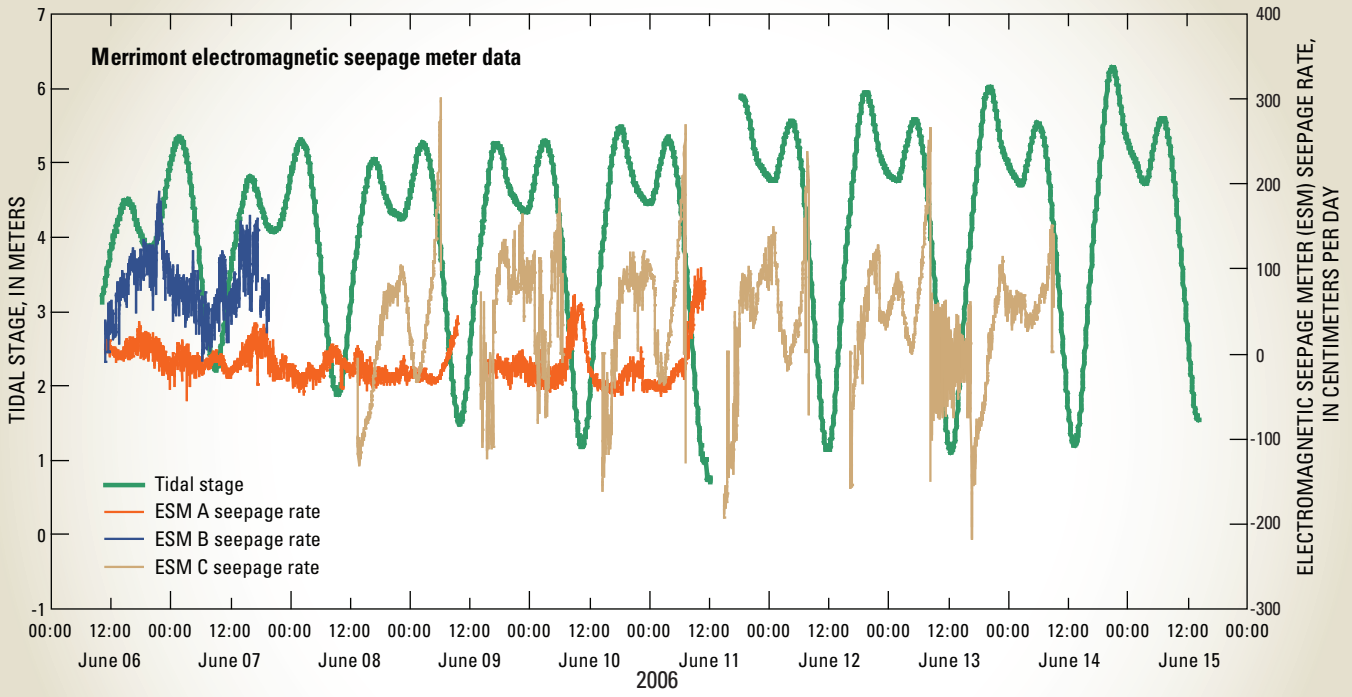

Figure 8. Continuous seepage data from two electromagnetic seepage meters (ESM) deployed in three positions at the Merrimont intensive study site, Lynch Cove area of Hood Canal, Washington. Gaps in ESM C data occurred during low tides when the instrument was not submerged.

Continuous specific conductance data (fig. 10*D*), collected using a Solinst™ Diver mounted on top of the seepage-meter dome, showed a sharp decrease during the last day of measurements. The conductance of bottom water decreased from a mean value of 40.7 mS/cm (salinity=26.0 ppt), to a value of less than 34 mS/cm (salinity=19.7 ppt) at low tide on June 10, 2006, a decrease that was not observed earlier in the time series. The conductance (salinity) of the water at the surface water sampling site at Merrimont likely reflects an integrated signal that responds to both SGD and the periodic transport of fresher water masses possibly derived from river discharge. The changes in salinity inside the ESM in some cases may be controlled by the salinity outside of the ESM and not by fresh ground-water discharge (fig. 10*D*). However, as the tidal range increased during the 5-day period, there is evidence of extended periods of decreasing salinities inside the ESM, even though recharge of higher salinity water should intuitively increase salinity inside the ESM. Nonetheless, the pronounced decline in conductance (salinity) precisely at low tide at the same time that radon activity and seepage rates measured by the ESM peak, confirms tidal modulation of ground-water/surface-water exchange at this site.

Time-series water temperature data (fig. 10*E*) also show delayed reaction inside the ESM to temperature variations outside the dome. Water temperature and conductivity both vary depending on the position of the probes relative to local stratification, currents and other local conditions.

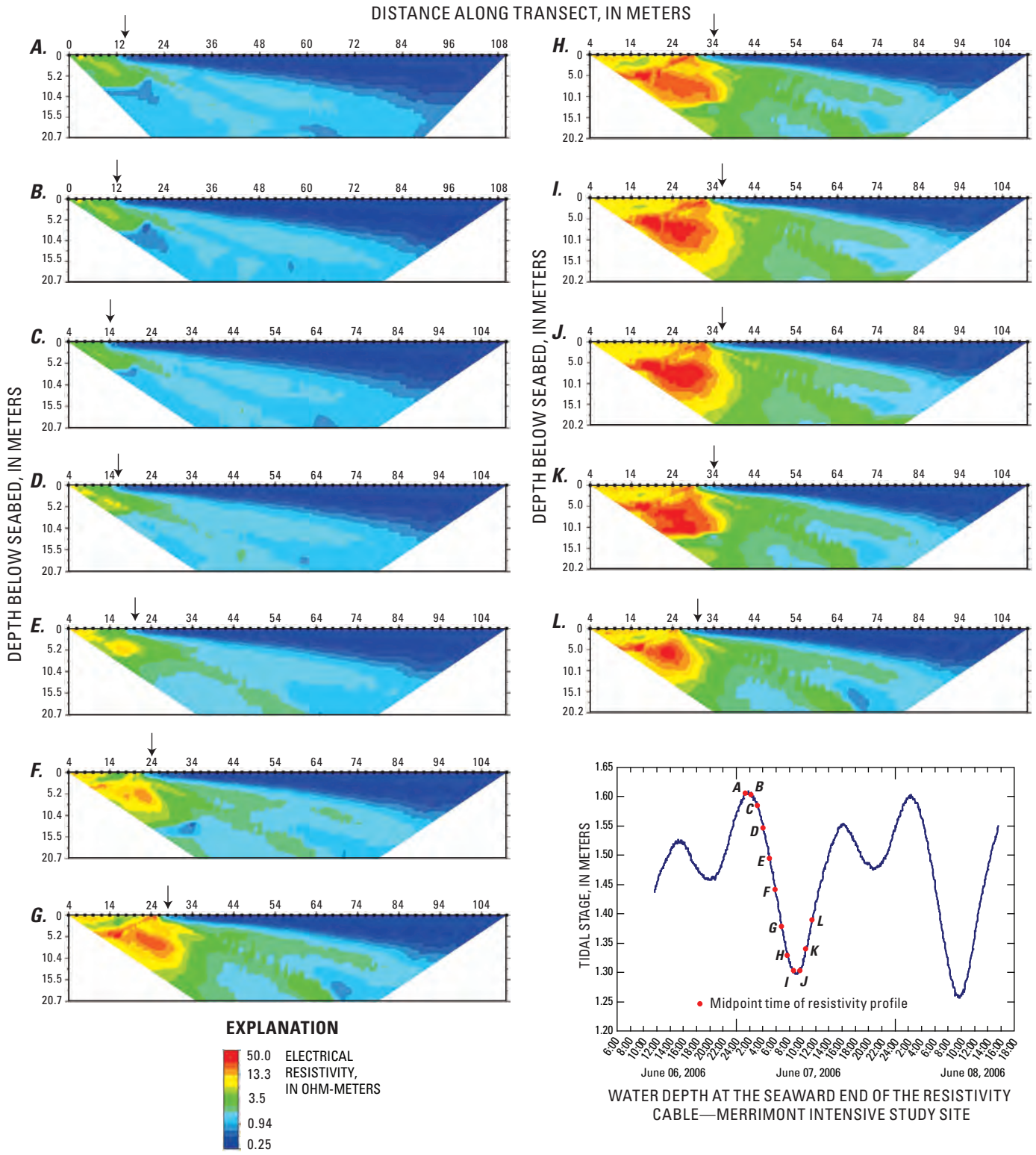

Figure 9. Electrical-resistivity profiles perpendicular to the shoreline at the Merrimont intensive study site, Lynch Cove area of Hood Canal, Washington. Each profile represents a snapshot of electrical resistivity along a cross-section of the intertidal area. Colors represent resistance in ohm-meters. Red colors indicate more electrically resistant fresh water, and blue colors indicate more electrically conductive saline water. Approximate position of the waterline on the beach is indicated by the arrow above the profile. The plot shows the midpoint time of the data acquisition interval relative to the tidal cycle.

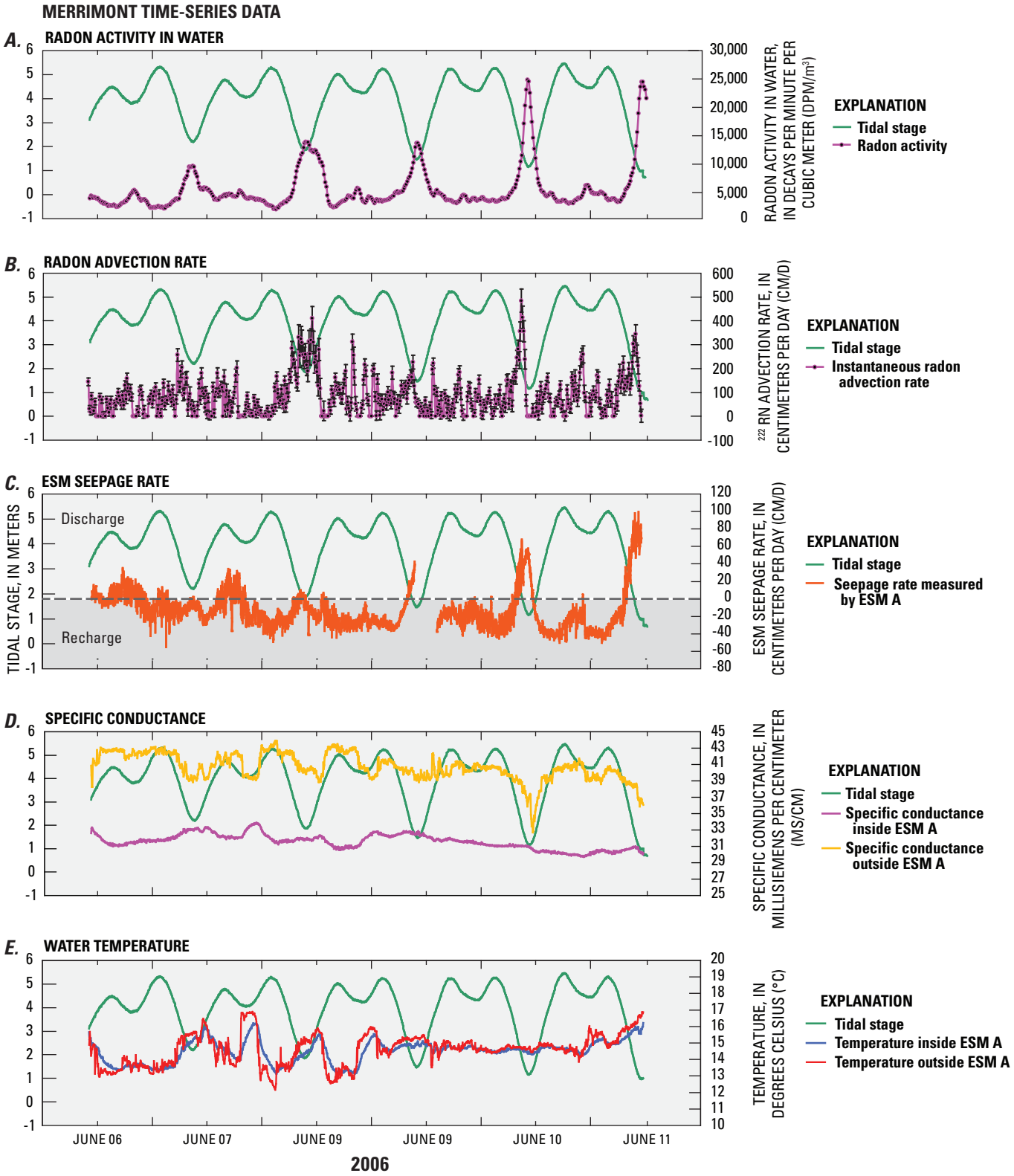

Figure 10. Relationship between tidal stage at the Merrimont intensive study site, Lynch Cove area of Hood Canal, Washington and (*A*) radon activity, (*B*) instantaneous advection rates, (*C*) continuous seepage rates measured by electromagnetic seepage meter ESM A, (*D*) conductivity of bottom water inside and outside ESM A, and (*E*) temperature of bottom water inside and outside ESM A.

Table 4. Radium, thorium, and radon activities in ground-water and surface-water samples at the Merrimont site, Lynch Cove area of Hood Canal, Washington, June 7 to October 2006.

[Locations of sampling sites are shown in figure 2. Expected error for radium 223 and 224 is about 10 percent. ppt, parts per thousand; dpm/100 L, decays per minute per 100 liters; dpm/L, decays per minute per liter; –, parameter not measured]

Sample name	Salinity (ppt)	Isotope activity					
		dpm/100 L					dpm/L
		Radium-226	Radium 228	Radium 223	Radium 224	Thorium 228	Radon 222
Merrimont spring sample							
35H01S	–	–	–	–	–	–	274 ± 21
Merrimont, ground-water samples from minipiezometer HC0606							
1 GW [1,2,3]	14.6	8.1 ± 1.2	25.5 ± 2.9	3	44.3	2.7	158 ± 11
5 GW	17.3	8.8 ± 1.2	34 ± 3	2.6	87.9	2.4	129 ± 25
10 GW	17.1	6.6 ± 1.1	5.1 ± 1.9	2.2	97.2	0	140 ± 35
Merrimont, surface-water samples from boat dock							
11 SW [2,3]	25.1	5 ± 0.4	1.7 ± 0.3	0.1	1.1	0.2	–
15 SW	25.9	4.6 ± 0.4	3 ± 0.5	.1	1	.4	–
20 SW	26.7	5.4 ± 0.4	1.1 ± 0.4	.1	1.5	.5	–
Lynch Cove, surface-water samples from estuary							
HC1[3]	24.4	2.9 ± 0.3	1.9 ± 0.5	0	0.8	0.2	–
HC2	23.5	3.2 ± 0.3	2.1 ± 0.4	0	1	.2	–
HC3	24.8	3.8 ± 0.3	1.9 ± 0.5	.2	.6	.3	–
HC4	24.3	3.8 ± 0.3	1.6 ± 0.5	.2	1	.4	–
HC5	21.5	5.9 ± 0.3	4.7 ± 0.5	.3	10.2	.4	–
Skokomish River samples							
SR1[3]	0.01	0.4 ± 0.1	0	0.1	0.2	0.2	–

[1]Sample collected using a drive-point piezometer from an equilibrated horizon 185 centimeters below the seabed near low-tide tide line at the Merrimont site.

[2]Numbering sequence and associated attributes in "Piezo" and "Surface" samples match those presented in table 2.

[3]All radium samples were collected by filtering water directly through preweighed manganese oxide cartridges with a peristaltic pump. Surface water, Lynch Cove estuary, and the Skokomish River samples were pumped from 0.5-meter water column depth.

Sunset Beach Site

The Sunset Beach site is located on the south shore of Lynch Cove close to its landward terminus (fig. 2). This site is characterized by low relief and a relatively wide intertidal zone (about 100 m). Nearshore sediments generally are finer grained than at the other intensive study sites; the area may be underlain by reworked fill material or possibly landslide deposits or other permeable geologic materials. A 2.5-m-tall cement seawall separates waterfront homes from the gently sloping beach. Minipiezometer and seepage meter arrays were installed and monitored at Sunset Beach in 2005 (locations 1 through 7, fig. 11) and 2006 (locations M20 through M80, fig. 11). Minipiezometers installed with water level recorders in 2005 did not provide useful information due to slow equilibration rates. Slug tests conducted in minipiezometers SB1, SB2, SB3, and SB6 indicated very low hydraulic conductivities at depths of 185 cm below the seabed while SB7 had a very high conductivity near the seawall (fig. 11). A slug test conducted at 0.6-m depth in minipiezometer SB3S indicated a higher conductivity zone near the surface. Average seepage rates from seepage meters installed in 2005 were either very small (SB3 and SB6) or generally negative (SB2, SB4, and SB5), indicating low rates of ground-water discharge or saline water recharge (table 3). The average net seepage rate for the array was -0.72 cm/d suggesting that recharge of saline water is slightly more dominant in this part of the beach. Data from seepage meter SB1 was not used because it was later determined to have been placed over a colony of ghost shrimp, thus the upward flow measured in this seepage meter was biologically induced. Cable and others (2006) noted that "bioirrigation" at a site in Florida resulted in upward seepage rates of about 5 cm/d. This illustrates one of the problems that can affect seepage-meter measurements.

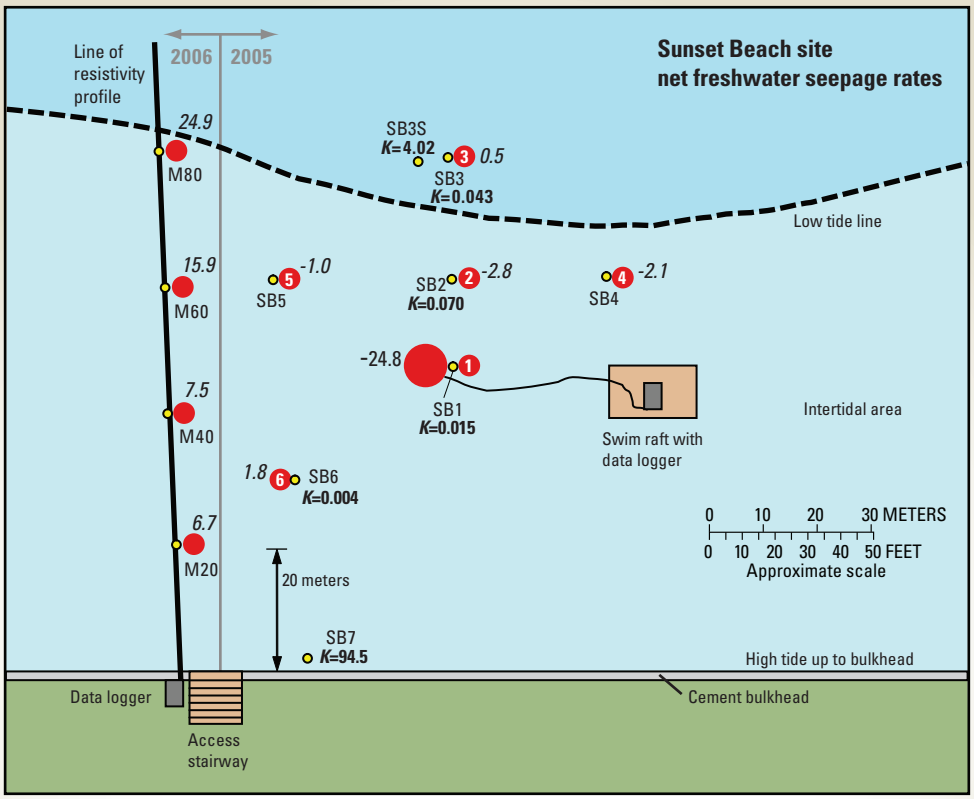

EXPLANATION

Net freshwater seepage rates—Calculated by adding average seepage rates during incoming tides (generally negative) and average seepage rates during outgoing tides (generally negative). Location of intensive study site shown on figure 2

-24.8 **Electromagnetic seepage meter (ESM)**—Number is average seepage rate, in centimeters per day, measured by ESM

-2.8 2 **Lee-type seepage meter and number**—Number is seepage meter number (see table 3). Italicized number is net freshwater seepage rate, in centimeters per day (see table 3), and represents the freshwater component of submarine ground-water discharge

K=0.015 **Minipiezometer**—Bold number is hydraulic conductivity (*K*), in meters per day, measured using slug tests in minipiezometers

Figure 11. Minipiezometer, electromagnetic-seepage-meter, and resistivity arrays at the Sunset Beach intensive study site, Lynch Cove area of Hood Canal, Washington.

Data from the ESM near the center of the 2005 array indicate nearly continuous downward flow (recharge) except during short duration events that do not seem to correlate well with the tidal cycle (fig. 12). Although low rates of ground-water discharge were observed in seepage meters SB3 and SB6, slightly higher rates of saline water recharge were observed in seepage meters SB2, SB4, and SB5, suggesting that this part of the beach undergoes seawater infiltration during all but the lowest tides (table 3). Data from the 2005 array was inconclusive and raised additional questions about the processes occurring at the Sunset Beach site. For this reason, the site was reoccupied in 2006 for a series of additional experiments.

In 2006, a line of minipiezometers and seepage meters were installed to the west of the 2005 array at distances of 20, 40, 60, and 80 m perpendicular to the cement bulkhead (fig. 11). Seepage measurements made along this transect during outgoing tides were positive, whereas those made during incoming tides were negative, except at station M80 (table 3). The net freshwater discharge rates along the 2006 transect increased from 6.7 to 24.9 cm/d with distance from the shoreline and indicated an average net discharge rate of 14 cm/d for the array. When the data from the 2006 array are combined with the 2005 data, the resulting average net discharge rate is 7 cm/d; a number that reflects the large spatial variability at Sunset Beach and perhaps at other

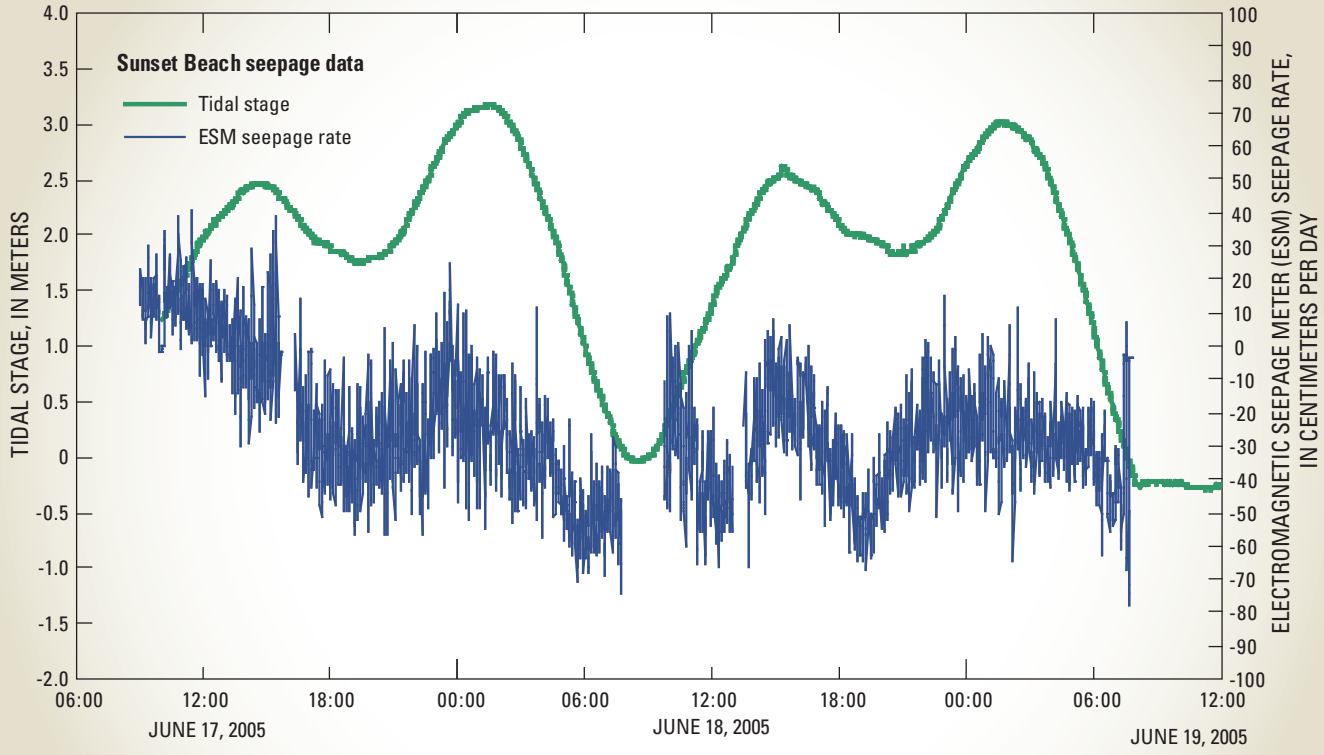

Figure 12. Continuous seepage data from the electromagnetic seepage meter at the Sunset Beach array relative to surface-water stage, Lynch Cove area of Hood Canal, Washington.

intertidal areas adjacent to low-relief uplands. For such intertidal areas, the process of seawater infiltration during incoming tides and ground-water discharge during outgoing tides is complicated by the particular geology of the site. Subtle topographic variations (ridges and swales), as well as buried confining layers like mudflat or marsh deposits, could provide preferential flowpaths or favor lateral ground-water movement over vertical movement (Bratton, 2007), thus directing SGD farther offshore.

An electrical-resistivity cable placed along the same line as the seepage meters was used to acquire 13 subsurface profiles during an incoming tide (fig. 13). The initial images clearly show a large resistive mass at a depth of 6 m that underlies a less resistive mass near the surface (fig. 13, profile A). This inferred mass of fresh ground water extended deeper than 20 m, the maximum depth electrical-resistivity method could image, and extended beyond the length of the cable (112 m). As the incoming tide spread across the low-angle beach the profiles show a rapid infiltration of saline water (fig. 13, profiles B, C, and D). At high tide, the surface water rose to as high as a meter above the base of the concrete bulkhead. As the tide receded, a shallow layer (less than 3 m deep) of fresher ground water appeared near the base of the cement bulkhead and began to spread seaward (fig. 13, profiles H, I, J, and K). This layer could represent a highly permeable sandy layer that is more conducive to flow or a lack of mixing that causes the freshwater to accumulate in the sandy layer. Although the signal could be partially blanked by the shallow resistive layer, some freshening also was evident at depth (fig. 13, profiles L and M). Freshening of the deeper parts of the system occurs much slower (10–12 hours) and may originate from longer, more regional ground-water flowpaths.

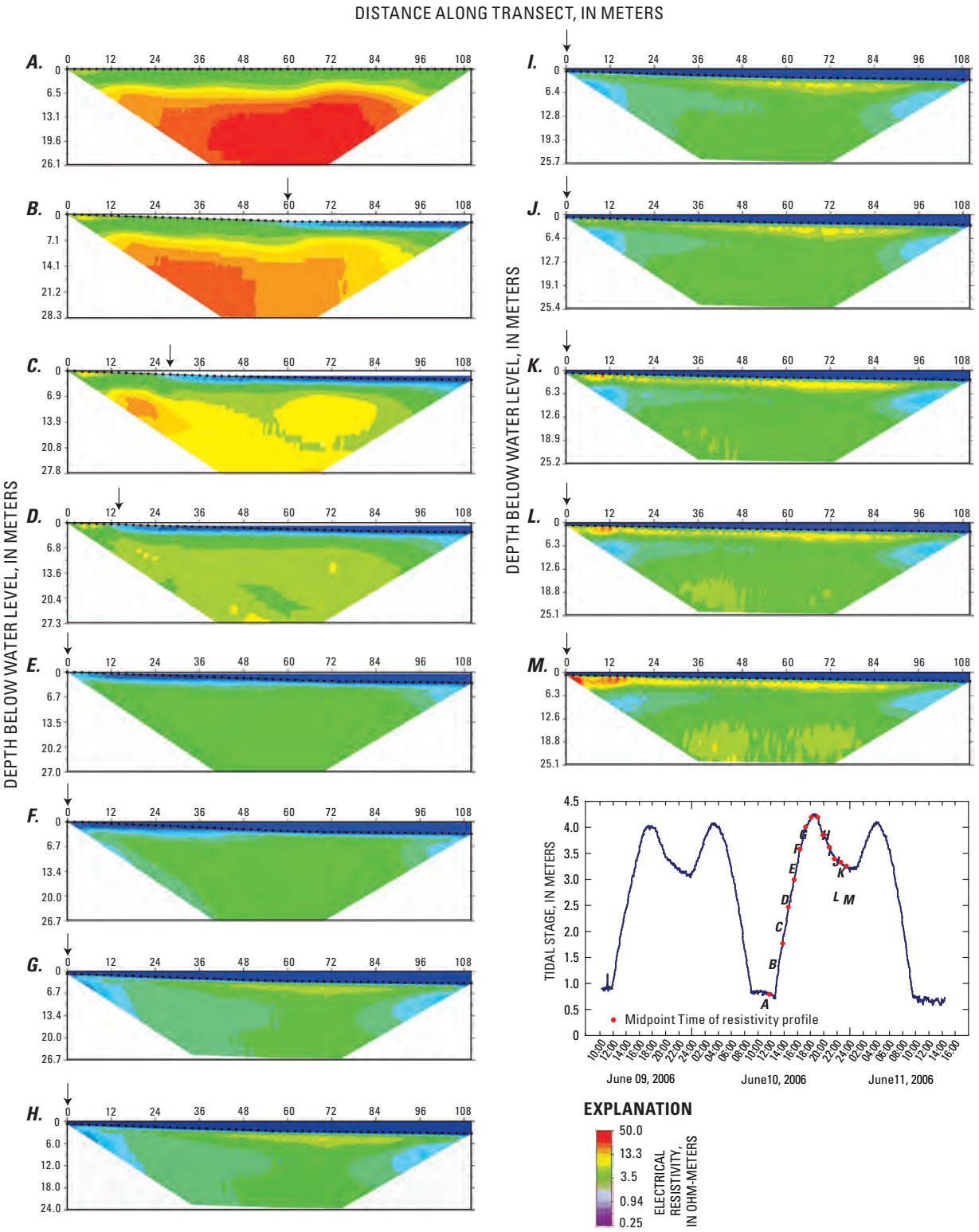

Figure 13. Resistivity profiles produced from data collected perpendicular to the shoreline at the Sunset Beach intensive study site, Lynch Cove area of Hood Canal, Washington. Each profile represents a snapshot of electrical resistivity along a cross-section of the intertidal area. Colors represent resistance in ohm-meters. Red colors indicate more electrically resistant fresh ground water and blue colors indicate more electrically conductive saline water. Approximate position of the waterline on the beach is indicated by the arrow above the profile. The plot shows the midpoint time of the data acquisition interval relative to the tidal cycle.

Landon Road Site

The north shore of Lynch Cove is exposed to more wind and wave energy than the south shore, so the seabed material is coarser grained and generally thinner than at the south shore sites (sidebar H). The Landon Road site is representative of a high-energy beach environment adjacent to a moderately steep slope. An array of minipiezometers and seepage meters similar to those used at the other intensive study sites were installed and monitored in 2005 (fig. 14). Minipiezometers in the upper intertidal zone penetrated a thin gravel veneer above compacted glacial sand and gravel. Slug tests conducted at a depth of 185 cm below the seabed indicated higher hydraulic conductivities in the sandy deposition zone just below the low tide-line (LR3, fig. 14), very low conductivities in the compacted glacial material near the low-tide line, and slightly higher conductivities in the slope-wash colluvium in the upper beach area (LR7, fig. 14). Despite the variations in hydraulic conductivity, the net freshwater discharge rates were similar (ranging from 7.0 to 24.2 cm/d), suggesting that the seabed sediments near the surface are more homogeneous due to the higher energy environment of deposition (table 3). The average net discharge rate of 13 cm/d for the Landon Road array is assumed to be representative of similar environments along the north shore of Lynch Cove.

The ESM data from a 2-day deployment showed relatively consistent discharge with short-term reversals that generally occurred during incoming tides (fig. 15). The average ESM seepage rate at the Landon Road site (7.6 cm/d) agreed closely with the apparent net seepage rates from the Lee-type seepage meters in the array (table 3). A prominent increase in ground-water discharge that occurred during the last low tide interval was not seen during the low tide of the first day of deployment. The second low tide was about 25 cm lower than the first, suggesting that there may be a threshold tidal stage below which ground-water discharge substantially increases.

Sidebar H. Conducting slug tests in a minipiezometer at the Landon Road intensive study site. The intertidal area on the north shore of Lynch Cove is composed of cobbles and gravel indicative of a higher energy environment. Photograph taken by F. William Simonds, U.S. Geological Survey, June 22, 2005.

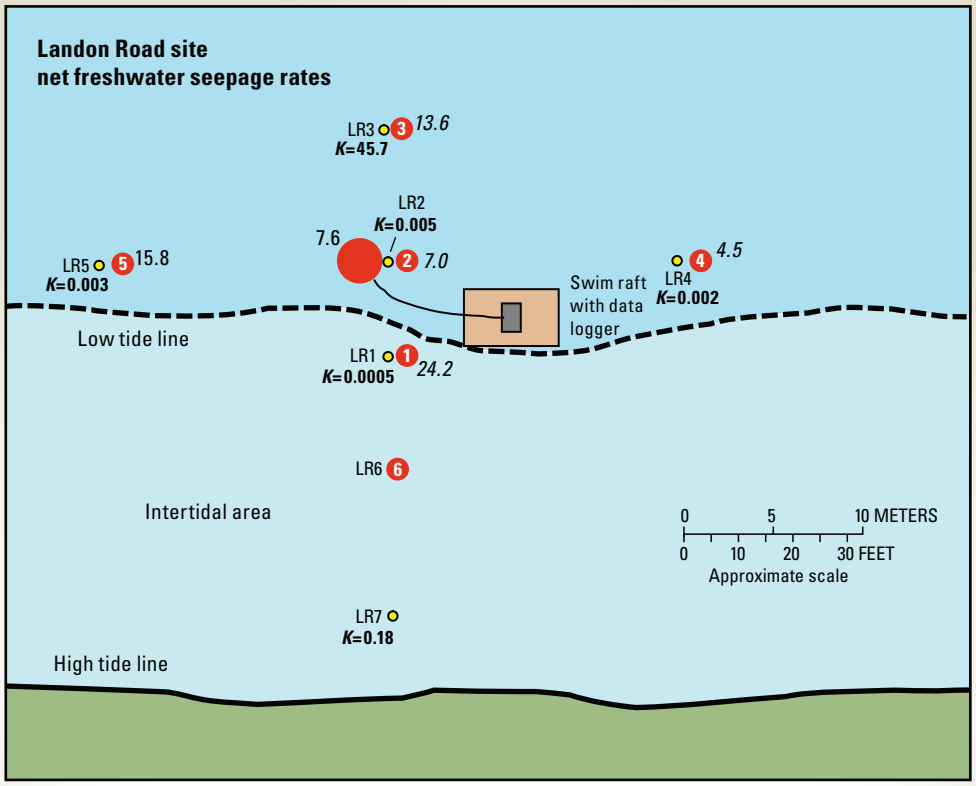

EXPLANATION

Net freshwater seepage rates—Calculated by adding average seepage rates during incoming tides (generally positive) and average seepage rates during outgoing tides (positive but smaller in magnitude). Location of intensive study site shown on figure 2

7.6 **Electromagnetic seepage meter (ESM)**—Number is average seepage rate, in centimeters per day, measured by ESM

24.2 1 **Lee-type seepage meter and number**—Number is seepage meter number (see table 3). Italicized number is net freshwater seepage rate, in centimeters per day (see table 3), and represents the freshwater component of submarine ground-water discharge

K*=0.18** **Minipiezometer**—Bold number is hydraulic conductivity (K***), in meters per day, measured using slug tests in minipiezometers

Figure 14. Minipiezometer and seepage meter arrays at the Landon Road intensive study site, Lynch Cove area of Hood Canal, Washington.

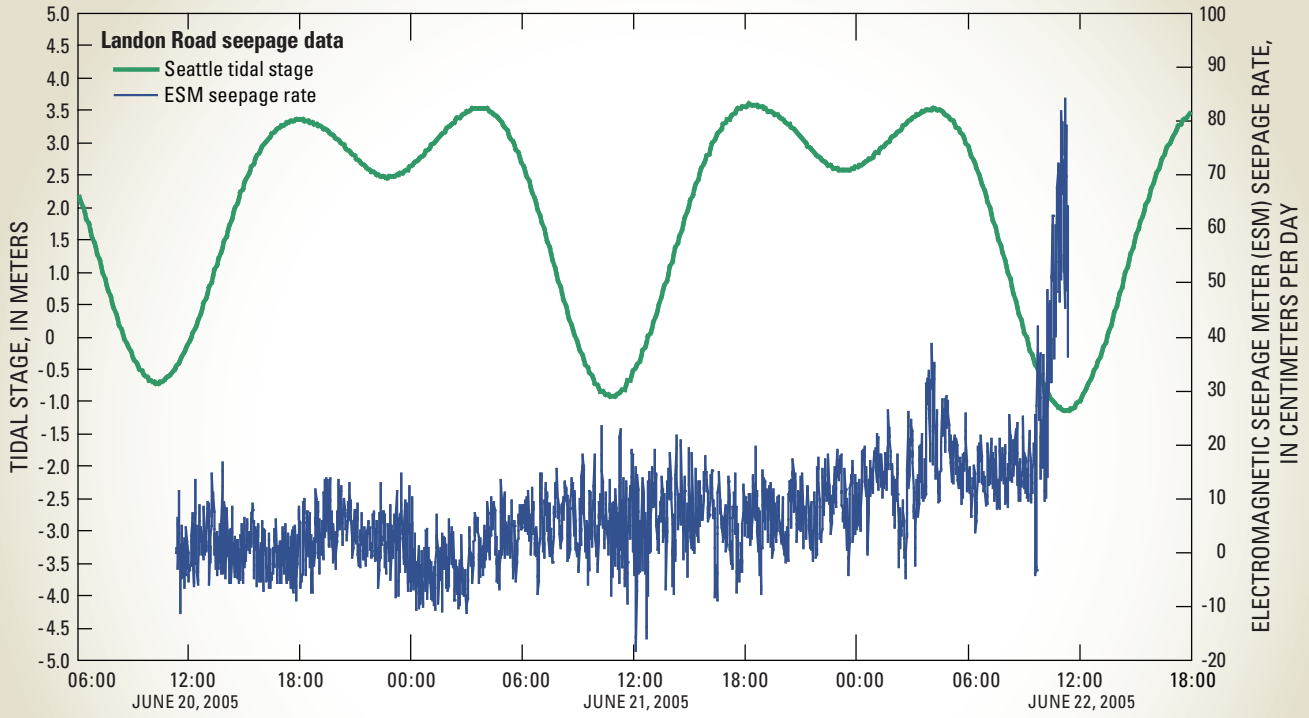

Figure 15. Continuous seepage data from the electromagnetic seepage meter (ESM) at the Landon Road intensive study site, Lynch Cove area of Hood Canal, Washington. Tidal data from Seattle closely matched the surface-water stage recorded at the other intensive study sites in Lynch Cove, so when pressure transducer data at this site were deemed unreliable the Seattle tidal data were used as a surrogate.

Spatial Variability of Submarine Ground-Water Discharge

Variability Within Intensive Study Sites

Measurements made at the intensive study sites indicate variability in ground-water discharge both parallel and perpendicular to the shoreline of Lynch Cove at the scale of an array (about 30×30 m). Slug tests conducted in minipiezometers and calculations of hydraulic conductivity (*K*) using the methods of Bouwer and Rice (1976), Bouwer (1989), and Yang and Yeh (2004) yielded *K* values that ranged over five orders of magnitude. Such variation in *K* values is likely due in part to the variety of geologic materials penetrated by the minipiezometers, although some variation also is likely due to installation problems that cause limited hydraulic connection between minipiezometers and the sediments. The hydrologic properties of the shoreline sediments, such as grain size, porosity, permeability, and thickness, stem from (1) shoreline coastal processes, which vary perpendicular to the shoreline and from site to site around the perimeter of Lynch Cove, and (2) original glacial and fluvial deposits, which vary as well in less predictable ways.

The net freshwater discharge (or recharge) rates calculated for individual seepage meters also illustrate the spatial variability at the scale of an array (table 3). At Sunset Beach, some parts of the 2005 array were dominated by recharge of saline water, whereas the 2006 array showed dominantly freshwater discharge. Such variability may be due to subtle topographic swales and the accumulation of fine-grained sediments in gentle depressions causing the low hydraulic conductivities measured in the 2005 array. However, in contrast to the magnitude of variability in hydraulic conductivity, the average net discharge rates calculated for each intensive study site fell into a fairly narrow range (-0.72 to +27 cm/d, table 3). This range of average net discharge rates is less than the variability of individual seepage meter measurements that were conducted over a typical tidal cycle. Thus, despite the large variability in hydraulic properties, when the component of saline water recharge is accounted for in the total SGD, the resulting freshwater discharge rates are relatively consistent among the intensive study sites.

Variability Throughout Lynch Cove

A streaming (marine based) electrical-resistivity survey was conducted around the perimeter of Lynch Cove to determine if the spatial variability observed at the intensive study sites could be put into a regional context. The survey was conducted over a 2-day period and consisted of 16 transects parallel to the shoreline covering a total of about 40 km (fig. 16). The surveys were conducted in 3 to 10 m of water at or near high tide so that the profiles generated would not be affected by tidal variation and would penetrate sediments within the submerged intertidal zone. The goal of the experiment was to explore the coastline of Lynch Cove and identify areas in the subsurface where fresh ground water might be present. One disadvantage of a streaming survey is that both fresh ground water and electrically resistant geologic formations can produce resistivity anomalies, although salinity differences usually produce much larger resistivity contrasts than geologic variations in marine settings (Manheim and others, 2004). Another disadvantage of these high tide surveys was the apparent limited freshwater discharge to Lynch Cove during high tides as inferred from the stationary resistivity data at the intensive study sites. Metal objects, wave action, and curvature of the towed cable also present problems when processing the data. Prominent indicators of fresh water at the mouths of several major drainages are likely occurrences of fresh ground water in coarse channel-fill deposits and suggest ground-water underflow beneath major streams entering Lynch Cove. Individual profiles from all survey transects can be found in appendix A.

Radon activity measured in surface water at the same time as the streaming electrical-resistivity survey also reveals information regarding spatial variability of SGD. A map of Lynch Cove showing continuous radon activities measured from a boat during the shore-parallel survey suggests areas where there might be ground-water discharge (fig. 17). The map shows higher activities of radon along portions of the south shore and north shore of Lynch Cove, with one “hot spot” near the mouth of Stimson Creek, located just northeast of the Landon Road intensive study site (fig. 2). Lower activities were found at the landward terminus of Lynch Cove and around Sisters Point. The presence of hot spots also could indicate areas where surface water from small creeks fed by ground-water discharge enter the Lynch Cove estuary; additional surveys would need to be conducted at low tide to confirm any conclusions based on the data. The radon data are useful, however, for reconnaissance and seem to show an area at the terminus of Lynch Cove where ground-water discharge might be more spread out or discharging farther offshore.

Temporal Variability of Submarine Ground-Water Discharge

The stationary (land based) electrical resistivity profiles taken perpendicular to the shoreline at Merrimont (fig. 9) and Sunset Beach (fig. 13) show how fresh water and saline water interact in the subsurface under the influence of a large tidal range. At the Merrimont site, continuous radon activities and continuous ESM data, which link subsurface ground-water movements spatially and temporally with discharge, helped confirm the observed temporal variations in seepage rates and their relations to the tidal cycle (fig. 10). Conductivity and temperature of bottom water inside the ESM at Merrimont, when compared with data from other sensors in the surface water outside of the dome, also yield useful temporal information. Taken together, these multiple datasets indicate that ground-water discharge is highly dynamic and strongly modulated by the tides.

Tidal Forcing

Data collected from these experiments confirm that the large tidal range of Hood Canal (3–5 m) is likely the primary driving force controlling temporal variability and mixing of fresh and saline water. The large changes in tidal stage influence both the rate of discharge and the position of maximum discharge within the intertidal zone. During each low tide, fresh ground water is able to flow freely seaward; during the successive high tide, saline seawater infiltrates into the sediments and mixes with fresh ground water. The higher density saline water may cause displacement of fresher ground water, driving circulation and saline recharge into the seabed (Moore, 1999; Bokuniewicz and others, 2004; Robinson and others, 2006). Random observations of downward flow in seepage meters during high tides at the onset of this study now make sense and provide additional evidence of these tidally induced processes.

Seasonal Fluctuations

Although the seasonal variation in ground-water discharge remains unknown, it is assumed to be relatively small compared to the total amount of ground-water discharge that enters Lynch Cove on an annual basis. Ground-water discharge is likely moderated by the large hydraulic head landward of the shoreline as indicated by springs on the hill slopes and small, baseflow-fed streams that flow year round.

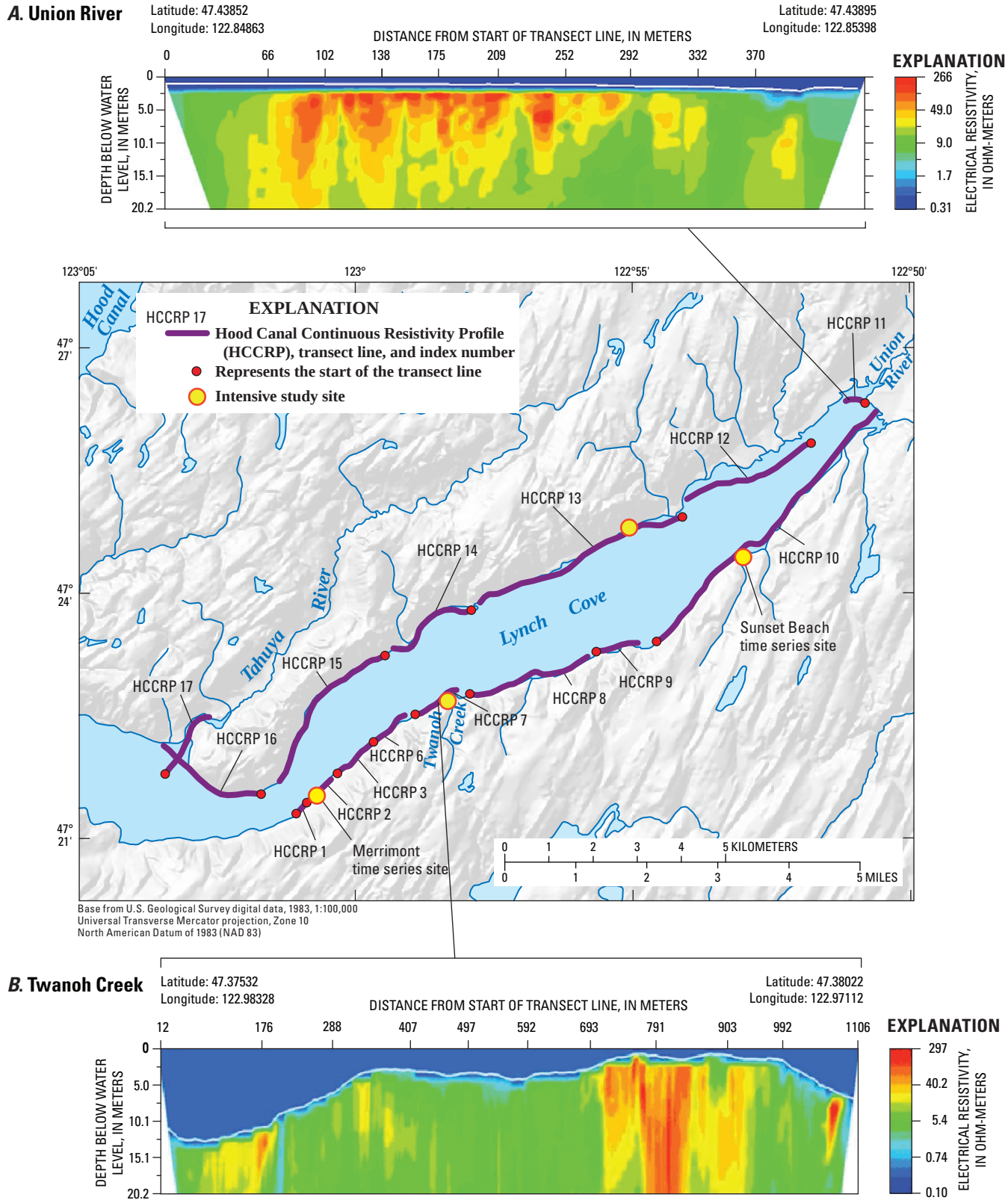

Figure 16. Trace of shore-parallel, streaming electrical-resistivity transects around the perimeter of Lynch Cove, Washington. Example profiles across the mouth of the Union River (*A*), and the mouth of Twanoh Creek (*B*) represent cross-sectional views into the sediments beneath the seabed (indicated with the white line), surface water is shown in blue. Additional profiles are included in appendix A.

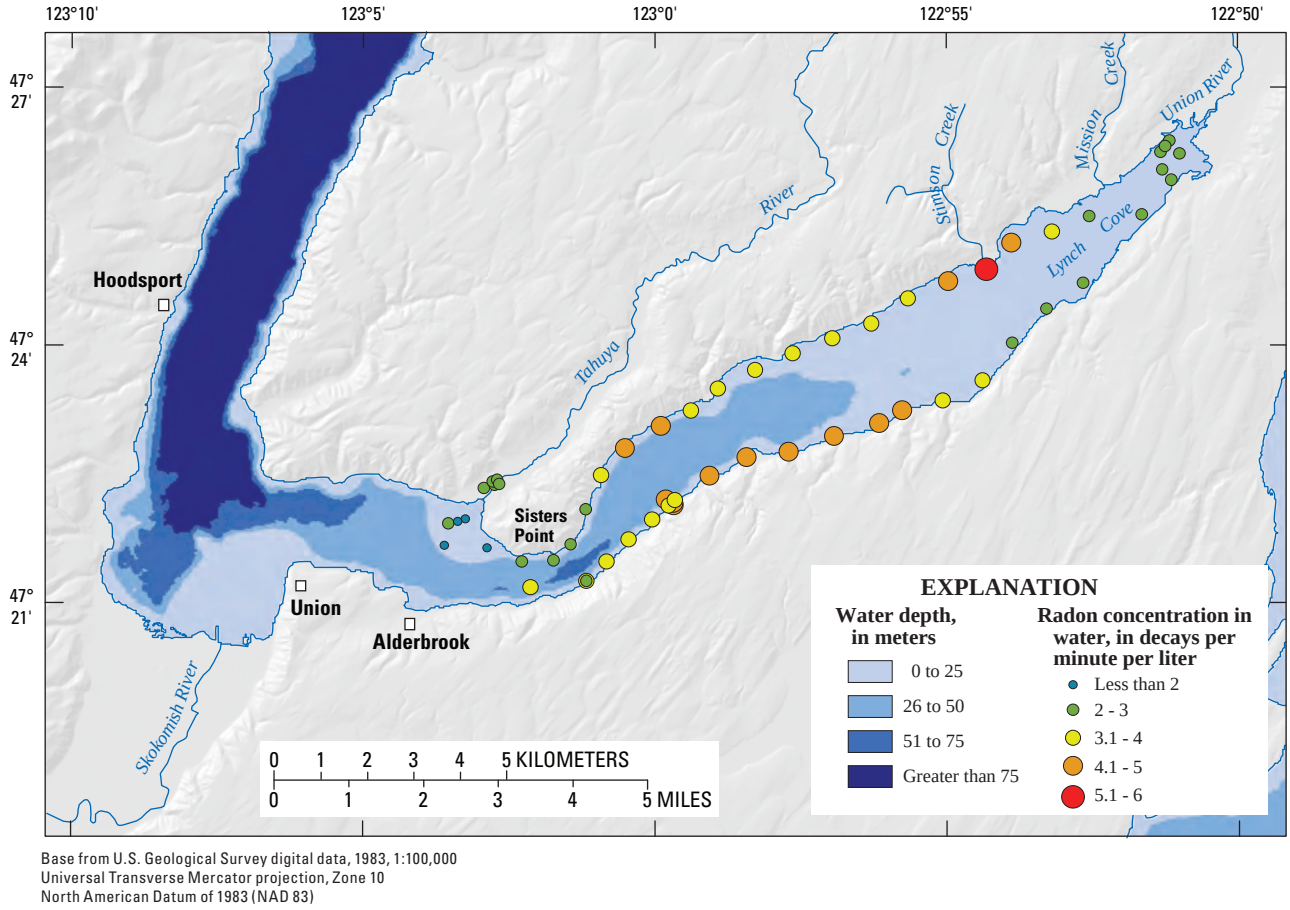

Base from U.S. Geological Survey digital data, 1983, 1:100,000
Universal Transverse Mercator projection, Zone 10
North American Datum of 1983 (NAD 83)

Figure 17. Radon activity measured during the streaming electrical-resistivity survey in the Lynch Cove area of Hood Canal, Washington.

Seasonal variation in ground-water discharge is manifest in streams that have slightly higher rates of flow in the early summer shortly after the rainy season ends and other small streams that dry up in the late summer. These seasonal fluctuations, however, generally are small, and baseflow discharge into streams is typically steady. Although seasonal maximums in ground-water flow can occur several months after the water table peaks in response to winter precipitation (Michael and others, 2005), the experiments conducted as part of this study were performed in the early summer, when ground-water levels typically are at their highest and ground-water discharge rates are assumed to be at a maximum value. Thus, for the purposes of estimating a ground-water discharge rate and nutrient loading into Lynch Cove, the estimates in this report may be maximum values. Topics worthy of further study include the delay between precipitation and ground-water discharge maximums and the effect of seasonal variations in ground-water discharge and implications of the associated nutrient loading.

Nutrient Loading to the Lynch Cove Area

Estimating nutrient loads entering the Lynch Cove area of Hood Canal by direct ground-water discharge requires knowledge of the rates of ground-water discharge, the area over which ground-water discharge occurs, and nutrient concentrations in discharging ground water. The product of the discharge (seepage) rate (in units of length per time) multiplied by the discharge area yields a ground-water flux (in units of volume per time). The nutrient-loading estimate is calculated by multiplying the ground-water flux by a representative nutrient concentration. As has been described earlier in this report, there are many complexities and uncertainties in each of these terms. To better understand how these complexities and uncertainties affect the estimated nutrient load, a suite of nutrient-loading estimates were calculated using three different methods to calculate ground-water flux and four or five different representative nutrient concentrations in ground water (table 5). The refined estimate of nutrient load was made using the average net discharge rates from each of the intensive study sites and spatially representative nutrient concentrations in ground water to calculate the nutrient load from each of three discrete zones of Lynch Cove—the south shore, the terminus of Lynch Cove, and the north shore (fig. 18). This final estimate allowed comparison of nutrient contributions from different areas around Lynch Cove. The nutrient-load calculations and results are described below and summarized in table 5.

In the following approximations, the ground-water flux entering Lynch Cove is estimated by taking the average seepage rate derived from three separate methodologies and multiplying by the intertidal area represented by a 5-m tidal cycle. The intertidal area was determined using the LIDAR digital elevation model for Lynch Cove (Puget Sound LIDAR Consortium) with contours drawn representing mean sea level plus 2.5 m, and mean sea level minus 2.5 m. Using the Grid module in ArcGIS version 9.0, the area between the two contours was calculated to be 4,614,078 m^2.

The first method is based on the residual ground-water term from the water mass-balance estimate of Paulson and others (2006) of 1.4 m^3/s. When this flux is divided by the 5-m intertidal area for Lynch Cove, it predicts an average seepage rate of 2.5 cm/d. Although this estimate is lower than the measured seepage rates, it is reasonable based on the available precipitation, accounting for surface-water runoff and evapotranspiration. When this flux is multiplied by the range of nutrient concentrations representing low and high extremes of TDN concentrations (mostly nitrate), from samples collected around the perimeter of Lynch Cove, the resulting nutrient load is 14.1 to 47.0 MT/yr (table 5). The ground-water flux and nutrient load calculated by this method provides a basis for comparison with other methods.

The second method simply takes the average of the net discharge rates from all intensive study sites (14 cm/d) multiplied by the intertidal area to calculate a ground-water flux of 7.5 m^3/s (table 5). This flux estimate was then multiplied by a range of nutrient concentrations from 0.33 to 1.1 mg/L to calculate a range of nitrogen loads to Lynch Cove from ground water of 77.8 to 259.4MT/yr (table 5). Although this simplistic approach accounts for the volume of recirculated seawater that temporarily enters the ground-water system with incoming tides, it averages the spatial and temporal variability in seepage rates for all of Lynch Cove. The ground-water flux calculated by this method is higher than the water mass-balance calculation would predict and implies that the majority of precipitation infiltrates to become ground-water recharge rather than surface-water runoff.

The third method for estimating the ground-water flux entering Lynch Cove was derived from the previously described radon-radium mass balance using indirect geochemical methods of Charette and others (2001), Burnett and Dulaiova (2003), Burnett and others (2003b), and Lambert and Burnett (2003). Using these methods at the Merrimont site (fig. 2), an advective ground-water flux was estimated based on continuous measurements of radon-222 activity over a 5-day period. Based on 501 individual measurements, the mean estimated total ground-water discharge rate at the Merrimont site was 85.8±84.5 cm/d. Multiplying this radon-derived value by the 5-m intertidal area for Lynch Cove yields a flux of 45.4 m^3/s. This approach represents a total (fresh plus saline) SGD flux, which is why this flux is six times larger than the flux calculated using average net discharge rates (method 2 in table 5).

Radium measurements can be used in conjunction with radon data to quantify the saline component of SGD in marine environments (Charette and others, 2001; Charette, 2007). This approach helps quantify the amount of seawater that is recirculated through the sediments of Lynch Cove by examining excess ^{226}Ra-flux-derived SGD rates for the entire Lynch Cove area of Hood Canal and comparing these rates to radon, ESM, or manual seepage-meter measurements. Excess ^{226}Ra fluxes were derived by subtracting the ^{226}Ra activity at HC1 (fig. 2) from a mean Lynch Cove ^{226}Ra activity, and then adjusting per the volume of Lynch Cove ($4.0\times10^8 m^3$) and the computed mean apparent residence time (32 days). Here, the end-member HC1 sample is assumed to reflect seawater most removed from Lynch Cove, wherein Ra isotopes are effectively at background activities. The influence of rivers in a mass balance of Ra in this system was ignored because the Ra activity was much lower than that in Lynch Cove proper. As in the radon model, a SGD rate for the entire water body could be derived by dividing the excess radium fluxes by a mean ^{226}Ra ground-water value (7.8 dpm/100L) from the excess Ra fluxs (table 4). This method yielded an SGD flux of 23.8 m^3/s for the Lynch Cove estuary, assuming that the area

Table 5. Comparison of calculated nutrient loads entering Lynch Cove using different methodologies.

[Delineation of zones shown in figure 18. **Average seepage rates:** Rates shown are calculated using different methods. **Area of submarine ground-water discharge (SGD)**: Represents the intertidal area spanned by a 5-meter tidal cycle. **Total dissolved nitrogen concentration**: Average total dissolved nitrogen concentrations derived from different datasets. **Total dissolved nitrogen load**: Total dissolved nitrogen load entering Lynch Cove (shown with different units of measure). **Abbreviations:** cm/d, centimeter per day; m/d, meter per day; m^2, square meter; m^3/s, cubic meter per second; ft^3/s, cubic foot per second; mg/L milligram per liter; mg/m^3, milligram per cubic meter; mg/d, milligram per day; MT/d, metric ton per day; MT/yr, metric ton per year; mol/d, moles per day; DIN, dissolved inorganic nitrogen; TDN, total dissolved nitrogen]

Average seepage rates		×	Area of SGD (m^2)	Equals (=)	Ground-water flux rate			×	Total dissolved nitrogen concentration		Equals (=)	Total dissolved nitrogen load			Total dissolved nitrogen (mol/d)
cm/d	m/d				m^3/s	ft^3/s	m^3/d		mg/L	mg/m^3		mg/d	MT/d	MT/yr	
Method 1 using seepage rates from the Paulson and others (2006) mass balance approach for Lynch Cove															
2.5	0.025		4,614,078		1.4	48	116,985		0.6	(Paulson and others, 2006) 600		70,191,000	0.0701910000	25.6	5,010
2.5	.025		4,614,078		1.4	48	116,985		.33	2005 data (this study) 330		38,605,050	.0386050500	14.1	2,756
2.5	.025		4,614,078		1.4	48	116,985		.41	2006 data (this study) 410		47,963,850	.0479638500	17.5	3,424
2.5	.025		4,614,078		1.4	48	116,985		.61	average of all data 610		71,360,850	.0713608500	26.0	5,094
2.5	.025		4,614,078		1.4	48	116,985		1.1	maximum 1,100		128,683,500	.1286835000	47.0	9,185
Method 2 using average net seepage rates from manual measurements of Lee-type seepage meters in 2005 and 2006															
14	0.14		4,614,078		7.5	264	645,970.9		0.33	2005 data (this study) 330		213,170,404	0.2131704036	77.8	15,216
14	.14		4,614,078		7.5	264	645,970.9		.41	2006 data (this study) 410		264,848,077	.2648480772	96.7	18,904
14	.14		4,614,078		7.5	264	645,970.9		.61	average of all data 610		394,042,261	.3940422612	143.8	28,126
14	.14		4,614,078		7.5	264	645,970.9		1.1	maximum 1,100		710,568,012	.7105680120	259.4	50,719
Method 3 using seepage rates based on radon-radium mass balance															
40.4	0.404		4,614,078		21.6	763	1,866,240		0.339	2006 data (DIN, this study) 339		632,655,360	0.6326553600	230.9	45,157
40.4	.404		4,614,078		21.6	763	1,866,240		.41	2006 data (TDN, this study) 410		765,158,400	.7651584000	279.3	54,615
40.4	.404		4,614,078		21.6	763	1,866,240		.61	average of all data 610		1,138,406,400	1.1384064000	415.5	81,257
40.4	.404		4,614,078		21.6	763	1,866,240		1.1	maximum 1,100		2,052,864,000	2.0528640000	749.3	146,528
Nutrient loads entering Lynch Cove based on zonal approach															
Zone 1 (south shore) using apparent net seepage rates and nutrient concentrations from within zone 1															
17.5	0.175		629,436		1.1	39	95,935.88		0.3	300		28,780,763	0.0287807625	10.5	2,054
Zone 2 (Lynch Cove terminus) using apparent net seepage rates and nutrient concentrations from within zone 2															
7	0.07		3,436,437		2.8	98	240,550.6		0.9792	979.2		235,555,913	0.2355559128	86.0	16,813
Zone 3 (north shore) using apparent net seepage rates and nutrient concentrations from within zone 3															
13	0.13		548,205		0.9	33	81,826.68		0.0600	60.0		4,909,601	0.0049096008	1.8	350
Total ground-water flow into Lynch Cove					4.8	170	418,313.1								
Total nutrient loads entering Lynch Cove based on zonal approach (MT/yr)														98.3	

over which radioactive decay processes operate is $2.7\times10^7 m^2$. This Ra approach represents an estimate of saline SGD only for the time period studied; more detailed information to better constrain end-member variability and seasonality would reduce the large errors associated with this estimate. However, when the saline flux derived from excess ^{226}Ra is subtracted from the total flux derived by the radon method, the resulting flux (21.6 m^3/s) represents the volume of fresh ground water entering Lynch Cove. Multiplying this ground-water flux by the range of fresh ground-water TDN concentrations (0.33 to 1.1 mg/L) yields a nitrogen load to Lynch Cove of 230.9 to 749.3 MT/yr (table 5). The ground-water flux calculated by this method is more than the available precipitation falling in the Lynch Cove watershed suggesting that the errors associated with this estimate are larger than the other methods.

Spatially distributed loading estimates were derived by subdividing the intertidal area around Lynch Cove into distinct geomorphic regions and performing loading calculations based on data from each zone. The zones were based on geographic and geomorphic characteristics (fig. 18), and also were supported by data from the streaming resistivity and radon surveys (figs. 16 and 17). An implicit assumption in the zone approach is that the limited data collected from within each zone are representative of the entire zone. Within each zone, average net discharge rates from manual seepage measurements at the intensive study sites were multiplied by the intertidal area within each zone to determine ground-water fluxes of 1.1 m^3/s for zone 1; 2.8 m^3/s for zone 2; and 0.9 m^3/s for zone 3 (fig. 18), giving a total ground-water flux of 4.8 m^3/s for Lynch Cove. Multiplying each flux by the average

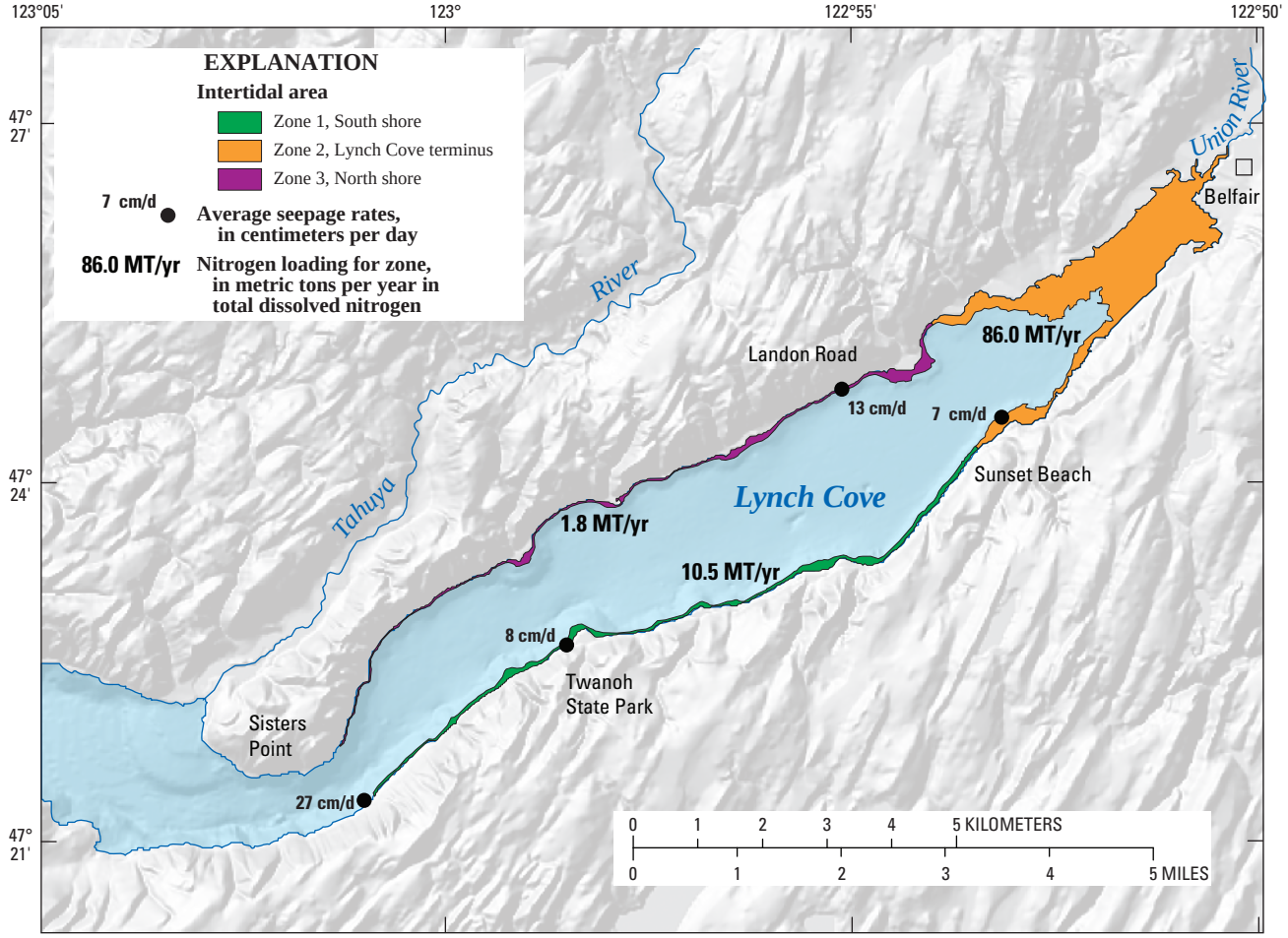

Base from U.S. Geological Survey digital data, 1983, 1:100,000
Universal Transverse Mercator projection, Zone 10
North American Datum of 1983 (NAD 83)

Figure 18. Intertidal areas of Lynch Cove, based on a 5-meter tidal range, subdivided into zones representing the south shore, the terminus of Lynch Cove, and the north shore areas of Hood Canal, Washington.

nutrient concentration from samples collected within each zone produced nutrient loads of 10.5 MT/yr for zone 1 (south shore), 86.0 MT/yr for zone 2 (terminus), and 1.8 MT/yr for zone 3 (north shore) (fig. 18; table 5). The ground-water flux calculated by this method is larger than the mass balance method but less than the flux calculated using manual seepage meter measurements.

Based on the limited seepage data collected during this study, the distribution of nutrient loading from ground-water discharge into Lynch Cove appears to be non-uniform. Average net discharge rates within each zone were similar (average of Twanoh and Merrimont sites=17.5 cm/d for the south shore, 7 cm/d for the terminus of Lynch Cove, and 13 cm/d for the north shore) and the mean TDN concentrations were 0.3, 0.98, and 0.06 mg/L within these respective zones. The smallest loading estimate was within the north shore zone (1.8 MT/yr), where both the average net discharge rates and average nutrient concentrations were the lowest. The loading estimate for the south shore zone (10.5 MT/yr) was intermediate between the north shore zone and the terminus area of Lynch Cove. The south shore zone had the highest measured discharge rates in the study; however, the average nutrient concentrations were generally lower. Both the north shore and south shore zones lie along steep coastlines, so the areal extent of the intertidal zone is small. The largest estimated loading of TDN occurs at the terminus of Lynch Cove (86.0 MT/yr). The terminus of Lynch Cove has relatively flat topography, so the intertidal area is much larger than that of the other zones. In addition, nutrient concentrations within this zone also were higher than in the other zones. Thus, one disadvantage of the zone method is that the size of the intertidal area affects the calculations by biasing flat areas with high discharge rates and steep areas with low discharge rates.

The location of the apparent maximum nutrient loading at the terminus of Lynch Cove could be due, in part, to the proximity of a large urban area (Belfair) and the increased population density in that area. Increased population density generally leads to more use of fertilizers, more septic systems, less natural evergreen forest, and more alders, all of which contribute to increased nutrients in ground water. The ground-water flow system within the Lynch Cove basin flows towards the shoreline, and flow lines tend to converge at the terminus of narrow water bodies like Lynch Cove. All these factors may contribute to enhanced nutrient loading around the terminus of Lynch Cove, which contributes to the chronic low oxygen condition that threatens marine wildlife. Fish kill events, however are caused by persistent southerly winds that push the surface-water layer aside and allow deeper water with a low dissolved-oxygen (DO) concentration to outcrop at the surface. Thus, fish kill events are more common near the Great Bend and west of Sisters Point than they are in Lynch Cove.

When the nutrient load entering Lynch Cove through the ground-water pathway is placed in context with other sources of nutrients, the importance of ground-water derived nutrients is clear. Estimated annual loads from estuarine circulation are the largest source of nutrients transporting 1,584 MT/yr DIN into Lynch Cove (Paulson and others, 2006). Nutrient loading from the ground-water pathway estimated by this study was 98 MT/yr. Surface-water sources contribute varying amounts of nutrients depending on the amount of flow; 10.8 MT/yr DIN during the dry season and about four times that amount during the wet season (Paulson and others, 2006). Septic sources also vary depending on the time of year; 10.1 MT/yr was estimated using September and October as a baseline (Paulson and others, 2006). Atmospheric deposition of nitrogen also varies annually; 1.68 MT/yr was estimated using September and October as a baseline (Paulson and others, 2006). These estimates rank ground water as the second largest source of nutrients that are delivered into Lynch Cove on an annual basis. Excluding estuarine circulation, surface water may be an important source of nutrients during the winter rainy season, but ground water is the dominant source during the summer dry season when low DO conditions are most chronic.

Uncertainty and Limitations of Nutrient-Loading Estimates

Comparison of nutrient loads calculated using the various methods described above shows that the geochemical method gave the widest range and the largest net loading of nutrients into Lynch Cove (230.9 to 749.3 MT/yr), followed by manual measurements of seepage (77.8 to 259.4 MT/yr). The manual seepage measurements were further refined by subdividing the area of ground-water discharge into three separate zones, and calculating an average net discharge rate for fresh ground water within each zone. An estimate of errors for fluxes, areas, and nutrient concentrations yielded TDN loads of 10.5±3.5 MT/yr for the south shore zone, 86.0±5.8 MT/yr for the terminus of Lynch Cove, and 1.8±0.97 MT/yr for the north shore zone, for a total refined estimate of 98±10.3 MT/yr. This refined estimate is 2 to 7 times larger than the TDN loads calculated using the residual ground-water term with the mass-balance approach (14 to 47 MT/yr) (Paulson and others, 2006). The large range of values is due to a combination of uncertainties in the collection and measurement of seepage rates, estimation of the areal extent of ground-water discharge, and estimation of the nutrient concentration in the water as it enters the Lynch Cove estuary. In this study, attempts were made to understand the spatial and temporal variability in

seepage rates, to identify the areal distribution of ground-water discharge, and to obtain a representative sample of nutrient concentrations in ground water adjacent to the shoreline. Uncertainties in each of the terms in the nutrient loading calculation, however, preclude a precise determination.

In this study, measured ground-water fluxes were 4.8 to 7.5 m^3/s, or 3.5 to 5 times larger than the residual ground-water term predicted using a mass-balance approach (1.4 m^3/s; Paulson and others, 2006). One possible reason for this discrepancy may be the fact that seepage measurements were made during the early summer when ground-water discharge rates would be at or near their seasonal maximum. If this were the case then the annual ground-water flux would be lower and in closer agreement to the mass balance estimate. In addition, processes such as denitrification, which affect nutrient concentrations at or near the sediment-water interface, were not addressed in this study. If denitrification was occurring then the overall amount of nitrogen available for uptake in the Lynch Cove estuary would be lower than estimated.

This study did not identify specific sources of nutrients in ground water, such as those derived from septic inputs. Properly functioning septic systems are designed to disperse nutrients into the environment, where geochemical processes determine the rate of denitrification. No failing systems were observed during the course of this study, although assessing the integrity of such systems was not an objective of this project. Future investigations should focus on seasonal and longer term climatic variations that relate specific natural and human-induced causes to ecosystem health and factors that contribute to fish kill events. The ground-water flux and nutrient loading estimates from this study are intended to verify previous estimates, and to provide a starting point for biogeochemical modeling of the Hood Canal marine ecosystem.

Summary and Conclusions

Natural and human-influenced factors that affect hypoxic conditions in the marine waters of Hood Canal are the subject of intensive study by the Hood Canal Dissolved Oxygen Program. This study contributes to the overall understanding of nutrient sources by looking specifically at the direct ground-water discharge pathway. The study focused on the Lynch Cove area, the most landward reach of Hood Canal, where low dissolved oxygen in surface waters are most chronic. Previously, little was known about how and where ground-water discharge was likely to occur in a fjord environment with a high-amplitude tidal cycle such as Lynch Cove. Previous estimates of ground-water discharge and nutrient loading were based on water mass-balance calculations using estimates of bulk precipitation, evapotranspiration, surface-water runoff, and ground-water recharge. The goal of this study was to better understand the processes that control ground-water discharge into Hood Canal and make measurements that could be used to better constrain previous nutrient-loading estimates.

Physical measurements of ground-water discharge were made using Lee-type seepage meters, minipiezometers, and electromagnetic seepage meters. These devices were deployed around the perimeter of Lynch Cove as an initial reconnaissance tool, and later in T-shaped arrays at four intensive study sites. Indirect measurements of ground-water discharge were made using geochemical tracers such as radon and radium. Continuous radon measurements provided temporal information about total (fresh plus saline) submarine ground-water discharge (SGD), whereas a radium-isotope mass-balance technique provided information about the role of seawater water recirculation at the estuary scale. Because radium is only mobilized in saline water, radium-isotopes can be used in conjunction with radon measurements to quantify both saline and fresh ground-water components of SGD. Nutrient concentrations in ground water were assessed by analyzing samples from domestic wells around the perimeter of Lynch Cove, natural flowing springs, and minipiezometers installed within the intertidal zone. Stationary and streaming electrical-resistivity surveys were extremely useful for visualizing the freshwater/saltwater interface and better understanding temporal effects of tidal forcing.

Estimating the volume of ground-water discharge into the Lynch Cove area of Hood Canal is complicated by spatial and temporal variability in the rate of discharge that occurs at various scales. Small-scale spatial variability was observed in the arrays at each of the four intensive study sites, whereas larger-scale variability was indicated by the shore-parallel radon and electrical-resistivity surveys. At the array scale, hydraulic conductivities varied by as much as five orders of magnitude, largely due to heterogeneities in the geologic materials penetrated by the minipiezometers. Hydraulic conductivity also affects the average seepage rate, which generally decreases with increasing distance from shore. Zones of preferential flow were inferred to follow areas with coarser grained or more permeable materials within the intertidal area. Sunset Beach, with its low-relief topography and finer grained sediments, represents a large intertidal area at the landward terminus of Lynch Cove. Low-relief mudflats have complicated freshwater-seawater interactions that occur over a broader area than was observed at steeper shoreline sites. Within the wide intertidal zone at such sites, infiltration of seawater takes place during incoming tides, and fresh ground-water discharge occurs over broad areas during outgoing tides. In some areas, such as subtle depressions, recharge of saline water may predominate, except during extreme low tides. Limited measurements at Sunset Beach suggest that additional areas of ground-water discharge could

occur farther offshore. Shore-parallel streaming electrical-resistivity and near-continuous radon measurements showed distinct along-shore spatial variations in Lynch Cove surveys. Prominent resistivity anomalies at the mouths of major drainages suggest the occurrence of freshwater underflow in localized high permeability zones in these settings, a previously unconsidered nutrient-input pathway.

Stationary electrical-resistivity surveys, radon time-series measurements, and continuous measurements of seepage proved useful in showing the temporal variability in ground-water discharge at high resolution. Taken together, these data provide an unprecedented level of temporal and spatial information. The electrical-resistivity profiles from the Merrimont site showed an upper saline cell and a "tongue" of freshwater discharge that are parts of a complex fresh-saline interface that moves seaward during outgoing tides and landward during incoming tides. The movement of this interface was about 30 meters horizontally and 20 meters vertically. Along steeper shorelines this process was restricted to a narrow intertidal zone, but at Sunset Beach the width of this zone of interface movement was greater than 100 meters. The resistivity profiles from Sunset Beach showed a large mass of fresh water about 6 meters below the seabed during low tide. As the incoming tide swept across Sunset Beach, the resistivity profiles showed significant infiltration of saline water, which displaced and (or) mixed with fresh ground water in the subsurface. When the tide receded, fresh water infiltrated into a shallow permeable layer first, followed by a slow freshening at depth, possibly from a deeper, more regional ground-water flowpath.

Both the ESM and radon data showed an inverse correlation with the tides, with increased ground-water discharge and radon activities during the lowest tides, and either decreased discharge or saline recharge during high tides. When total seepage measured during incoming tides was compared to seepage measured during outgoing tides, the outgoing-tide interval had higher total seepage rates in every case. Thus, the sum of seepage rates measured during incoming and outgoing tides was assumed to represent the net freshwater discharge entering Lynch Cove. The range of average net discharge rates, based on measurements at the four intensive study sites, were relatively small (27 centimeters per day [cm/d] at Merrimont; 8 cm/d at Twanoh State Park; 7 cm/d at Sunset Beach (when 2005 and 2006 data are combined); and 13 cm/d at Landon Road). This range of average net discharge rates is approximately 3.5 to 5 times larger than the residual ground-water term predicted using a mass-balance approach for Hood Canal.

The rate of fresh ground-water discharge into Lynch Cove is one of the variables necessary to calculate a nutrient load. When average net discharge rates from all intensive study sites (14 cm/d) are used, the result is a flux of 7.5m^3/s and a nutrient load of 77.8 to 259.4 metric tons per year (MT/y;TDN) to the Lynch Cove area. This estimate was refined by subdividing the intertidal area into three geomorphic zones. When the average net discharge rates from each zone are used the resulting loading estimate for TDN is 10.5±3.5 MT/yr for the south shore zone, 86±5.8 MT/yr for the terminus of Lynch Cove, and 1.8±0.97 MT/yr for the north shore zone, and a total refined estimate of 98±10.3 MT/yr for the Lynch Cove area. This estimate is higher than the previously reported mass-balance estimate, but lower than the estimate based on indirect geochemical tracer methods. Although the zone approach suggests that the bulk of the loading may come from the mudflat areas at the terminus of Lynch Cove, there is significant uncertainty about the source of nutrients and the role of denitrification at or near the sediment-water interface.

Although the location of the maximum nutrient loading appears to correlate with population density, further examination of the Lynch Cove terminus is warranted. Studying the temporal and spatial variations in ground-water discharge, the influence of tidal forcing, and the role of seawater recirculation are keys to understanding the delivery of nutrients into the marine ecosystem through the ground-water pathway. Although estuarine circulation of seawater may be the largest source of nutrients into Lynch Cove, the role of ground water is at least as important as surface water. Ground water may be the most significant source of nutrients to the shallow marine layer during the late summer when Hood Canal is most susceptible to phytoplankton blooms.

Acknowledgments

We gratefully acknowledge the support of the Hood Canal Dissolved Oxygen Program (HCDOP) and the close partnership with its codirectors, Jan Newton and Dan Hannafous. Support and encouragement were provided by all members of the HCDOP, the Salmon Enhancement Group, Hood Canal Coordinating Council, the Puget Sound Action Team, and many other participating groups. We are especially grateful to the many local residents and concerned citizens who let us access their wells and beach property. Special thanks are offered to Bob Hagar, Mike Dully, Al Adams, and Dr. William Portuese for allowing access to their property, as well as to the staff of Twanoh State Park. In the field, Seth Book (Mason County Health Department), Suzanne Osborn (University of Washington) and Reagan Huffman (USGS) helped with sampling, piezometer installations, and seepage-meter measurements and Jason Greenwood helped run the resistivity surveys. The manuscript benefitted from reviews by John Bratton (USGS, Woods Hole Oceanographic Institute), Eric Richard (USGS, California Water Science Center), and Richard Dinicola (USGS, Washington Water Science Center).

References Cited

Anderson, J.K., Wondzell, S.M., Gooseff, M.N., and Haggerty, R., 2005, Patterns in stream longitudinal profiles and implications for hyporheic exchange flow at the H.J. Andrews Experimental Forest, Oregon, USA: Hydrological Processes, v. 19, p. 2931-2949.

Atekwana, E.A., and Krishnamurthy, R.V., 2004, Investigating landfill-impacted ground-water seepage into headwater streams using stable carbon isotopes: Hydrological Processes, v. 18, p. 1915–1926.

Baxter, C., Hauer, F.R., and Woessner, W.W., 2003, Measuring ground water-stream water exchange— New techniques for installing minipiezometers and estimating hydraulic conductivity: Transactions of the American Fisheries Society, v. 132, p. 493–502.

Belanger, T.V., and Montgomery, M.T., 1992, Seepage meter errors: Limnology and Oceanography, v. 37, no. 8, p. 1787-1795.

Bencala, K.E., 2000, Hyporheic zone hydrological processes: Hydrological Processes, v. 14, p. 2797-2798.

Bencala, K.E., McKnight, D.M., and Zellweger, G.W., 1990, Characterization of transport in an acidic and metal-rich mountain stream based on a lithium tracer injection and simulations of transient storage: Water Resources Research, v. 26, no. 5, p. 989-1000.

Bokuniewicz, H., Pollock, M., Blum, J., and Wilson, R., 2004, Submarine ground water discharge and salt penetration across the sea floor: Ground Water–Oceans Special Issue, v. 42, no. 7, p. 983–989.

Bouwer, H., 1989, The Bouwer and Rice slug test—An update: Ground Water, v. 27, p. 304-309.

Bouwer, H., and Rice, R.C., 1976, A slug test for determining hydraulic conductivity of unconfined aquifers with completely or partially penetrating wells: Water Resources Research, v. 12, p. 423-428.

Bratton, J.F., 2007, The importance of submarine confining units to submarine groundwater flow, *in* A New Focus on Groundwater-Seawater Interactions: International Association of Hydrological Sciences (IAHS) Publication 312, p. 28-36.

Burnett, W.C., Bokuniewicz, H., Huettel, M., Moore, W.S., and Taniguchi, M., 2003a, Ground water and porewater inputs to the coastal zone: Biogeochemistry, v. 66, p. 3-33.

Burnett, W.C., Cable, J.E., and Corbett, D.R., 2003b, Radon tracing of submarine ground-water discharge in coastal environments, *in* Taniguchi, M., Wang, K. and Gamo. T., eds., Land and Marine Hydrogeology: Elsevier, p. 25-43.

Burnett, W.C., Chanton, J., Christoff, J., Kontar, E., Krupa, S., Lambert, M., Moore, W., O'Rourke, D., Paulsen, R., Smith, C., Smith, L., and Taniguchi, M., 2002, Assessing methodologies for measuring ground-water discharge to the ocean: EOS, v. 83, p. 117-123.

Burnett, W.C., and Dulaiova, H., 2003, Estimating the dynamics of ground-water input into the coastal zone via continuous radon-222 measurements: Journal of Environmental Radioactivity, v. 69, p. 21-35.

Burnett, W.C., and Dulaiova, H., 2006, Radon as a tracer of submarine ground-water discharge into a boat basin in Donnalucata, Sicily: Continental Shelf Research, v. 26, p. 862-873.

Burnett, W.C., Santos, I., Weinstein, Y., Swarzenski, P.W., and Herut, B., 2007, Remaining uncertainties in the use of Rn-222 as a quantitative tracer of submarine groundwater discharge, *in* A New Focus on Groundwater-Seawater Interactions: International Association of Hydrological Sciences (IAHS), Publication 312, p. 109-118.

Cable, J.E., Burnett, W.C., Chanton, J.P., Corbett, D.R., and Cable, P.H., 1997, Field evaluation of seepage meters in the coastal marine environment: Estuarine, Coastal and Shelf Science, v. 45, p. 367-375.

Cable, J.E., Martin, J.B., and Jaeger, J., 2006, Exonerating Bernouilli? On evaluating the physical and biological processes affecting marine seepage meter measurements: Limnology and Oceanography: Methods 4, 2006, p. 172-183.

Capone, D.G., and Bautista, M.F., 1985, A ground-water source of nitrate in near shore marine sediments, Nature, v. 313, p. 214-216.

Charette, M.A., 2007, Hydrologic forcing of submarine groundwater discharge—Insight from a seasonal study of radium isotopes in a groundwater-dominated salt marsh estuary: Limnology and Oceanography, v. 52, no. 1, p. 230-239.

Charette, M.A., Buesseler, K.O., and Andrews, J.E., 2001, Utility of radium isotopes for evaluating the input and transport of ground water-derived nitrogen to a Cape Cod estuary: Limnology and Oceanography, v. 46, p. 465-470.

Conant, B., Jr., 2004, Delineating and quantifying ground water discharge zones using streambed temperatures: Ground Water, v. 42, no. 2, p. 243–257.

Constantz, J., Thomas, C.L., and Zellweger, G., 1994, Influence of diurnal variations in stream temperature on streamflow loss and ground-water recharge: Water Resources Research, v. 30, no. 12, p. 3253-3264.

Crecelius, E.A., Brandenburger, J., Louchouarn, P., Cooper, S., Leopold, E., Gengwu, L., and McDougall, K., 2007, History of hypoxia recorded in sediments of Hood Canal, Puget Sound: Proceedings, Georgia Basin Puget Sound Research Conference, Vancouver, BC, 26-29 March 2007.

Crusius, J., Koopmans, D., Bratton, J., Charette, M., Kroeger, K., Henderson, P., Ryckman, L., Halloran, K., and Colman, J., 2005, Submarine groundwater discharge to a small estuary estimated from radon and salinity measurements and a box model: Biogeosciences, v. 2, p. 141-157.

Dulaiova, H., Peterson, R., Burnett, W.C., and Lane-Smith, D., 2005, A multi-detector continuous monitor for assessment of ^{222}Rn in the coastal ocean: Journal of Radioanalytical and Nuclear Chemistry, v. 263, p. 361-365.

Easterbrook, D.J., 1979, The last glaciation of northwest Washington, *in* Armentrout, J.M., Cole, M.R., Ter Best, Harry Jr., eds., Cenozoic Paleogeography of the Western U.S.: Society of Economic Paleontologists and Mineralogists Symposium Volume, p. 177-189.

Fishman, M.J., ed., 1993, Methods of analysis by the U.S. Geological Survey National Water Quality Laboratory—Determination of inorganic and organic constituents in water and fluvial sediments: U.S. Geological Survey Open-File Report 93-125, 217 p.

Fokkens, B., and Weijenberg, J., 1968, Measuring the hydraulic potential of ground water with the hydraulic potential probe: Journal of Hydrology, v. 6, p. 306-313.

Giblin, A., and Gaines, A., 1990, Nitrogen inputs to a marine embayment—The importance of ground water: Biogeochemistry, v. 10, p. 309–328.

Gobler, C.J., and Sanudo-Wilhelmy, S.A., 2001, Temporal variability of ground-water seepage and brown tide blooms in a Long Island embayment: Marine Ecology Program Series, v. 217, p. 299-309.

Gooseff, M.N., LaNier, J., Haggerty, R., and Kokkeler, K., 2005, Determining in-channel (dead zone) transient storage by comparing solute transport in a bedrock channel–alluvial channel sequence, Oregon: Water Resources Research, v. 41, W06014, doi:10.1029/2004WR003513.

Greene, K.E., 1997, Ambient quality of ground water in the vicinity of Naval Submarine Base Bangor, Kitsap County, Washington, 1995: U.S. Geological Survey Water-Resources Investigations Report 96-4309, 46 p.

Harvey, J.W., and Bencala, K.E., 1993. The effect of streambed topography on surface-subsurface water exchange in mountain catchments: Water Resources Research, v. 29, no. 1, p. 89-98.

Hatch, C.E., Fisher, A.T., Revenaugh, J.S., Constantz, J., and Ruehl, C., 2006, Quantifying surface water–ground water interactions using time series analysis of streambed thermal records—Method development: Water Resources Research, v. 42, W10410, doi:10.1029/2005WR004787.

Hu, C., Muller-Karger, F., and Swarzenski, P.W., 2006, Hurricanes, submarine ground-water discharge and west Florida's red tides: Geophysical Research Letters, v. 33, L11601, doi:10.1029/2005GL025449.

Hwang, D.W., Kim, G., Lee, Y.W., and Yang, H.S., 2005, Estimating submarine inputs of ground water and nutrients to a coastal bay using radium isotopes: Marine Chemistry, v. 96, p. 61-71.

Inkpen, E.L., Tesoriero, A.J., Ebbert, J.C., Silva, S.R., and Sandstrom, M.W., 2000, Ground-water quality in the Puget Sound Basin, Washington and British Columbia, 1996-1998: U.S. Geological Survey Water-Resources Investigations Report 00-4100, 66 p.

Johannes, R., 1980, The ecological significance of the submarine discharge of ground water: Marine Ecology Program Series, v. 3, p. 365–373.

Jones, J.B., and Mulholland, P.J., 2000, Streams and Ground Waters: Academic Press, San Diego, 425 p.

Lambert, M.J., and Burnett, W.C., 2003, Submarine groundwater discharge estimates at a Florida coastal site based on continuous radon measurements: Biogeochemistry, v. 66, p. 55-73.

Landon, M.K., Rus, D.L., and Harvey, F.E., 2001, Comparison of instream methods for measuring hydraulic conductivity in sandy streambeds: Ground Water, v. 39, no. 6, p. 870-885.

LaRoche, J., Nuzzi, R., Waters, R., Wyman, K., Falkowski, P.G., and Wallace, D.W.R., 1997, Brown tide blooms in Long Island's coastal waters linked to inter-annual variability in ground-water flow: Global Change Biology, v. 3, 397-410.

Lee, D.R., 1977, A device for measuring seepage flux in lakes and estuaries: Limnology and Oceanography, v. 22, no.1, p. 140-147.

Lee, D.R., and Cherry, J.A., 1978, A field exercise on ground-water flow using seepage meters and minipiezometers: Journal of Geological Education, v. 27, p. 6-10.

Liu, F., Williams, M.W., and Caine, N., 2004, Source waters and flow paths in an alpine catchment, Colorado Front Range, United States: Water Resources Research, v. 40, W09401, doi:10.1029/2004WR003076.

Malcolm, I.A., Soulsby, C., Youngson, A.F., Hannah, D.M., McLaren, I.S., and Thorne, A., 2004, Hydrological influences on hyporheic water quality—Implications for salmon egg survival: Hydrological Processes, v. 18, p. 1543–1560.

Malcolm, I.A., Soulsby, C., Youngson, A.F., and Petry, J., 2003, Heterogeneity in ground water–surface water interactions in the hyporheic zone of a salmonid spawning stream: Hydrological Processes, v. 17, p. 601–617.

Manheim, F.T., Krantz, D.E., and Bratton, J.F., 2004, Studying ground water beneath Delmarva coastal bays using electrical resistivity: Ground Water, v. 42, no. 7, p. 1052-1068.

Martens, C.S., Kipphut, G.W., and Klump, J.V., 1980, Sediment-water chemical exchange in the coastal zone traced by in situ radon-222 flux measurements: Science, v. 208, p. 285-288.

Michael, H.A., Mulligan, A.E. and Harvey, C.F., 2005, Seasonal oscillations in water exchange between aquifers and the coastal ocean: Nature, v. 436, no. 7054, p. 1145–1148.

Moore, W.S., 1996, Large ground-water inputs to coastal waters revealed by ^{226}Ra enrichment: Nature, v. 380, p. 612-614.

Moore, W.S., 1999, The subterranean estuary—A reaction zone of ground water and sea water: Marine Chemistry, v. 65, p. 111–125.

Moore, W.S., 2000, Determining coastal mixing rates using radium isotopes: Continental Shelf Research, v. 20, p. 1993-2007.

Moore, W.S., 2003, Sources and fluxes of submarine ground-water discharge delineated by radium isotopes: Biogeochemistry, v. 66, p. 75-93.

Moore, W.S., 2006, Radium isotopes as tracers of submarine ground-water discharge in Sicily: Continental Shelf Research, v. 26, 852-861.

Murdoch, L.C., and Kelly, S.E., 2003, Factors affecting the performance of conventional seepage meters: Water Resources Research, v. 39, no. 6, 1163 p., doi:10.1029/2002WR001347.

Mutz, M., and Rohde, A., 2003, Processes of surface-subsurface water exchange in a low energy sand-bed stream: International Review of Hydrobiology, v. 88, p. 290–303.

Noble, M.A., Gartner, A.L., Paulson, A.J., Xu, J., Josberger, E.G., and Curran, C., 2006, Transport pathways in the lower reaches of Hood Canal: U.S. Geological Survey Open-File Report 2006-1001 [http://pubs.usgs.gov/of/2006/1001/].

Paulson, A.J., Konrad, C.P., Frans. L.M., Noble, Marlene, Kendal, Carol, Josberger, E.G., Huffman, R.L., and Olsen, T.D., 2006, Freshwater and saline loads of dissolved inorganic nitrogen to Hood Canal and Lynch Cove, western Washington: U.S. Geological Survey Scientific Investigations Report 2006-5106, 91 p.

Robinson, C., Li, L., and Prommer, H., 2006, Tide-induced recirculation across the aquifer-ocean interface: Water Resources Research, v. 43, W07428, doi:10.1029/2006WR005679.

Rosenberry, D.O., and Menheer, M.A., 2006, A system for calibrating seepage meters used to measure flow between ground water and surface water: U.S. Geological Survey Scientific Investigations Report 2006-5053.

Rosenberry, D.O., and Morin, R.H., 2004, Use of an electromagnetic seepage meter to investigate temporal variability in lake seepage: Ground Water, v. 42, no. 1, p. 68-77.

Salehin, M., Packman, A.I., and Paradis, M., 2004, Hyporheic exchange with heterogeneous streambeds—Laboratory experiments and modeling: Water Resources Research, v. 40, no. 11, W11504, doi:10.1029/2003WR002567.

Scott, D.T., Gooseff, M.N., Bencala, K.E., and Runkel, R., 2003, Automated calibration of a stream solute transport model—Implications for interpretation of biogeochemical parameters: Journal of the North American Benthological Society, v. 22, no. 4, p. 492-510.

Shaw, R.D., and Prepas, E.E., 1990, Ground water-lake interactions: I. Accuracy of seepage meter estimates of lake seepage: Journal of Hydrology, v. 119, p. 105-120.

Shinn, E.A., Reich, C.D., and Hickey, T.D. 2002, Seepage meters and Bernoulli's revenge: Estuaries, v. 25, no. 1, p. 126-132.

Silliman, S.E., and Booth, D.F., 1993, Analysis of time-series measurements of sediment temperature for identification of gaining vs. losing portions of Juday Creek, Indiana: Journal of Hydrology, v. 146, p. 131-148.

Stanford, J.A., and Ward, J.V., 1988, The hyporheic habitat of river ecosystems: Nature, v. 335, no. 1, p. 64-66.

Stonestrom, D.A., and Constantz, J., 2004, Using temperature to study stream-ground water exchanges: U.S. Geological Survey Fact Sheet 2004-3010.

Storey, R.G., Howard, K.W.F., and Williams, D.D., 2003, Factors controlling riffle-scale hyporheic exchange flows and their seasonal changes in a gaining stream—A three-dimensional ground-water flow model: Water Resources Research, v. 39(2), 1034 p., doi:10.1029/2002WR001367.

Swarzenski, P.W., 2007, U/Th series radionuclides as tracers of coastal ground water: Chemical Reviews, v. 107, p. 663-674, doi:10.1021/cr0503761.

Swarzenski, P.W., Burnett, W.C., Greenwood, W.J., Herut, B., Peterson, R., Dimova, N., Shalem, Y., Yechieli, Y., and Weinstein, Y., 2006a, Combined time-series resistivity and geochemical tracer techniques to examine submarine ground-water discharge at Dor Beach, Israel: Geophysical Research Letters, v. 33, L24405, doi:10.1029/2006GL028282.

Swarzenski, P.W., Charette, M., and Langevin, C., 2004, An autonomous, electromagnetic seepage meter to study coastal ground water/surface water exchange: U.S. Geological Survey Open-File Report 2004-1369, 4 p.

Swarzenski, P.W., Orem, W.G., McPherson, B.F., Baskaran, M., and Wan, Y., 2006b, Biogeochemical transport in the Loxahatchee River estuary—The role of submarine ground-water discharge: Marine Chemistry, v. 101, p. 248–265.

Swarzenski, P.W., Reich, C., Kroeger, K., and Baskaran, M., 2007a, Ra and Rn isotopes as natural tracers of submarine ground-water discharge in Tampa Bay, Fla.: Marine Chemistry, v. 104, p. 69–84.

Swarzenski, P.W., Simonds, F.W., Paulson, A.J., Kruse, Sarah, and Reich, Chris, 2007b, Geochemical and geophysical examination of submarine groundwater discharge and associated nutrient loading estimates into Lynch Cove, Hood Canal, Washington: Environmental Science and Technology, v. 41, no. 20, p. 7022–7029.

Triska, F.J., Duff, J.H., and Avanzino, R.J., 1993, The role of water exchange between a stream channel and its hyporheic zone in nitrogen cycling at the terrestrial-aquatic interface: Hydrobiologia, v. 251, p. 167–184

U.S. Geological Survey, variously dated, National field manual for the collection of water-quality data: U.S. Geological Survey Techniques of Water-Resources Investigations, Book 9, chaps. A1-A9, [http://pubs.water.usgs.gov/twri9A].

U.S. Soil Conservation Service, 1965, Mean annual precipitation, 1930-1957, Portland, Oregon: State of Washington, Map M-4430.

Vacarro, J.J., Hansen, A.J., Jr., and Jones, M.A., 1998, Hydrogeologic framework of the Puget Sound aquifer system, Washington and British Columbia: U.S. Geological Survey Professional Paper 1424-D, 77 p.

Valett, H.M., Fisher, S.G., Grimm, N.P., and Camill, P., 1994, Vertical hydrologic exchange and ecological stability of a desert stream ecosystem: Ecology, v. 75, no. 2, p. 548-560.

Winter, T.C., LaBaugh, J.W., and Rosenberry, D.O., 1988, The design and use of a hydraulic potentiomanometer for direct measurement of differences in hydraulic head between ground water and surface water: Limnology and Oceanography, v. 33, no. 5, p. 1209-1214.

Woessner, W.W., 2000, Stream and fluvial plain ground water interactions—Rescaling hydrogeologic thought: Ground Water, v. 38, no. 3, p. 423-429.

Worman, A., Packman, A.I., Johansson, H., and Jonsson, K., 2002, Effect of flow-induced exchange in hyporheic zones on longitudinal transport of solutes in streams and rivers: Water Resources Research, v. 38, no. 1, doi:10.1029/2001WR00.

Yang, S.Y., and Yeh, H.D., 2004, A simple approach using Bouwer and Rice's method for slug test data analysis: Ground Water, v. 42, p. 781-784.

This page intentionally left blank

Appendix A.—Streaming Electrical-Resistivity-Survey Profiles

A series of streaming electrical resistivity surveys were conducted on June 7 and 8, 2006, along the perimeter of Lynch Cove. The surveys were performed by trailing a floating, 130-m electrode cable behind a boat traveling at 2-4 knots while maintaining a water depth of 3 to 10 m as data were collected in a series of transects. The surveys began on June 7, 2006, near Merrimont; data were acquired as the boat traveled northeast along the south shoreline to the terminus of Lynch Cove. On June 8, 2006, the surveys continued as the boat traveled southwest along the north shore past Sisters Point, ending west of the Tahuya River. All data were acquired during or near high tide. The data from each survey line were processed using AGI's 2D EarthImager™ software and are shown as profiles. Profiles represent a cross-sectional view through the water column (blue) to the sea floor (shown as the white line) and into the sediments below the seabed (colored section). Color scales represent electrical resistivity in ohm-meters with more electrically resistant materials shown in red and yellow colors and less electrically resistant materials shown in green and blue colors (note the scales are variable). Vertical axes are depth below surface water elevation at or near high tide. Horizontal axes represent horizontal distance traveled between latitude-longitude coordinates at the beginning and end of each profile.

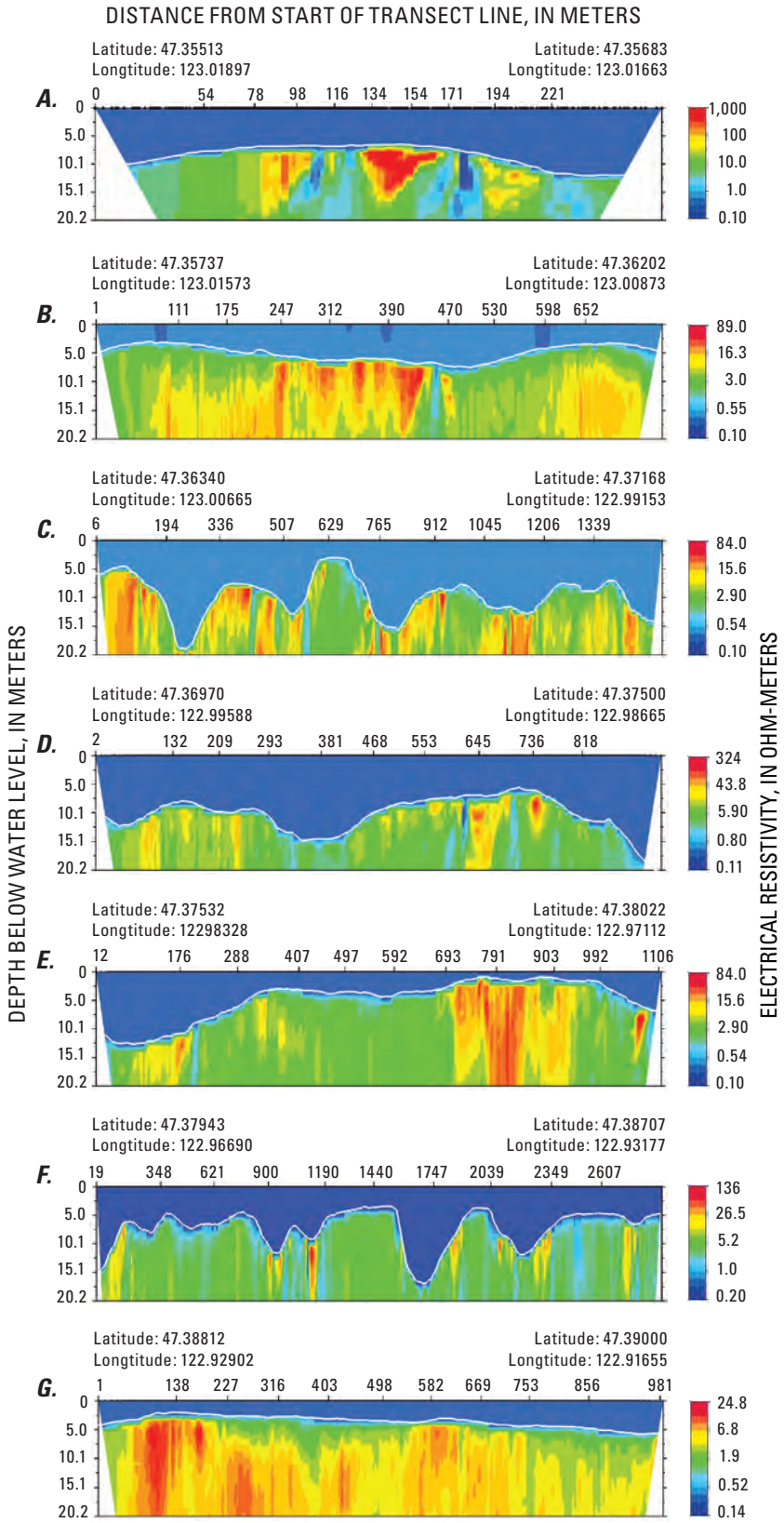

Figure A1. Electrical-resistivity profiles, June 7–8, 2008, Lynch Cove area of Hood Canal, Washington.

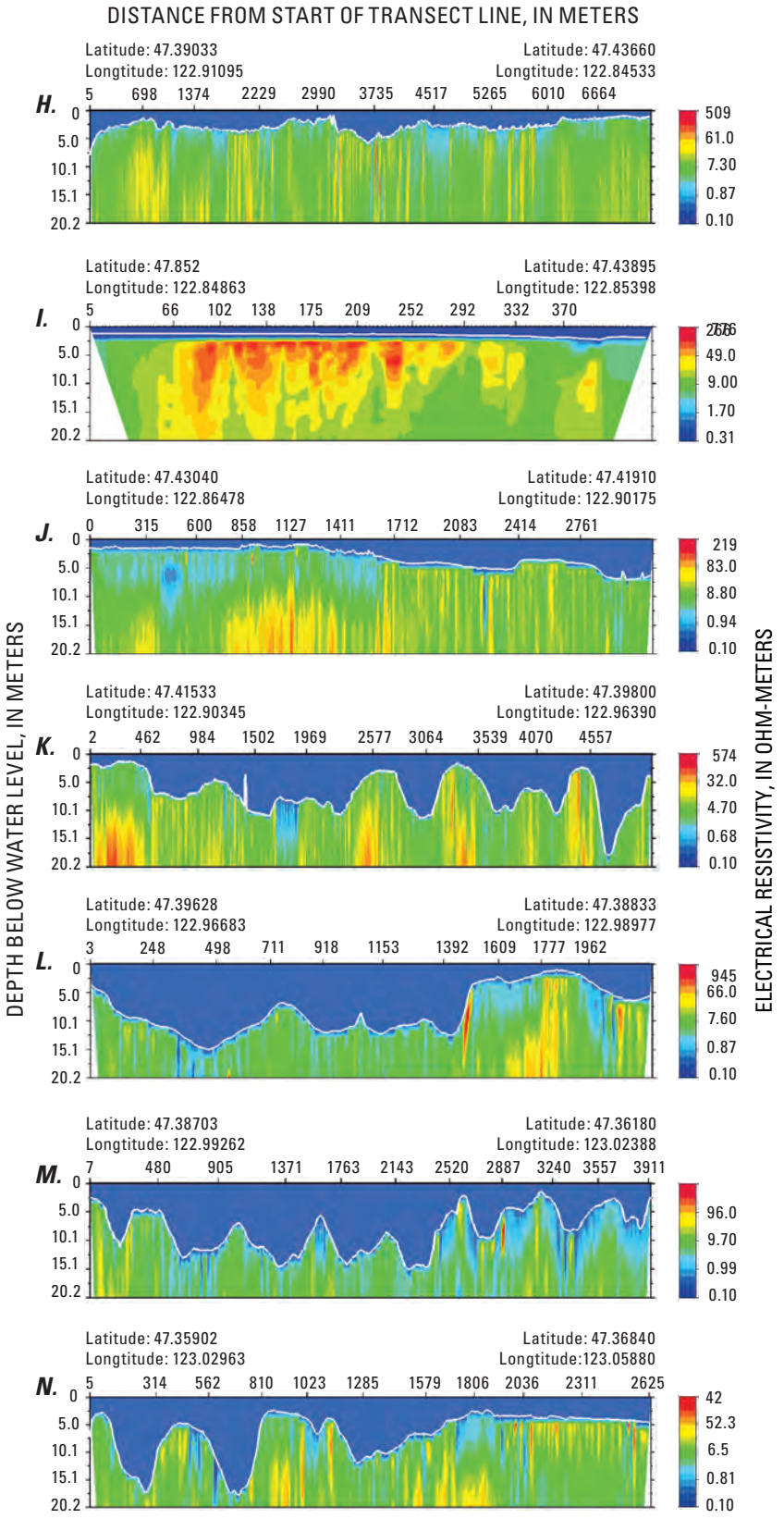

Figure A1. Continued.

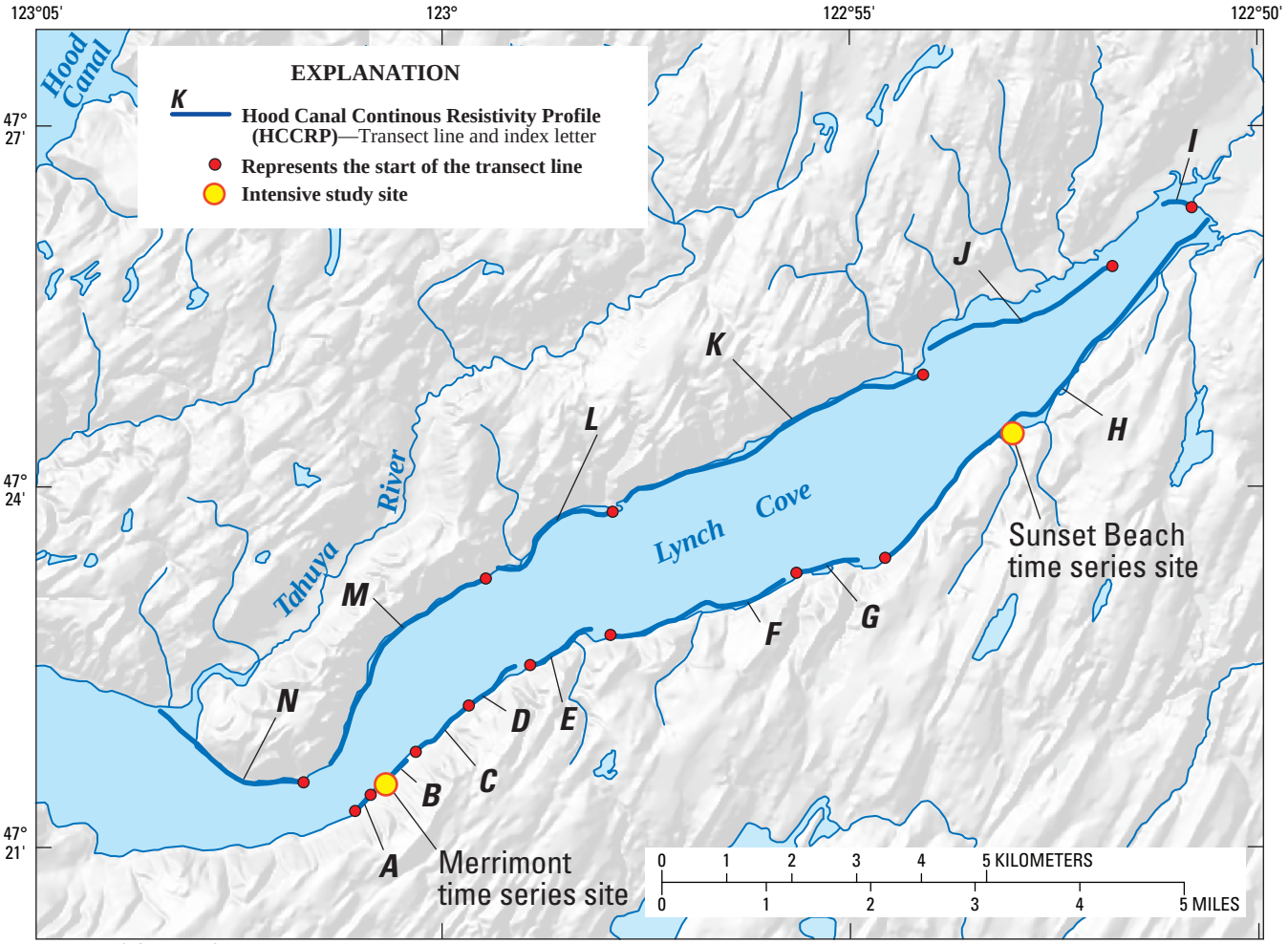

Figure A2. Hood Canal Continuous Resistivity Profile transects and intensive study sites, Lynch Cove area of Hood Canal, Washington.

Manuscript approved for publication, May 9, 2008
Prepared by the USGS Publishing Network,
Bob Crist
Bill Gibbs
Debra Grillo
Bobbie Jo Richey
Linda Rogers
For more information concerning the research in this report, contact the
Director, Washington Water Science Center
U.S. Geological Survey, 934 Broadway—Suite 300
Tacoma, Washington 98402
http://wa.water.usgs.gov